

BIOPROCESSING OF RECOMBINANT PROTEINS PRODUCED IN THE  
CHLOROPLAST OF *CHLAMYDOMONAS REINHARDTII*

A Thesis

by

KATELYN MARIE QUINONES

Submitted to the Office of Graduate and Professional Studies of  
Texas A&M University  
in partial fulfillment of the requirements for the degree of

MASTER OF SCIENCE

Chair of Committee,	Zivko L. Nikolov
Committee Members,	R. Karthikeyan
	Arul Jayaraman
Head of Department,	Steve Searcy

August 2015

Major Subject: Biological and Agricultural Engineering

Copyright 2015 Katelyn Marie Quinones

## ABSTRACT

The chloroplast of eukaryotic green algae, *Chlamydomonas reinhardtii*, is a relatively new and unexplored platform for the production of human therapeutics, vaccines, and human monoclonal antibodies. To accurately determine the viability of algae as a production platform, not only does the titer of correctly folded proteins have to be competitive to existing platforms (insect, yeast, plants, and bacteria) but the ease of downstream processing must also be taken into consideration. Two proteins expressed in the chloroplast of *C. reinhardtii* were studied, a malaria vaccine candidate (*Plasmodium falciparum* surface protein 25 (Pfs25)) and a single-chained antibody fragment ( $\alpha$ CD22scFv). The first part of this study (Chapter II) had two objectives: (i) increase the accumulation of Pfs25 and (ii) characterize the Pfs25-aggregates. By suspending algal cells in fresh media after 5 days of growth, the accumulation of Pfs25 increased 1.7-fold. The Pfs25-aggregates were separated by size exclusion chromatography (SEC) and found to range in size from 25 kDa to >600 kDa; even in the presence of reducing agents and detergent the higher molecular (MW) aggregates remained intact. Due to the wide variances of Pfs25, evaluating the ease of downstream processing of algae with Pfs25 would prove to be difficult. Previously, our lab used  $\alpha$ CD22scFv to compare three pretreatment methods (ammonium sulfate precipitation at pH 8.0, isoelectric precipitation at pH 4.5, and chitosan precipitation at pH 5.0) on residual chlorophyll, DNA, host cell protein, and  $\alpha$ CD22scFv yield. However, the pretreatment methods were compared using anti-FLAG-affinity resin (a very specific yet highly expensive resin).

Therefore, the second part of this study (Chapter III) used  $\alpha$ CD22scFv to (i) test the effect of pretreatment methods on  $\alpha$ CD22scFv adsorption to Capto Q and Phenyl Sepharose resins and (ii) develop a purification process resulting in >98% purity. Isoelectric precipitation at pH 4.5 and anion exchange chromatography (AXC) combination was determined to be the best combination for initial recovery and concentration of  $\alpha$ CD22scFv. After isoelectric precipitation and AXC, anti-FLAG-affinity resin was the only resin scouted that showed a >98%  $\alpha$ CD22scFv purity and 77% yield.

## DEDICATION

To my wonderful mother for her unconditional love and support.

## ACKNOWLEDGEMENTS

I would first like to thank my committee chair, Dr. Zivko L. Nikolov, for his patience, dedication, and guidance. I also want to extend my thanks to my committee members, Dr. R. Karthikeyan and Dr. Arul Jayaraman, for their guidance and support throughout the course of this research.

I would like to acknowledge the funding of this work by the National Science Foundation (Chemical, Bioengineering, Environmental, and Transport Systems Grant #1160117). A thank you to Stephen Mayfield and his laboratory, at the University of California San Diego, for providing transgenic strains of *C. reinhardtii* and collaboration. Also, a thank you to Dr. Larry Dangott for running purified recombinant proteins on 2-D electrophoresis gels.

Thanks also go to my friends and colleagues and the department faculty and staff for making my time at Texas A&M University a great experience.

Finally, thanks to my mother and father for their encouragement and to my wonderful husband for his patience and love through this whole experience.

## NOMENCLATURE

AP	Alkaline Phosphatase
BCIP	5-Bromo-4-Chloro 3''-Indolyphosphate p-Toluidine Salt
CTB	Cholera Toxin Beta Subunit
CVs	Column Volumes
EPA	ExoProtein A
ER	Endoplasmic Reticulum
FDA	US Food and Drug Administration
GLA	Glucopyranosal Lipid A
GPI	Glycosylphosphatidylinositol
GRAS	Generally Regarded As Safe
HAC	Hydroxyapatite Affinity Chromatography
HAP	Hydroxyapatite
HIC	Hydrophobic Interaction Chromatography
IEX	Ion-Exchange Chromatography
IMAC	Immobilized Metal Affinity Chromatography
LicKM	Lichenase Carrier Molecule
LDS	Lithium Dodecyl Sulfate
mAb	Monoclonal Antibody
MS	Mass Spectroscopy
MTP	Muramyl Tripeptide

MW	Molecular Weight
NaOH	Sodium Hydroxide
NBT	Nitro-Blue Tetrazolium
Ni-NTA	Nickel Nitrile-Triacetic Acid
OMPC	Outer-Membrane Protein Complex
PBST	Phosphate Buffered Saline with 0.1% Tween 20
PES	Polyethersulfone
Pfs25	<i>Plasmodium falciparum</i> Surface Protein 25
pI	Isoelectric Point
PpL	Peptostreptococcal Protein L
RO	Reverse Osmosis
RPC	Reverse-Phase Chromatography
Rubisco	Ribulose Bis-phosphate Carboxylase/Oxygenase
scFvs	Single-Chained Antibody Fragments
SEC	Size Exclusion Chromatography
SEC-MALLS	Size Exclusion Chromatography with Multi-Angle Laser Light Scattering
SMFA	Standard Membrane Feeding Assay
TAP	Tris-Acetate-Phosphate
TB	Transmission Blocking
TBS-T	Tris-Buffered Saline and Tween 20
TBVs	Transmission Blocking Vaccines

TEV

Tobacco Etch Virus

UTRs

Untranslated Regions

## TABLE OF CONTENTS

	Page
ABSTRACT .....	ii
DEDICATION .....	iv
ACKNOWLEDGEMENTS .....	v
NOMENCLATURE .....	vi
TABLE OF CONTENTS .....	ix
LIST OF FIGURES .....	xii
LIST OF TABLES .....	xvii
CHAPTER I INTRODUCTION AND BACKGROUND .....	1
1.1 Introduction.....	1
1.2 Background.....	2
1.2.1 Expression systems for recombinant protein production.....	2
1.2.2 Recovery and purification of high-value proteins (native and recombinant) from microalgae.....	5
1.3 Objectives .....	13
1.4 Thesis organization .....	14
CHAPTER II INCREASED ACCUMULATION AND CHARACTERIZATION OF PFS25 PRODUCED IN THE CHLOROPLAST OF <i>CHLAMYDOMONAS REINHARDTII</i> .....	16
2.1 Overview.....	16
2.2 Introduction.....	17
2.2.1 Malaria disease .....	17
2.2.2 Production systems for Pfs25 .....	21
2.3 Materials and methods .....	29
2.3.1 Gene constructs for Pfs25 .....	29
2.3.2 Cultivation of recombinant Pfs25 <i>Chlamydomonas reinhardtii</i> strains.....	29
2.3.3 Protein Extraction .....	30
2.3.4 Protein Analysis.....	31
2.3.5 FLAG-affinity capture and purification.....	32

2.3.6 Characterization of purified Pfs25 by SEC.....	33
2.3.7 ELISA .....	34
2.4 Results and discussion .....	35
2.4.1 Cell resuspension increases Pfs25 accumulation.....	35
2.4.2 Purification and partial characterization of Pfs25.....	38
2.4.3 Characterization of purified Pfs25 by SEC .....	40
2.5 Summary.....	49
CHAPTER III DEVELOPMENT OF A NON-AFFINITY PURIFICATION METHODS FOR RECOMBINANT PROTEINS PRODUCED IN <i>CHLAMYDOMONAS</i> <i>REINHARDTII</i> .....	52
3.1 Overview.....	52
3.2 Introduction.....	54
3.2.1 Single-chain antibody fragments ( $\alpha$ CD22scFv) applications .....	54
3.2.2 Purification of scFv.....	55
3.2.3 Purification of scFv from algae .....	58
3.3 Materials and methods .....	59
3.3.1 Gene construct for $\alpha$ CD22scFv .....	59
3.3.2 Cultivation of $\alpha$ CD22scFv <i>Chlamydomonas reinhardtii</i> strains.....	60
3.3.3 Protein Extraction .....	60
3.3.4 Pretreatment of cell free lysates.....	61
3.3.5 Anion exchange chromatography (AXC) .....	62
3.3.6 Hydrophobic interaction chromatography (HIC) .....	63
3.3.7 Mixed-mode chromatography.....	65
3.3.8 Anti-FLAG-affinity purification.....	65
3.3.9 Protein Analysis.....	67
3.4 Results and discussion .....	68
3.4.1 Stability of $\alpha$ CD22scFv during adsorption to Capto Q resin.....	68
3.4.2 Comparing effect of pretreatment methods with $\alpha$ CD22scFv adsorption to Capto Q and Phenyl Sepharose resin.....	71
3.4.3 Screening of Phenyl Sepharose and HAP as possible intermediate purification steps.....	75
3.4.4 Purification of $\alpha$ CD22scFv by Capto Q and FLAG-affinity chromatography .....	81
3.5 Summary.....	87
CHAPTER IV CONCLUSIONS AND RECOMMENDATIONS .....	90
4.1 Conclusions.....	90
4.2 Recommendations.....	92

REFERENCES.....	94
APPENDIX.....	104

## LIST OF FIGURES

	Page
Figure 1. Ordering of water molecules around hydrophobic residues on the surface of a protein. ....	7
Figure 2. Protein interaction caused by disruption of hydrogen layer. ....	8
Figure 3. Solubility of a globulin-type protein close to its pI. ....	10
Figure 4. Mechanism of polymer precipitation. ....	11
Figure 5. The effect of cell resuspension and light exposure ( $100\mu\text{mol m}^{-2} \text{s}^{-1}$ ) on <i>C. reinhardtii</i> cell concentration and Pfs25 accumulation (% total soluble protein). Average of 3 replicates. TAP: Tris-Acetate-Phosphate. ....	36
Figure 6. SDS-PAGE gels of Pfs25 affinity purification from (a) non resuspended cell lysate (control) and (b) resuspended cell lysates. Lane 1: molecular weight marker (kDa); Lanes 7-10: Pfs25 eluted fractions at pH 3.5. ....	37
Figure 7. Analysis of resin wash and eluted Pfs25 fractions. (a) SDS-PAGE gel of Pfs25 affinity purification and (b) Western blot analysis of Pfs25 from resuspended cell lysate. (b) Lane 1: molecular weight marker (kDa); Lane 2: 1st CV of wash before elution; Lane 3: 10X dilution of 1 <sup>st</sup> CV of wash before elution; Lane 4-5: 2 <sup>nd</sup> and 3 <sup>rd</sup> CV of wash before elution; Lane 7-10: elution 1-4 at pH 3.5. ....	39
Figure 8. 2-D electrophoresis gel of FLAG-purified Pfs25 separated first by isoelectric point and then by molecular weight. ....	40
Figure 9. Calibration curve used for analysis of Pfs25 aggregates. ....	41
Figure 10. Chromatogram of Pfs25 without Tween 20 purified by anti-FLAG affinity chromatography separated by SEC TSKGEL G3000SWxl. ....	43
Figure 11. Western blotting of FLAG-purified Pfs25 separated by SEC using anti-FLAG-AP conjugated antibody (a) under non-reducing conditions, (b) under reducing conditions without Tween 20, and (c) under reducing conditions in the presence of Tween 20. ....	44
Figure 12. Chromatogram of Pfs25 with 0.25% Tween 20 purified by anti-FLAG affinity chromatography separated by SEC TSK GEL G3000SWxl. ....	47

Figure 13. Chromatogram of FLAG-purified Pfs25 eluted using FLAG-peptide pH 8.0, separated using SEC. ....	48
Figure 14. Reactivity of selected fractions from SEC probed with dilutions of 4B7 mAb on ELISA. ....	49
Figure 15. Stability of $\alpha$ CD22scFv bound to Capto Q resin in clarified lysate for 7 hours at room temperature. Western Blot analysis of $\alpha$ CD22scFv using anti-FLAG-AP conjugated antibody. Lane 1: molecular weight marker (kDa); Lane 2: 10X diluted supernatant after sonication of cells; Lane 3: 10X diluted supernatant after filtration through PES 0.22 $\mu$ m syringe filter; Lane 4: 10X diluted supernatant after dialysis; Lane 5: 10X diluted supernatant after 7 hours binding with anti-FLAG resin; Lane 6: 10X diluted washes before elution; Lane 7-10: 50mM Tris-base, 1M NaCl pH 8.0 eluted fractions. ....	70
Figure 16. (a) 1M ammonium sulfate precipitation Western blot analysis of $\alpha$ CD22scFv using anti-FLAG-AP conjugated antibody. Lane 1: supernatant after 30 minutes of binding with Phenyl Sepharose resin; Lane 2: wash of Phenyl Sepharose resin after 30 minutes of incubation with supernatant. (b) Chitosan precipitation Western blot analysis of $\alpha$ CD22scFv using anti-FLAG-AP conjugated antibody. Lane 1: supernatant after 30 minutes of binding with Capto Q resin; Lane 2: wash of Capto Q resin after 30 minutes of incubation with supernatant. (c) Isoelectric precipitation at pH 4.5 Western blot analysis of $\alpha$ CD22scFv using anti-FLAG-AP conjugated antibody. Lane 1: supernatant after 30 minutes of binding with Capto Q resin; Lane 2: wash of Capto Q resin after 30 minutes of incubation with supernatant. ....	73
Figure 17. Purification of $\alpha$ CD22scFv after isoelectric precipitation and AXC. (a) Coomassie-stained SDS-PAGE of $\alpha$ CD22scFv. Lane 1: molecular weight marker (kDa); Lane 2: clarified algae extract; Lane 3: supernatant after isoelectric precipitation from pH 4.5 to pH 8.0; Lane 4: supernatant after 30 minutes of binding with Capto Q resin at room temperature; Lane 5: washing of Capto Q resin before elution; Lane 6-10: elution fractions by step-wise elutions with increasing concentrations of salt. (b) Western blot analysis of $\alpha$ CD22scFv samples run on SDS-PAGE using anti-FLAG-AP conjugated antibody. Black arrow indicates $\alpha$ CD22scFv. ....	75
Figure 18. Purification of $\alpha$ CD22scFv using Phenyl Sepharose resin as intermediate purification step after isoelectric precipitation and AXC. Coomassie-stained SDS-PAGE of $\alpha$ CD22scFv. Lane 1: molecular weight marker (kDa); Lanes 2-3: 1.2M ammonium sulfate elution fractions; Lanes 4-5: 1.0M ammonium sulfate elution fractions; Lanes 6-7: 0.8M ammonium sulfate elution	

fractions; Lanes 8-9: 0.6M ammonium sulfate elution fractions; Lanes 10-11: 0.4M ammonium sulfate elution fractions; Lanes 12-13: 0.2M ammonium sulfate elution fractions; Lanes 14-15: 0M ammonium sulfate elution fractions. Black arrow indicates  $\alpha$ CD22scFv. ....77

Figure 19. Western blot analysis of reduced  $\alpha$ CD22scFv using anti-FLAG-AP conjugated antibody after elution from Phenyl Sepharose resin as an orthogonal step to isoelectric precipitation at pH 4.5 and elution from Capto Q resin. Lane 1: molecular weight marker (kDa); Lanes 2-3: 1.2M ammonium sulfate elution fractions; Lanes 4-5: 1.0M ammonium sulfate elution fractions; Lanes 6-7: 0.8M ammonium sulfate elution fractions; Lanes 8-9: 0.6M ammonium sulfate elution fractions; Lane 10: 0.4M ammonium sulfate elution fractions. ....78

Figure 20. Coomassie-stained SDS-PAGE of highly concentrated  $\alpha$ CD22scFv after HIC as orthogonal chromatography step. Lane 1: molecular weight marker (kDa); Lane 2: concentrated pooled elution fractions (Lanes 2-5 from Figures 19 and 20). Black arrow indicates  $\alpha$ CD22scFv. ....79

Figure 21. Purification of  $\alpha$ CD22scFv using HAP as intermediate purification step after isoelectric precipitation and AXC. (a) Coomassie-stained SDS-PAGE of reduced  $\alpha$ CD22scFv. Lane 1: molecular weight marker (kDa); Lane 2: Pooled elutions from Capto Q resin; Lane 3: partially purified sample after buffer exchange into 5mM sodium phosphate pH 6.8; Lane 4: supernatant after 30 minutes binding with HAP resin; Lane 5: washing HAP resin before elution; Lanes 6-7: 200mM sodium phosphate pH 6.8 elutions; Lane 8-9: 500mM sodium phosphate pH 6.8 elutions. (b) Western blot analysis of  $\alpha$ CD22scFv using anti-FLAG-AP conjugated antibody on same samples as SDS-PAGE. ....80

Figure 22. Chromatogram of *Chlamydomonas reinhardtii* and pretreated lysate purified using AXC Capto Q resin. The chromatogram is plotted with absorbance at 280nm (mAU) and conductivity (mS/cm) against time (min). Sample Injection is marked by pink dashed line and each sample collected are labeled at the bottom of the chromatogram. ....82

Figure 23. Analysis of fractions collected by AktaPurifer after binding and elution to Capto Q column. (a) Western blot analysis of  $\alpha$ CD22scFv using anti-FLAG-AP conjugated antibody. Lane 1: molecular weight marker (kDa); Lane 2-10: Fractions collected from AktaPurifier. (b) Coomassie-stained SDS-PAGE of same samples on Western blot. ....83

Figure 24. Chromatogram of partially purified *Chlamydomonas reinhardtii*  $\alpha$ CD22scFv, by Capto Q resin, further purified using anti-FLAG affinity resin. The chromatogram is plotted with absorbance at 280nm (mAU)

against time (min). Injection of sample is marked by pink dashed line and fractions collected are noted at the bottom of the chromatogram. ....84

Figure 25. (a) Western blot analysis of concentrated  $\alpha$ CD22scFv using anti-FLAG-AP conjugated antibody. Lane 1: molecular weight marker (kDa); Lane 2: concentrated Fraction D5; Lane 3: 2X diluted pooled Fractions E8-E12; Lane 4: 4X diluted pooled Fractions E8-E12; Lane 5: 8X diluted pooled Fractions E8-E12; Lane 6: concentrated pooled Fractions D13-D14. (b) Coomassie-stained SDS-PAGE of concentrated  $\alpha$ CD22scFv purified with FLAG affinity chromatography. Lane 1: : molecular weight marker (kDa); Lane 2: concentrated Fraction D5; Lane 3: concentrated pooled Fractions E8-E12; Lane 4: 2X diluted pooled Fractions E8-E12; Lane 5: concentrated pooled Fractions D13-D14. ....85

Figure 26. Chromatogram of FLAG-purified Pfs25 separated by QA monolithic disk.105

Figure 27. Uptake experiment with Capto Q resin. Western Blot of  $\alpha$ CD22scFv using anti-FLAG-AP conjugated antibody. Lane 1: molecular weight marker (kDa); Lane 2: 10X diluted supernatant after centrifugation; Lane 3: 10X diluted supernatant after filtration through PES 0.22 $\mu$ m syringe filter; Lane 4: 10X diluted supernatant after dialysis; Lane 5: 10X diluted supernatant after 5 minutes of binding with Capto Q resin; Lane 6: 10X diluted supernatant after 15 minutes of binding with Capto Q resin; Lane 7: 10X diluted supernatant after 30 minutes of binding with Capto Q resin; Lane 8: 10X diluted supernatant after 60 minutes of binding with Capto Q resin. ....107

Figure 28. Uptake experiment with 1M ammonium sulfate and Phenyl Sepharose resin. Western Blot using anti-FLAG-AP conjugated antibody to detect  $\alpha$ CD22scFv. Lane 1: molecular weight marker (kDa); Lane 2: supernatant after centrifugation; Lane 3: supernatant of clarified lysate; Lane 4: supernatant after 1M ammonium sulfate precipitation; Lanes 5, 7, 9, and 11: supernatant after mixing with Phenyl Sepharose resin for 5, 15, 30, and 60 minutes; Lanes 6, 8, 10, and 12: 1<sup>st</sup> and 2<sup>nd</sup> CVs of washing column before elution; Lanes 13-17: elution fractions of resin mixed with clarified lysate for 60 minutes at room temperature..... 109

Figure 29. Uptake experiment with 1.5M ammonium sulfate and Phenyl Sepharose resin. Western blot analysis of  $\alpha$ CD22scFv, using anti-FLAG-AP conjugated antibody. Lane 1: supernatant of clarified lysate; Lane 2: Supernatant after 1.5M sodium phosphate precipitation; Lane 3: supernatant after 5 minutes of binding with Phenyl Sepharose resin; Lane 4: wash of Phenyl Sepharose resin after 5 minutes of incubation with supernatant; Lane 5: supernatant after 15 minutes of binding with Phenyl Sepharose resin; Lane 6: wash of Phenyl Sepharose resin after 15 minutes of incubation with

supernatant; Lane 7: supernatant after 30 minutes of binding with Phenyl Sepharose resin; Lane 8: wash of Phenyl Sepharose resin after 30 minutes of incubation with supernatant; Lane 9: supernatant after 60 minutes of binding with Phenyl Sepharose resin; Lane 10: wash of Phenyl Sepharose resin after 30 minutes of incubation with supernatant..... 112

Figure 30. 2D electrophoresis gel on FLAG-purified  $\alpha$ CD22scFv..... 113

## LIST OF TABLES

	Page
Table 1. Elution of calibration proteins from TSKGel G3000SWxl column from TOSOH. ....	41
Table 2. Effect of pretreatment method stage of implementation on residual DNA, chlorophyll, host cell protein, and $\alpha$ CD22scFv yield in algae extract. Values given are averages from 3 replicates $\pm$ standard deviations. <sup>a,b,c,d,e</sup> For each observation that do not share a common superscript letter are significantly different from the control no pretreatment ( $P < 0.05$ ). ....	72
Table 3. Purity and yield of $\alpha$ CD22scFv after each clarification/chromatography step. .	86

# CHAPTER I

## INTRODUCTION AND BACKGROUND

### 1.1 Introduction

Over the past 25 years, protein therapeutics has become the fastest growing sector in drug development. During this period, US Food and Drug Administration (FDA) have approved over 130 protein therapeutics including. These bio-therapeutics are produced in several heterologous protein expression systems each possessing advantages and disadvantages relating to ease of manipulation, cost of operation, and protein yield [1]. Protein-based therapeutics are produced in several different heterologous expression systems (mammalian, plant, and bacteria cell lines), each system possessing distinct advantages and disadvantages pertaining to the type of protein produced, the quantity and quality of protein, ease of manipulation, and cost of manufacture [1].

The chloroplast of eukaryotic green algae, *Chlamydomonas reinhardtii*, is a relatively new and unexplored recombinant production system. With simple and cheap growth requirements, short generation times, and a lack of human pathogens, prions, or other harmful toxins has shown algae to be a viable competitor to current production systems of recombinant therapeutic proteins. Our collaborators have shown that *C. reinhardtii* has the ability to correctly produce malaria transmission blocking vaccine candidate, *Plasmodium falciparum* surface protein 25 (Pfs25), and single-chained antibody fragment,  $\alpha$ CD22scFv [2, 3]. However, to truly be demonstrated as a viable

production system, recombinant proteins produced in the chloroplast of algae must be produced and purified at a competitive cost on a commercial scale.

This project addresses two main bioprocess challenges: (i) increasing recombinant Pfs25 accumulation in the chloroplast and characterize the extracted protein (Chapter II) and (ii) maximizing  $\alpha$ CD22scFv purity and yield using commercial grade chromatographic resins (Chapter III).

## **1.2 Background**

Utilizing microalgae as a platform for the production of recombinant protein production has grown in success over the past couple of decades. Human monoclonal antibodies [4, 5], human protein therapeutics [6], and subunit vaccines [7] have all been properly produced in the chloroplast of eukaryotic microalgae *C. reinhardtii*. However, there is little data available on the purification methods of the therapeutics. Because the most expensive portion of the total manufacturing cost of therapeutic proteins is the downstream processing, it is vital for recovery and purification of the protein to be highly selective and efficient.

### *1.2.1 Expression systems for recombinant protein production*

The most popular expression system for producing complex proteins and monoclonal antibodies are transgenic mammalian cells. However, mammalian cells necessitate complex growth media, specialized bioreactors, have poor oxygen and nutrient distribution, produce waste accumulation, require a long generation time, are

easily contaminated by pathogens, and cells have a high sensitivity to shear stress [8, 9]. These limitations force scientists to search for other platforms to correctly produce complex proteins quicker and cheaper [10]. Bacterial systems like *Escherichia coli* have a much faster doubling time than mammalian cultures, possess easily manipulated genomes, and are able to produce large quantities of recombinant proteins at very low cost [11]. Unfortunately, bacterial systems lack the machinery to properly fold complex proteins with disulfide bonds [12], a requirement for the correct folding of complex proteins. Transgenic plants, like tobacco and yeast, have also been explored as possible systems to produce high value proteins as they are free from human pathogens, less expensive than mammalian cells, resistant to most animal-infecting pathogens, and are capable of post-translational modifications. However, there have been reports linking plant-derived proteoglycans to allergic reactions [13], there is a risk of environmental contamination, and transgenic plants have slow growth cycles [14, 15].

Microalgae are being explored as an alternative protein therapeutic production platform as they have several advantages to mammalian, plant, and bacteria cell cultures. Compared to mammalian, plant, and bacteria expression systems, microalgae, specifically *C. reinhardtii* has several advantages as an alternative platform for recombinant proteins. The main advantages include: a short generation time, can be cultivated in enclosed bioreactors at a low cost, and possess the ability to fold complex human proteins due to chaperones and cellular machinery [16]. *C. reinhardtii* does not contain endotoxins, human pathogens, or any other known toxic compounds that are harmful to humans. Also, *C. reinhardtii* and several other green algae species have

GRAS (generally regarded as safe) status [17], permitting their formulation for oral or topical delivery of therapeutic proteins. To help offset the cost of algal biomass production, algae could co-produce triglycerides that can be used as a potential source of renewable fuel. However, several challenges arise when using microalgae as the platform for producing high-value recombinant proteins. These include recombinant protein recovery, protein stability, and the use of less expensive (non-affinity) chromatography methods for protein purification. All of these variables need to be fully understood to make an optimally-designed purification procedure.

#### **1.2.1.1 Microalgae as an expression system for high-value proteins**

The majority of current knowledge is established by using single-celled eukaryotic algae, *C. reinhardtii*, which is the most characterized genus of the microalgae species [18]. This strain allows recombinant proteins to be synthesized in the chloroplast, mitochondrial, and nuclear genomes [18]. Each genome has its own transcriptional, translation, and post-translational properties that make them unique. The organelle chosen for protein production is determined by the size and complexity of the protein structure along with the stability of the protein in the target site. Ideally, the location of protein accumulation would aid in protein functionality and ease of purification.

If expressed in the nucleus, recombinant proteins can either be targeted to go to the cytoplasm or secreted out of the cell through the endoplasmic reticulum and Golgi apparatus [19]. Nuclear gene expression allows regulated and tissue-specific expression, as well as posttranslational modifications including glycosylation [16]; however, for the

two proteins explored in this thesis, glycosylation of the protein will result in inactivation. Secretion of recombinant proteins is a common strategy in heterologous production systems [20, 21]. The microalgae *C. reinhardtii* is cultured in a water-like media, secretion of the proteins into the media will simplify purification as there are very few other impurities in the media[22]. However, recovering the secreted proteins from large volumes of media prove to be challenging, especially if the proteins have a small yield [23].

If proteins are synthesized in the chloroplast, they will also accumulate in the chloroplast. In algae grown non-photosynthetically, the chloroplast provides a protected intracellular space (~40% of the cell volume) that is non-essential to growth. The chloroplast has a higher level of accumulation than the other genomes because it is able to overexpress proteins and lacks gene silencing mechanisms that reduce recombinant protein production. Also, the chloroplast envelope may protect the protein from degradation [24]. Chloroplasts have multiple insertion sites and have the ability to process polycistronic transcripts allowing an entire gene cassette to be regulated by a single promoter.

### *1.2.2 Recovery and purification of high-value proteins (native and recombinant) from microalgae*

During cell disruption impurities such as DNA, proteases, chlorophyll, polysaccharides, alkaloids, phenolics, and other host cell proteins are released into the lysis buffer as well as the target protein. These impurities can diminish the final product

quality and yield by binding to or degrading the target protein. They can also reduce the purification efficiency due to membrane or resin fouling. Therefore, extraction conditions should try to reduce the impurities from the extract while providing a safe environment for the protein from proteolytic degradation.

#### **1.2.2.1 Primary protein recovery by precipitation**

During protein purification, after cell lysis, the next process should rapidly remove the protein of interest from other proteins and macromolecules in a cell extract. Most often, a precipitation step is implemented after cell lysis by altering the solvent conditions and the solubility differences between your protein and undesired proteins in the extract. In this thesis, three methods of precipitation will be tested for protein purification: ammonium sulfate, isoelectric, and polymer.

Knowledge of a protein's amino acid composition is essential to determine the ideal precipitation method. The solubility of a protein depends on the distribution of hydrophilic and hydrophobic amino acids on the protein's surface. A protein with a high percentage of hydrophobic amino acids on its surface will have low solubility in an aqueous solvent. When proteins are dissolved in a solvent, repulsive electrostatic forces are formed between proteins; these repulsive forces prevent aggregation and facilitate suspension. Solvent counterions travel towards the dissolved protein's charged surface, creating a firm solvation layer. Another layer of counterions forms next to the solvation layer but of a lesser concentration of counterions (Figure 1).



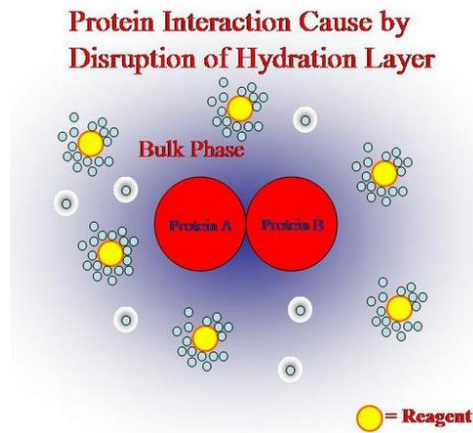


**Figure 2.** Protein interaction caused by disruption of hydrogen layer.

Several steps need to take place before a protein precipitate forms. First, a precipitating agent is added to the solution and thoroughly mixed. Enough mixing time is required for the molecules to diffuse across the fluid eddies and allow the precipitant and protein to collide. Next, submicroscopic sized protein particles are generated. Under Brownian diffusion control, the particles will begin to grow by colliding with other particles until the particles reach a critical size and begin dropping out of solution.

### **1.2.2.2 Fractionation by ammonium sulfate precipitation**

Ammonium sulfate precipitation, or salting out, is the most common method used to precipitate a target protein. Adding ammonium sulfate, a neutral salt, compresses the solvation layer and increases protein-protein interactions. The added salt interacts with the charges on the surface of the protein and exposes hydrophobic patches on the

surface of the protein, encouraging protein-protein attractive forces to surpass the repulsive forces between the proteins.

### **1.2.2.3 Fractionation by isoelectric precipitation**

The isoelectric point (pI) is the pH of the solution at which the net charge of a protein reaches zero. In a solution with a pH below the pI of the protein, the surface of the protein is predominantly positively charged and creates repulsive forces between like-charged proteins. Likewise, in a solution with a pH above the pI of the protein, the surface of the protein is predominantly negatively charged and repulsion between like-charged proteins occurs. However, at the pI the positive and negative charges cancel, resulting in a net charge of zero on the surface of the protein. With a net charge of zero, repulsive electrostatic forces are reduced and the attraction forces dominate between proteins resulting in precipitation of proteins (Figure 3). However, the greatest disadvantage of isoelectric precipitation is the irreversible denaturation of proteins. Therefore, this precipitation is most often used to precipitate contaminant proteins rather than the target protein.

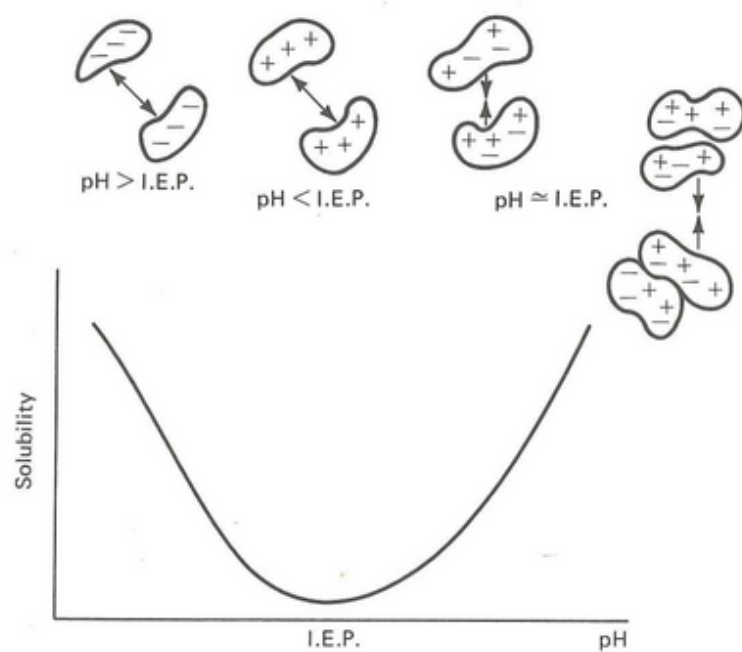


**Figure 3.** Solubility of a globulin-type protein close to its pI.

#### 1.2.2.4 Fractionation by polymer precipitation

Chitosan is a cationic linear polymer of beta-(1-4) linked D-glucosamine monomers is generated by chemical deacetylation of chitin [25-27]. The polymer is a natural polyelectrolyte that becomes charged when dissociated in an aqueous solution. The charge on the polymer is electrostatically attracted to the surface of proteins with the opposite charge, creating a bridging effect (Figure 4). Many factors affect polymer precipitation with the protein, including: the charge, molecular weight, and concentration of the polyelectrolyte, ionic strength, pH, and concentration of proteins in the solution [28].

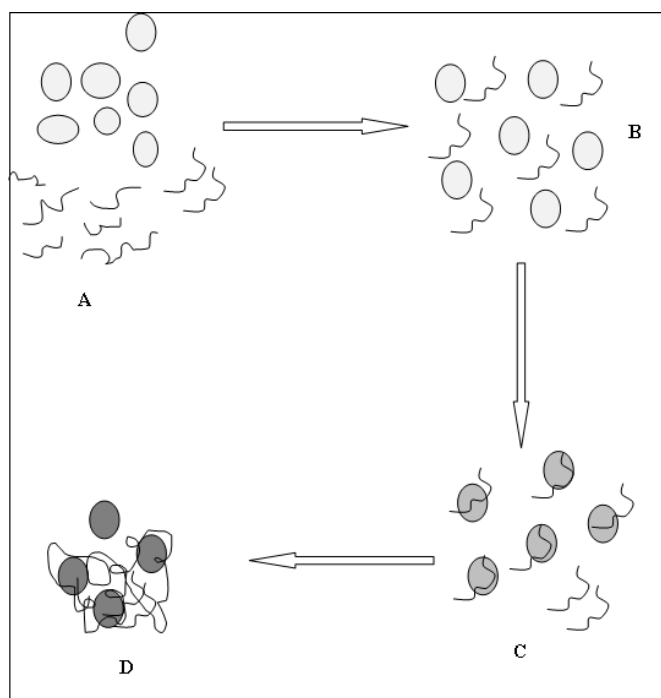


**Figure 4.** Mechanism of polymer precipitation.

### 1.2.2.5 Purification of native and recombinant proteins

Chromatography methods have been used for the purification of phycobiliproteins produced and recovered from blue-green algae, *Spirulina platensis*, and red algae species, *Porphyridum cruentum* and *Coralline elongate* [29-31]. For purification of C-phycoyanin and allophycoyanin from *Spirulina*, 70% ammonium sulfate precipitation was used to precipitate all proteins. The pellet was resuspended and purified by two chromatography steps (size exclusion using Sephadex G-100, followed by ionic exchange process using DEAE cellulose column) [30].

The purity ( $A_{620}/A_{280}$  ratio) of C-phycoyanin reached was 2.87 with a yield of 31 mg/g of dry *S. platensis*. Likewise, 32 % of B-phycoerythrin and 12 % of R-

phycoerythrin present in the biomass of red algae *P. cruentum*, were recovered and purified using one step anionic chromatography (DEAE cellulose column).

Furthermore, the phycoerythrin from the *Coralline elongate* species was purified with a simple process and low cost resin (hydroxyapatite chromatography resin), which allowed ~ 0.06 % recovery of purified biliprotein with a purity index of  $A_{566}/A_{280} = 6.67$ ,  $A_{566}/A_{495} = 1.44$  and  $A_{620}/A_{566} = 0.001$ . The ratio of the absorbance values indicate high purity and identity of the biliprotein with respect to other contaminant proteins in the sample [31].

Large scale recovery and purification of C-phycoerythrin from inferior *S. platensis* was performed in three steps using phenyl-Sepharose chromatography in an expanded bed adsorption column for protein recovery, followed by anion-exchange chromatography, and in the last step hydroxyapatite chromatography for purification [32]. Expanded bed chromatography with Streamline-DEAE was also tested to purify C-phycoerythrin; successfully demonstrating scalability and reduced cost [29].

There are only few examples of purification of recombinant proteins produced in the chloroplast of *C. reinhardtii* and those rely on affinity tags, such as MAT and FLAG [2-4]. The two proteins studied in this thesis contain a FLAG-tag, making purification using FLAG affinity chromatography easy and highly specific [2, 4, 16]. Binding of the FLAG-tagged recombinant proteins is accomplished during batch binding on a small scale by mixing the clarified lysate and FLAG-affinity resin. After the recombinant proteins are absorbed onto the FLAG-affinity resin, the resin was washed to

remove non-specific binding proteins from the column and then eluted the FLAG-tagged recombinant proteins off the resin using an elution buffer at a low pH [2, 16].

Using FLAG-affinity resin to purify recombinant proteins from clarified lysate is not a scalable solution for several main factors: (i) the resin cannot handle high pressure necessitating the lysate to be loaded onto the column under gravity flow; (ii) the resin extremely expensive; and (iii) the binding capacity of the resin is only 0.6mg/mL requiring a large bed volume, increasing the volume of washing and elution buffers. FLAG-affinity resin is more suitable as an analytical tool in batch purification methods for FLAG-tagged proteins from cell lysates.

Other resins will need to be scouted to identify resins that are scalable, economical, and provide minimal losses of the target protein. Several types of non-affinity chromatography are available for commercial processes: reverse-phase chromatography, ion exchange chromatography (IEX), size exclusion chromatography (SEC), hydrophobic interaction chromatography (HIC), mix-mode chromatography columns. Pre-packed disposable chromatography columns are also possible alternatives to reduce production costs.

### **1.3 Objectives**

The overall objective of this research is to further investigate the practicality of using the chloroplast of *C. reinhardtii* as a competitive production system for recombinant proteins. This project will characterize high molecular weight Pfs25 proteins reported by Mayfield and Vinetz's laboratories [2, 33]. Then, a purification

process on  $\alpha$ CD22scFv will be designed using pretreatment methods explored previously by our lab [34]. The specific objectives of this research are:

1. Increase Pfs25 accumulation in the chloroplast of *C. reinhardtii*.
2. Determine the size and stability of Pfs25-aggregates.
3. Compare effects of pretreatment methods on  $\alpha$ CD22scFv adsorption to Capto Q and Phenyl Sepharose resins.
4. Scout Phenyl Sepharose and hydroxyapatite resins as possible intermediate chromatography steps.
5. Determine purity and yield of  $\alpha$ CD22scFv after isoelectric precipitation at pH 4.5, anion exchange chromatography, and FLAG-affinity polishing step.

#### **1.4 Thesis organization**

This thesis is arranged into chapters. Each chapter begins with an introduction of the main findings concerning the specific chapter; followed by previous work and the purpose of the study. A material and methods section follows the introduction in Chapters II and III and is concluded with a presentation of the results and a discussion of the main findings.

Chapter I: titled “Introduction and literature review” begins with an introduction of the overall work presented in this thesis. A literature review covering basic concepts and background of the topics studied follows the introduction. Chapter I concludes with objectives and organization of the thesis.

Chapter II: titled “Increased accumulation and characterization of Pfs25 produced in chloroplast of *Chlamydomonas reinhardtii*” includes a literature review on the progression of Pfs25 expression and purification. This chapter focuses on purifying and characterizing Pfs25 from the chloroplast of *C. reinhardtii* as a possible “model” protein to evaluate downstream processing technology.

Chapter III: titled “Development of a purification train for recombinant protein produced in *C. reinhardtii*” begins with a literature review on the single chain antibody fragment ( $\alpha$ CD22 scFv) along with previous work on different primary recovery methods for clarification of algae extract. This chapter evaluates the effectiveness of different primary recovery methods on further downstream processing.

Concluding the thesis, chapter IV: titled “Conclusions and recommendations” states the main findings of the study and recommendations for future work.

## CHAPTER II

### INCREASED ACCUMULATION AND CHARACTERIZATION OF PFS25 PRODUCED IN THE CHLOROPLAST OF *CHLAMYDOMONAS REINHARDTII*

#### 2.1 Overview

Decades of research have been devoted to the development of a malaria vaccine that not only addresses morbidity but the transmission of the disease as well. One of the leading transmission blocking vaccines (TBVs) is the *Plasmodium falciparum* surface protein 25 (Pfs25). Due to the high cost of vaccines, various expressions are being explored to successfully produce active vaccines at the lowest price possible. Algae is an attractive and relatively unexplored production platform because of its simple and inexpensive growth requirements, short generation time, and absent of human pathogens, prions, or other harmful toxins. The chloroplast of *Chlamydomonas reinhardtii* has been proven to successfully fold recombinant proteins, including the complex structure of Pfs25. Steven Mayfield and Joseph Vinetz's laboratory both reported high molecular weight bands seen on Western blots when reacted with Anti-Pfs25-4B7 monoclonal antibody (mAb). This current study is aimed at enhancing the current production level of Pfs25 1.7-fold by resuspending the culture in fresh media before light induction. Also, the Pfs25-aggregates were characterized and found to range from 25 to 600 kDa in size. The aggregates proved to be stable in the presence of reducing agents and detergents. Thus, the chloroplast of *C. reinhardtii* is a promising production platform for Pfs25 and the aggregates should be further investigated for possible immunogenicity and TBA.

## **2.2 Introduction**

### *2.2.1 Malaria disease*

Malaria is an infectious and parasitic disease that has claimed the life of millions of children and adolescents, the leading cause of morbidity and mortality worldwide. Rainfall, consistent high temperatures, high humidity, and stagnant waters provide a breeding ground for mosquitos in tropical and subtropical regions. In poverty-stricken countries, there are limited resources to combat the disease, resulting in many lives lost. Without a proper labor force, the country is unable to develop, preventing the country from growing economically, keeping the country poor and unable to buy supplies to keep their citizens disease free (a vicious cycle). Many attempts to eradicate malaria have been made over the past couple hundred years, starting with natural remedies and evolving to sophisticated medicinal therapies. Since the 1600s, quinine, a material acquired from the bark of a cinchona tree, has been known to be effective against malaria [35]. After the transmission of malaria was better understood, scientists believed that by focusing on destroying the vector the cycle of infection could be halted. Thus, DDT and other insecticides began being used to kill mosquitoes; however, insecticide-resistant mosquitoes and drug-resistant parasites have forced the development of malaria vaccines.

To completely eradicate malaria, the life cycle of the disease must be fully understood. Malaria is caused by the parasite *Plasmodium*, a single-celled organism that has multiple life stages and requires more than one host for its survival. When a mosquito infected with malaria feeds on a human, the parasite, in the mosquito's saliva

glands, enters the human's body as a sporozoite. The sporozoite travels directly to the human's liver where it infects the liver cells and undergoes rounds of asexual reproduction to produce merozoites; one sporozoite can asexually reproduce to form 40,000 merozoites. A high concentration of merozoites can seriously challenge a human's immune system's ability to battle the parasite. The merozoites leave the liver and enter into the bloodstream and infect healthy red blood cells. In the red blood cells, the merozoites asexually reproduce hundreds of new merozoites. The merozoites burst the red blood cell and are released back into the blood stream, infecting more healthy red blood cells. It is during this phase that some merozoite-infected blood cells will stop asexually reproducing and instead mature into sexual forms of the parasite: male and female gametocytes. When a female *Anopheles* mosquito ingests the gametocytes during a blood meal, the gametocytes form gametes upon entering the midgut of the mosquito, which then fuse to form zygotes and are then transformed into elongated motile ookinetes. The ookinetes cross the mosquito's midgut and are transformed into spherical oocysts. Every surviving oocyst produces thousands of sporozoites which migrate to the mosquito's salivary glands and infect another human host during the next blood meal [36]. Malaria vaccines are being developed against different stages in the parasite's life cycle: sporozoite also referred to pre-erythrocytic (the liver stage, or the stage before the parasite infects red blood cells), asexual (when the parasite is infecting red blood cells), and sexual stage (when the parasite has been taken up by the mosquito during a blood meal and is being reproduced in the midgut of the mosquito) [37]. Sporozoite vaccines are designed to prevent mosquito-induced infection [38]. Targeting the asexual stage is

designed to prevent infection and to reduce disease severity. However, targeting the sexual stage blocks the transmission of the disease from mosquito to human hosts by inducing antibodies in the human host [37].

Even though there are several different anti-malaria drugs are under development targeting different stages of the parasite, there are many hurdles for the vaccine candidates to become a viable tool against the eradication of malaria. The countries that have a high rate of mortality due to malaria do not have many proper medical facilities and many citizens do not have access to them, either due to money or distance to the facility. Therefore, there is a great need to produce a malaria vaccine that is low cost and scalable production, with high, correctly folded, protein yields. The vaccine must also be able to travel long distances, without refrigeration, without losing its specificity. Then, once the vaccine arrives at its destination, it must be easily administered, either orally as a heat-stable capsule or as a nasal-spray, to prevent further infections due to misadministration or poor hygiene. The successful vaccine must completely adhere to all of these criteria.

Two main malaria vaccines have been developed by scientists, each targeting different life stages of the parasite: the sporozoite and sexual stage of the parasite (unfortunately there are no successful vaccines that target the asexual stage). The RTS,S vaccine is a vaccine that targets the sporozoite stage of the parasite's life cycle. The aim of this vaccine is to either prevent the sporozoites from entering into the liver cells or to destroy infected liver cells. RTS,S is in Phase III of clinical trials and have had very promising results. Children ages 5-17 months showed a reduced risk of clinical malaria

and severe malaria by 56% and 47%, respectively [39]. However, in infants ages 6-12 weeks only 33% had fewer episodes of both clinical and severe malaria [40]. Currently, scientists are working on improving the efficacy of the RTS,S vaccine to at least 50% effective by employing boost technology, adjuvants, and antigen optimization. The second vaccine is known as a transmission blocking vaccine (TBV), developed to prevent the sexual stage parasites from undergoing successful sporogonic development in the midgut of mosquitoes, stopping the transmission from human to mosquito and subsequent spread of the parasites [41]. One TBV candidate vaccine, Pfs25-EPA, is being developed by US National Institute of Allergy and Infectious Diseases Laboratory of Malaria Immunology and Virology and Johns Hopkins University Center for Vaccine Research. TBVs do not directly protect vaccinated individuals from infection; they only contribute to elimination of the disease. Therefore, by combining TBVs with vaccines targeting other stages of the infection the transmission of parasites that have escaped the immune response could be better prevented [42]. Recently, the Malaria Eradication Research Agenda Consultative Group on Vaccines has set as a core goal that any malaria vaccine program needs to reduce transmission as well as morbidity [43]. Therefore, only vaccines targeting the sexual stage of the parasite are being investigated in this study.

There are five species of the parasite known to cause disease in humans:

*Plasmodium falciparum*, *P. vivax*, *P. ovale*, *P. malariae*, and *P. knowlesi*. Of the five *Plasmodium* species, *P. falciparum* causes the highest mortality rate and *P. vivax* causes the highest morbidity rate. Even though all the species of the parasite must be addressed to completely eliminate malaria, only TBV candidates targeting *P. falciparum* will be

studied. The long-term success of a TBV depends upon induction of high functional antibody titers in order to effectively block the parasite transmission cycle. In *P. falciparum* three antigens have been identified whose antibodies have the ability to effectively reduce malaria transmission: Pfs230, Pfs48/45, and Pfs25 [44-49]. Of the three target antigens, Pfs25 has shown the most significant progress in clinical trials.

Pfs25, with a molecular mass  $M_r$  25,000 (25K), is the leading TBV candidate. This protein is expressed on the zygotes and ookinetes during the sexual stage of the *P. falciparum* life cycle. Pfs25 is a flat triangular molecule having four epidermal growth factor (EGF)-like motifs. The vaccine also possesses 22 conserved cysteines in the oxidized form creating eleven disulfide bonds buried within the protein [36] (a crucial element in the stability of this surface protein). Most importantly the protein possesses a C-terminal glycosylphosphatidylinositol (GPI) moiety anchoring the protein to the parasite surface [47, 50, 51]. Therefore, the protein must remain un-glycosylated to maintain its activity.

### 2.2.2 Production systems for Pfs25

The first platform explored as a possibility of producing Pfs25 was *Escherichia coli*, chosen for its ease and low overall costs. The bacteria produced an abundant amount of recombinant protein in the form of inclusion bodies. However, the transmission blocking antibodies to Pfs25 did not recognize the resulting fusion protein, revealing that the important conformational target epitopes were not recreated. Pfs25 was injected into mice and rabbits to determine if the protein would provoke an immune

response. The animals elicited antibodies that recognize the native protein; however, it failed to block transmission [52]. However, very recently, codon harmonization of the coding-gene sequence has allowed scientists to successfully express and purify recombinant Pfs25 protein from inclusion bodies upon resolubilization and successful refolding. Codon-harmonized recombinant Pfs25 elicited high titers of specific antibodies capable of recognizing Pfs25 protein in the mosquito midgut along with potent TBA in mice [53].

The first efforts to produce large quantities of recombinant Pfs25 were made using *Saccharomyces cerevisiae* in 1991 in California [48]. Barr et al. removed the glycosylation sites of the encoded protein to facilitate secretion from the yeast; this protein was labeled as Pfs25-B. The protein was purified using ion-exchange chromatography (IEX) on Fast Flow Q resin then by gel filtration on S-100 HR Sepharose. The purified protein was analyzed by immunoblotting using rabbit polyclonal antisera to Pfs25 and with mAb 1C7, a transmission blocking (TB) mAb that only recognizes natural Pfs25 under nonreducing conditions. The purified protein was conjugated with the muramyl tripeptide (MTP) adjuvant MF59 to immunize mice and monkeys. Even though Pfs25-B was only partially conformationally correct (based on weak interactions with mAb 1D2 and P7), the protein was still able to elicit TB antibodies in both the mice and monkeys. Kaslow continued Barr's work and adsorbed Pfs25-B to alum to induce TB antibodies in both mice and monkeys [54]. He also reported that the antisera to Pfs25-B adsorbed to alum appeared to block the in vivo development of zygotes to ookinetes, compared to mAbs to Pfs25 which block

transmission only after ookinete development. To overcome potential production problems with Pfs25-B, three modifications were made to create a second generation malaria TBV candidate:(1) the last cysteine residue of the fourth EGF-liked domain was added back in, (2) three of the four potential N-linked glycosylation sites were mutated by substituting glutamine for asparagine residues, and (3) a six histidine tag was added to the carboxy-terminus for ease of purification and detection [55]. Because the transmission-blocking vaccine was based on Pfs25 with a histidine tag, the protein was renamed TBV25H. Affinity chromatography using a nickel nitrile-triacetic acid (Ni-NTA) agarose resin and Sephadex-75 size exclusion chromatography (SEC) was used to achieve highly purified TBV25H. After three doses of 5 µg alum-adjuvanted TBV25H, the mice developed Abs to TBV25H and elicited TBA, significantly suppressing oocyst development [55]. TBV25H vaccine candidate was tested on mice, rabbits and monkeys, all of which induced TB Abs [49, 54, 56]. After taking TBV25H to Phase I clinical trials, it was found that humans elicited an immune response, but the antibody titers were too low to continue [57]. It was hypothesized that the Phase I clinical trials in humans were unsatisfactory because Pfs25H, purified by Ni-NTA chromatography, was a mixture of two structural conformers, Pfs25H-A and Pfs25H-B. Zou et al. further purified the secreted protein using Ni-NTA Superflow, phenyl Sepharose hydrophobic interaction chromatography (HIC) column, and a Superdex 75 SEC to separate the two conformers [58]. Only ScPfs25H-A was strongly recognized by conformation-dependent mAbs, 1D2 and 4B7, and it elicits TB antibodies in mice. However, Pfs25H-A is less than 1% of the total Pfs25H; therefore, to improve the production levels of Pfs25H-A,

the recombinant protein was produced and secreted from the yeast *Pichia pastoris*, PpPfs25H-A. Identical to *S. cerevisiae*, two structural conformers were produced and purified in *P. pastoris*. Even though the yield of PpPfs25H is comparable to ScPfs25H, 60% of PpPfs25H is the correctly-folded PpPfs25H-A (characterized using monoclonal anti-Pfs25H antibody 1D2 and 4B7) [58]. When PpPfs25H-A proceeded to Phase I human trials, with Montanide ISA 51 as an adjuvant, the vaccine elicited significant antibody titers and high levels of TBA in the human volunteers [59]. However, there were several cases of erythema nodosum and leukemoid reactions causing the trials to cease [59]. Montanide ISA 51 was previously believed to be generally well tolerated in human trials, but because of the adverse effects of PpPfs25/ISA 51, only human use-compatible adjuvants are being considered as possible carrier proteins. A series of studies were performed to improve the immunogenicity and TBA of PpPfs25H-A by chemically conjugating the protein to different carrier proteins. PpPfs25H-A was chemically conjugated to the outer-membrane protein complex (OMPC) of *Neisseria meningitidis* serogroup B by Wu et al.; they reported the induction of high, continual levels of Ab responses in mice, rabbits, and rhesus monkeys [60]. It was also reported that there was a rapid boost response in rhesus monkeys (already primed with PpPfs25H-OMPC) with nonconjugated PpPfs25H [60]. At the same time, Kubler-Kielb et al. reported that by conjugating PpPfs25H to itself, recombinant *Pseudomonas aeruginosa* endotoxin A, or ovalbumin, long-lasting and high levels of TB antibodies were induced in mice after three injections (2.5 µg Pfs25 conjugate per injection) [61]. Qian et al. conjugated PpPfs25H to the mutant, nontoxic *Pseudomonas aeruginosa* ExoProtein A

(EPA) and reported a 1,000-fold increase in Ab titers and significantly higher TBA in mice after two injections of only 0.5  $\mu$ g of PpPfs25-EPA [62]. To further the initial results of Qian et al., Shimp et al. characterized PpPfs25-EPA to better understand its potential for increased immunogenicity and its safety profile in humans [63]. Shimp found that the soluble PpPfs25-EPA conjugate appeared to be a spherical nanoparticle (~600kDa) and increased specific Abs in mice 75-110 fold when adsorbed on Alhydrogel® [63]. By adding CPG 7909 to PpPfs25-EPA conjugates formulated on Alhydrogel®, the specific antibody responses in mice further increased, resulting in Ab levels much higher than what was required for TBA [64]. PpPfs25-EPA, administered with Alhydrogel® was administered to humans in a Phase 1 clinical trial [65]. It was seen that Pfs25-EPA/Alhydrogel was well tolerated in humans and increased the immunogenic response with each successive dose, inducing Ab titers that correlated with TBA [65].

Through extensive studies, it was found that *P. falciparum* has is unable to form N-glycosylations and O-linked glycosylation is almost undetectable [66, 67]; therefore, the addition of N- or O-linked carbohydrates on recombinant malaria vaccine proteins is undesirable. Even though the N-glycosylation sites were removed from Pfs25 to facilitate secretion from yeast, the level and position of O-glycosylation in *P. pastoris* is impossible to predict due to the mannose residues added to the protein while moving through the endoplasmic reticulum (ER). The Malaria Vaccine Development Branch at the National Institute of Allergy and Infectious Disease in the US showed that overproduction of *P. pastoris* protein disulfide isomerase significantly reduced the level

of glycosylation in Pfs25 while also increasing the quantity of Pfs25 secreted by 3-fold, providing evidence of unintended glycosylation of Pfs25 in *P. pastoris* [68]. To enhance the immunogenicity with long-lasting TBA of the vaccine candidate and prevent O-linked glycosylation due to Pfs25 moving through the ER, the Fraunhofer USA group successfully produced four recombinant, full-length, 6× His-tagged Pfs25 proteins produced in *Nicotiana benthamiana* (non-secreted): (1) a glycosylated (wild-type) protein (Pfs25F1E), (2) a non-glycosylated (mutant) protein (Pfs25MF1E), (3) a glycosylated protein fusion to the modified lichenase carrier molecule (LicKM) (Pfs25F3E), and (4) a non-glycosylated protein fusion to LicKM (Pfs25MF3E) [69]. After immobilized metal affinity chromatography (IMAC), IEX, and hydrophobic interaction chromatography (HIC), the purified protein was analyzed by SDS-PAGE and an immunoblot probed with an anti-His mAb, both revealing one prominent band. The biochemical and biophysical characterization of the Pfs25 constructs was analyzed by N-terminal sequencing, *in vitro* de-glycosylation reactions, electrospray ionization mass spectroscopy (MS) mass determination, Coomassie-stained SDS-PAGE, and size-exclusion chromatography combined with multi-angle laser light scattering (SEC-MALLS) to show that each construct had greater than 90-95% purity. Serum samples from immunized mice were analyzed by ELISA for Pfs25-specific IgG responses and TBA was determined by running a standard membrane feeding assay (SMFA) on the serum samples. It was determined that mice immunized with Pfs25MF1E, Pfs25F3E, or Pfs25MF3E with Alhydrogel® as an adjuvant generated Abs that resulted in 97-100% reduction in the number of oocysts and mean oocyst reduction of 47% [69]. By

introducing mutations into the LicKM carrier molecule, the non-glycosylated version of the Pfs25-based subunit vaccine, Pfs25-FhCMB, was further optimized [70]. Pfs25-FhCMB was purified using a three-column chromatographic method: IMAC, HIC, and IEX. Analysis by SDS-PAGE under reducing conditions revealed a single band; analytical reverse-phase chromatography (RPC) provided a  $\geq 95\%$  purity; and target identity was confirmed by western blotting using anti-Pfs25, anti-LicKM, and anti-4 $\times$ His Abs. Serum samples were tested for Pfs25-specific IgG responses using ELISA and for TBA using SMFA. These tests proved that Pfs25-FhCMB elicits long-lasting and potent TBA in mice and rabbits [70].

Microalgae *C. reinhardtii* offers several advantages to current TBV expression systems. Not only are they generally recognized as safe (GRAS) by the US Food and Drug Administration (FDA), inexpensive, and easily scalable, but their lack of human pathogens, prions, or other harmful toxins reduces the risk of residual contamination following purification. Mayfield's lab in San Diego, California demonstrated that the chloroplast of *C. reinhardtii* could produce correctly folded Pfs25 that was recognized by TB mAb, 4B7 [2]. This was accomplished because the chloroplast lacks the machinery for post-translational glycosylation (a huge advantage for production of Pfs25) and contains nuclear encoded chaperones that assist in the correct folding of the complex EGF-like domains [71]. To overcome the poor immunogenicity of Pfs25, Gregory fused Pfs25 with cholera toxin beta subunit (CTB) and orally delivered the fusion to BALB/c mice. CTB-Pfs25 elicited CTB specific IgG antibodies and secretory IgA antibodies to both CTB and Pfs25. However, Pfs25 IgG antibodies are needed for

TBA during a mosquito blood meal, not IgA. Therefore, different adjuvants need to be explored to increase Pfs25-specific IgG antibodies. Due to erythema nodosum and leukemoid reactions being observed in humans during the Phase I clinical trial of Montanide ISA 51 oil-in-water adjuvant [59], only human use-compatible adjuvants are being explored, regardless of the heterologous expression system. Joseph Vinetz's laboratory compared rPfs25 with four different human compatible adjuvants (alum; TLR4 agonist (glucopyranosyl lipid A, GLA) plus alum; squalene oil-in-water emulsion; and GLA plus squalene oil-in-water emulsion) and compared their ability to induce malaria TBAs. They found that rPfs25 plus GLA plus squalene oil-in-water adjuvant induced the highest titer and avidity IgG antibodies [33]. Vinetz reported a Western immunoblot of affinity purified Pfs25 reacting with 4B7 (anti-Pfs25) at 25, 50, and 75 kDa markers, under non-reduced conditions; Gregory also reported that even higher molecular weight proteins were found in the purified sample, between 100 and 130 kDa, under the same conditions [2, 33]. Based on the data indicating that self-conjugated Pfs25 as well as other conjugated constructs elicit a higher immunogenic response than Pfs25 monomeric form, in this study we extended the work of Gregory et al. (2012) and Vinetz et al. (2015) with the objectives to increase accumulation of Pfs25 in *C. reinhardtii* biomass and characterize Pfs25-produced protein forms (aggregates).

## 2.3 Materials and methods

### 2.3.1 Gene constructs for Pfs25

The Pfs25 gene construct was designed by our collaborators at the University of California in San Diego. In the construct, the endogenous psbA locus was replaced by Pfs25 by direct homologous recombination. Thus, transgene expression in these strains is regulated by the psbA promoter and the 5' and 3' untranslated regions (UTRs) and, therefore, is light inducible. A kanamycin resistance cassette was incorporated for selection. The gene cassette was ligated with a sequence coding for a 1xFLAG peptide (DYKDDDDKS) and separated by a sequence that encodes a tobacco etch virus (TEV) protease cleavage site (ENLYFQG) [71].

### 2.3.2 Cultivation of recombinant Pfs25 *Chlamydomonas reinhardtii* strains

Algal biomass from a single agar plate (Tris-Acetate-Phosphate (TAP) agar with 150 µg/mL kanamycin) was transferred to 100 mL of TAP media without kanamycin and grown for 3 days. A subsequent volumetric culture scale up was performed using 10% inoculum in the exponential phase (100 mL) in 1 L of fresh TAP media containing 25 µg/mL kanamycin. One-liter cultures were grown heterotrophically for 5 days, reaching  $\sim 4$  to  $5 \times 10^5$  cells/mL. For resuspension experiments at the end of the fifth day, the biomass from 1-L cultures was resuspended in 1-L of fresh TAP media containing 25 µg/mL kanamycin and grown for 1 day, reaching about  $10^6$  cells/mL. The latter cultures were then exposed to light at a photon irradiance of  $300 \mu\text{mol m}^{-2} \text{s}^{-1}$  to induce recombinant protein synthesis. Control experiments without resuspension were

performed under the same time and light regimes. For each recombinant protein, three replicate batches were grown in different conditions (resuspension vs. non-resuspension) followed by light induction. Cell growth and cell concentration were monitored daily by counting cells using a hemocytometer (Bright Line, Hausser Scientific, Horsham, PA, USA) and by measuring the optical density at a 750-nm wavelength using a DU640 spectrophotometer (Beckman Coulter, Brea, CA, USA).

### 2.3.3 Protein Extraction

*C. reinhardtii* cultures producing recombinant proteins were grown in liquid media until they reached the desired cell concentration of  $\sim 10^6$  cells/mL. At the end of the light exposure period, cells were harvested by centrifugation at  $10,000\times g$  for 15 min at 4°C. Pelleted algal biomass was washed with fresh TAP media, weighed and then resuspended at a 1:5 biomass-to-lysis buffer ratio (50 mM Tris-HCl, 400 mM NaCl and 0.5% Tween, pH 8.0). The buffer contained a complete protease inhibitor cocktail (Roche, Mannheim, Germany) dissolved in 200 mL of the buffer. Algal cells were lysed by sonication for 8 min with 30 s on/off intervals at 4 °C using a sonicator (Sonifier 250, Branson, Danbury, CT, USA) at 30% output control and 30% duty cycle with a micro probe (1/8" microtip A3-561 Branson, Danbury, CT, USA). Cell lysates were centrifuged ( $10,000\times g$  for 10 min) to produce clarified crude extracts.

#### 2.3.4 Protein Analysis

Filtered algal crude extract and purified samples were analyzed by SDS-PAGE and Western blot, and the total eluted protein was determined by the Bradford assay [18]. Total soluble protein from crude extracts and purified samples were quantified using the microplate protocol (working range from 1 to 25  $\mu\text{g}/\text{mL}$  and 25 to 1,500  $\mu\text{g}/\text{mL}$ ) Coomassie plus (Bradford) assay kit (Thermo Scientific, Waltham, MA, USA). Absorption at 595 nm was measured using the VERSA max microplate reader (Molecular Devices, Sunnyvale, CA, USA).

NuPAGE Novex Bis-Tris pre-cast gradient gels (4%–12%) from Invitrogen™ (Carlsbad, CA, USA) (1.5 mm  $\times$  10 wells), were used for SDS-PAGE electrophoresis. Reducing buffer was prepared using lithium dodecyl sulfate (LDS) sample buffer (4 $\times$ ) (NuPAGE) containing 10% of reducing agent. Reduced samples were prepared using a 1:4 reducing buffer to sample ratio and heated at 70 °C for 10 min. MES SDS Running Buffer (20 $\times$ ) stock solution was used to prepare 1 $\times$  running buffer in reverse osmosis (RO) water. Antioxidant (NuPAGE, Invitrogen™, Carlsbad, CA, USA) was added to ensure reduced samples during electrophoresis. Gels were run for 35 min at a constant voltage (200 V). For SDS 25 analysis, the gels were blocked with a solution of 50% RO water, 40% ethanol, 10% acetic acid for 45 minutes. Then, the gels are rinsed with RO water and stained in Coomassie™ (Thermo Fisher Scientific, Waltham, MA, USA) G-250 stain for 3 hours. The gels are finished by destaining in RO water. For western blot analysis, the gel was transferred to nitrocellulose membranes using the iBlot® 7-Minute Blotting System, Life Technologies Corporation (Carlsbad, CA, USA).

After protein transfer to a nitrocellulose membrane, the membrane (free sites) was blocked with 2.5% non-fat milk in TBS containing 0.05% Tween 20 at pH 7.5 buffer for 1 h to prevent nonspecific binding of the detection antibodies. FLAG-tagged recombinant proteins ( $\alpha$ CD22scFv and Pfs25) were detected by using anti-FLAG M2-AP (alkaline phosphatase conjugated) antibody from Sigma Aldrich (St. Louis, MO, USA) at a concentration of 1:2000. After incubation with the antibody for 1 h, the membrane was washed with TBS containing 0.05% Tween 20 at pH 7.5; buffer and blots were visualized (developed) with nitro-blue tetrazolium (NBT) and 5-bromo-4-chloro 3'-indolyphosphate p-toluidine salt (BCIP) (Sigma FAST, St. Louis, MO, USA) dissolved in 10 mL of filtered RO water.

### *2.3.5 FLAG-affinity capture and purification*

Crude extracts were filtered using a polyethersulfone (PES) 0.45- $\mu$ m filter and mixed with anti-FLAG affinity resin (Sigma Aldrich A4596, St. Louis, MO, USA) equilibrated in the same lysis buffer used for protein extraction. Approximately 1 mL of resin was used per every 4 g of wet algal biomass. Binding of the recombinant protein to the affinity resin was performed for 2 h at 4 °C by continuous end-over-end mixing in a Glas-Col rotor (Glas-Col LLC, Terre Haute, IN, USA) at ~33 rpm (40% speed control). After the incubation period, the affinity resin was transferred into Bio Spin disposable chromatography columns (Bio Rad, Cat No. 732-6008, Hercules, CA, USA) for protein elution at room temperature. Affinity resin was washed with 10 column volumes (CVs) of lysis buffer without Tween 20. Recombinant protein was eluted using 5 CV of 100

mM glycine buffer, pH 3.5, which contained 400 mM NaCl. Eluted protein fractions were collected in 5 tubes containing a predetermined amount of 1M Tris-HCl, pH 8.0, to immediately increase the pH of the eluted protein and avoid protein denaturation. Typically, three elution fractions (E2 to E4) were used for the estimation of purity and yield, although some losses occurred by not taking into account E1 (Elution Fraction 1). By pooling these three fractions, more than 80% of extracted FLAG-tagged proteins were recovered. Extraction buffer and all of the materials used, including the sonication probe (1/8" microtip A3-561 Branson, Danbury, CT, USA), were cooled in advance.

The FLAG affinity adsorption and elution was used as a convenient analytical tool to determine the recombinant extraction yield. The resin was added in sufficient amounts to bind all available FLAG fusion protein present in clarified extracts. Cell debris and supernatants at the end of the batch adsorption period were regularly analyzed by western blotting to assure complete extraction and adsorption, respectively. Although minor recombinant protein losses have occurred during resin washing and pH 3.5 elution from the anti-FLAG resin, this determination of recombinant protein concentration was considered appropriate for estimating recombinant protein in crude extracts.

### *2.3.6 Characterization of purified Pfs25 by SEC*

To determine the size and range of multimeric forms of Pfs25, 100 µl of concentrated FLAG-purified Pfs25 protein in 100mM Glycine, 400mM NaCl, pH 8.0 buffer were loaded on a TSKgel G3000SWxl SEC (Tosho Bioscience LLC, Minato, TKY) at a flowrate of 0.5 mL/min.

Analysis of FLAG-purified Pfs25 by anion exchange chromatography was performed using CIM QA monolith disk (BIA Separations d.o.o., Ljubljana, SVN) at a flowrate of 3 mL/min. The monolith disk was washed with 10 CVs of 20mM Tris pH 8.0 and bound protein eluted with a 20 CV gradient to 100% 20mM Tris, 0.7M NaCl, pH 8.0.

Two-dimensional gel electrophoresis of FLAG-purified Pfs25 samples was done by Texas A&M Protein Chemistry Lab.

### 2.3.7 ELISA

Selected fractions of FLAG-purified Pfs25 separated by SEC were diluted 2, 4, and 8-fold with RO water, with triplicates of each dilution. NUNC-Immuno™ MicroWell™ Maxisorb 96-well plate (Thermo Fisher Scientific, Waltham, MA, USA) were coated in triplicate with 100 µl of each diluted sample and incubated overnight at 4°C. Wells were washed three times with Phosphate Buffered Saline with 0.1% Tween 20 (PBST) and blocked with 3% BSA in PBS for 2 hours at room temperature. Pfs25 was detected with 4B7 mAb (1:50 dilution) for 2 hours at room temperature followed by anti-mouse IgG (whole molecule)-peroxidase antibody produced in goat (Sigma Aldrich, St. Louis, MO, USA) at 1:5000 for 1 hour at room temperature. Antibody binding was detected using the TMB substrate kit (Thermo Fisher Scientific, Waltham, MA, USA) and read with a Molecular Devices VersaMax reader at a wavelength of 450nm.

## 2.4 Results and discussion

### 2.4.1 Cell resuspension increases Pfs25 accumulation

From a downstream processing viewpoint, the initial concentration of target protein in crude lysate is of paramount importance because it directly impacts overall process yield and final purity of the recombinant protein. In an earlier study using a different recombinant protein ( $\alpha$ CD22scFv), our group established that suspension of algal cells in fresh media before light induction was beneficial to both cell concentration and recombinant protein accumulation. In this work the same method was applied to induce higher production levels of Pfs25. The effect of cell resuspension on final cell concentration (Figure 5) and Pfs25 accumulation (Figure 6) was compared to non-resuspended control cultures. Both cultures, resuspended and non-resuspended, initially start with the same cell concentration ( $5 \times 10^4$  cells/mL) in one liter cultures with 10% inoculum. The cultures follow the same growth pattern the first 5 days of growth, doubling in cell concentration every 2 days. The control (non-resuspended) culture grows for an additional 24 hours before being exposed to  $101 \mu\text{molm}^{-2}\text{s}^{-1}$  of light for 24 hours. However, after 5 days of growth, the resuspended culture was centrifuged down, waste media removed, and algal cells suspended in new culture media. The resuspended culture was then allowed to grow for 24 hours before being exposed to  $101 \mu\text{molm}^{-2}\text{s}^{-1}$  of light for 24 hours, same as control culture. The addition of fresh nutrients produced the intended effect on the resuspended culture by generating a 30% increase in cell concentration at the end of the 6 day growth period (Figure 5). Because *psbA* is a light inducible gene promotor, Pfs25 will only be produced in the chloroplast during days 6 to

7. Therefore, a 30% increase in cell concentration will theoretically also increase Pfs25 production by 30%.

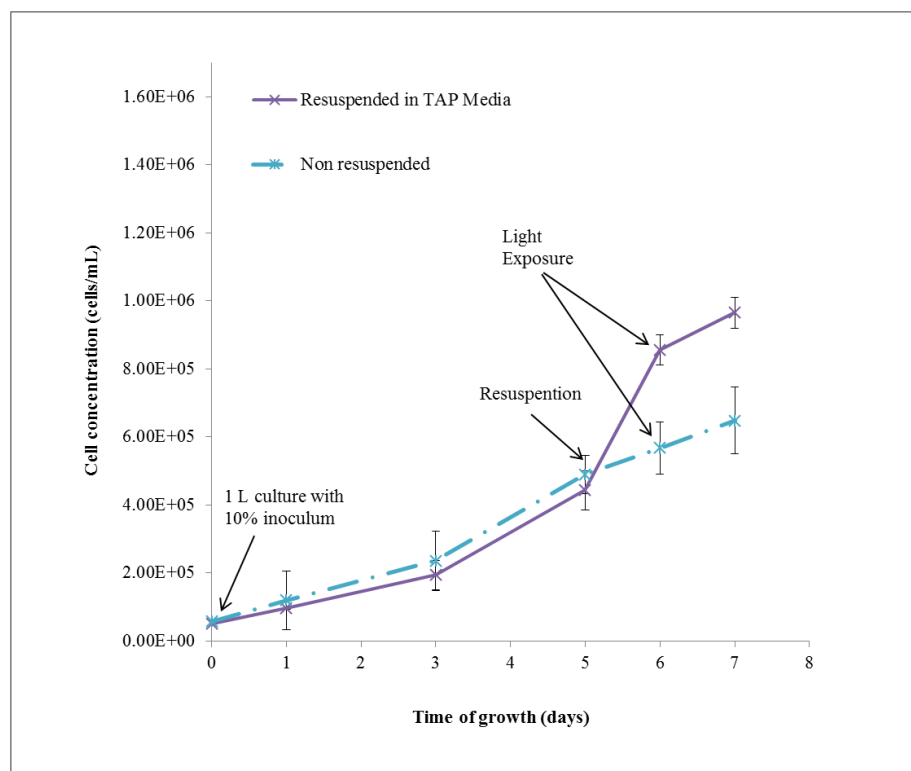


**Figure 5.** The effect of cell resuspension and light exposure ( $100\mu\text{mol m}^{-2} \text{s}^{-1}$ ) on *C. reinhardtii* cell concentration and Pfs25 accumulation (% total soluble protein). Average of 3 replicates. TAP: Tris-Acetate-Phosphate.

The amount of accumulated Pfs25 at the end of the cultivation was estimated by FLAG-affinity adsorption. The effect of resuspension on the amount of affinity purified Pfs25 is shown in lanes 8 to 10 in Figure 6. Comparing elution 2 and 3 of the two SDS-PAGE gels (Figures 6a and 6b) it is observed that the 28 kDa band (Pfs25) is thicker and darker in the culture that was resuspended in fresh media on day 5. Total Pfs25 protein

eluted from affinity resin (Lanes 8, 9, and 10 in Figure 6) was 309 ug of protein/L culture for resuspended vs 133 ug/L culture for the non-resuspended control. Therefore, the 30% increase in cell concentration for resuspended culture resulted in a 2.3-fold increase in Pfs25 protein. Considering there was also a 1.3-fold increase in total host protein accumulation, we estimate that Pfs25 accumulation increased 1.7-fold (from 1.5% TSP in the control to 2.5% TSP in the resuspended culture). An increase in product titer is always a welcome improvement because it translates more efficient downstream processing.

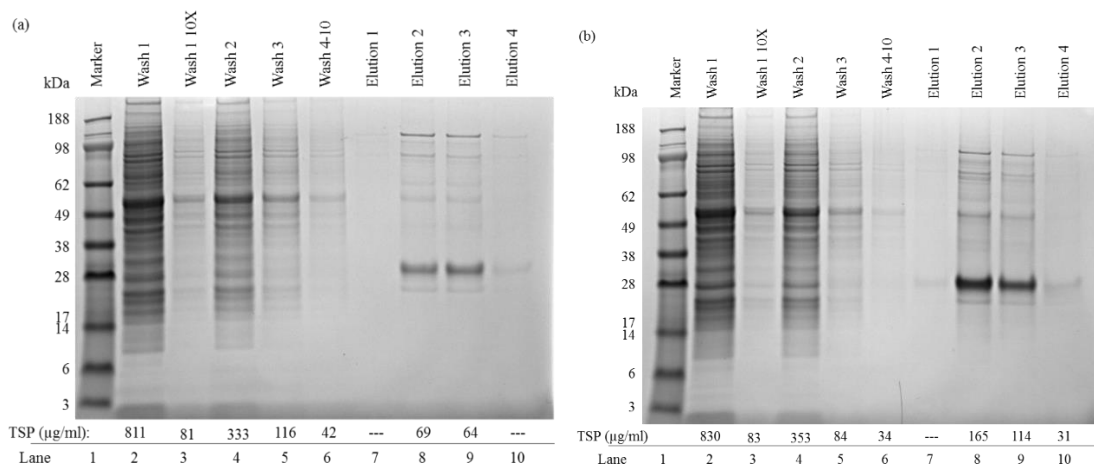


**Figure 6.** SDS-PAGE gels of Pfs25 affinity purification from (a) non resuspended cell lysate (control) and (b) resuspended cell lysates. Lane 1: molecular weight marker (kDa); Lanes 7-10: Pfs25 eluted fractions at pH 3.5.

#### 2.4.2 Purification and partial characterization of Pfs25

Pfs25 produced in resuspended *C. reinhardtii* was purified by batch adsorption, followed by low pH elution, using anti-FLAG-affinity resin. SDS-PAGE and Western blot in Figure 7 shows fractions of host cell protein and Pfs25 that were obtained during affinity resin washes and Pfs25 desorption. Nonspecifically adsorbed host cell protein was removed during the 10 CV washes before elution (Lanes 5 and 6), with Rubisco (~50 kDa band) being one of the most prominent protein. Based on Western blot analysis, the supernatant after adsorption did not possess measureable amounts of Pfs25; however, the wash fractions did contain detectable amounts of Pfs25 (Figure 7b), suggesting that a decent amount of Pfs25 was unable to specifically bind to the resin. The loss of Pfs25 in the wash fractions could be resolved by adding a larger amount of resin to the algae lysate, to provide more binding sites for Pfs25. The SDS-PAGE shows several minor protein bands in the elution fraction (Lanes 7-10) which are presumed to be Pfs25 aggregates, as indicated by the Western blot. ImageJ analysis indicates that about 25% of total Pfs25 in the elution lanes was aggregated.

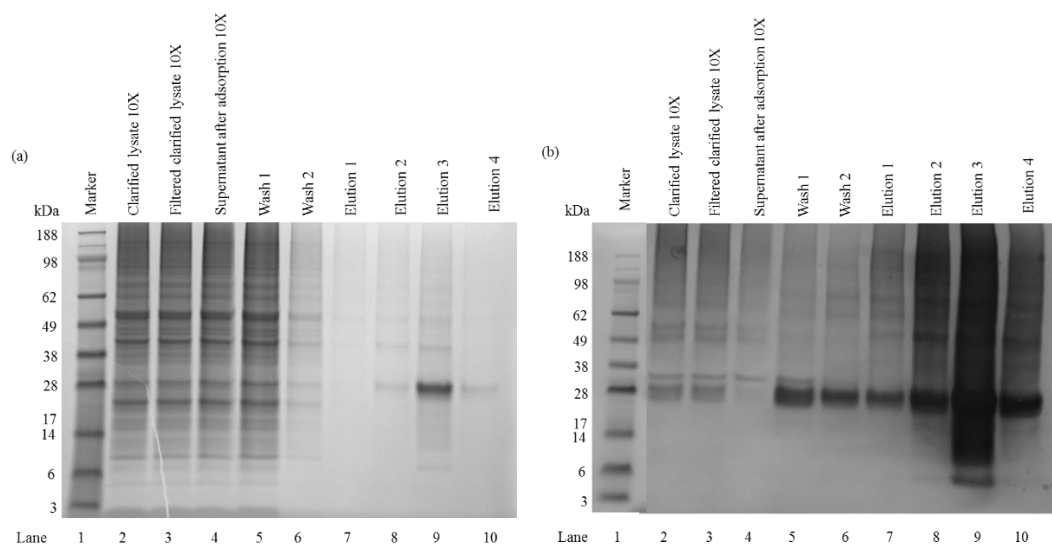


**Figure 7.** Analysis of resin wash and eluted Pfs25 fractions. (a) SDS-PAGE gel of Pfs25 affinity purification and (b) Western blot analysis of Pfs25 from resuspended cell lysate. (b) Lane 1: molecular weight marker (kDa); Lane 2: 1<sup>st</sup> CV of wash before elution; Lane 3: 10X dilution of 1<sup>st</sup> CV of wash before elution; Lane 4-5: 2<sup>nd</sup> and 3<sup>rd</sup> CV of wash before elution; Lane 7-10: elution 1-4 at pH 3.5.

Elution fractions 2 and 3 from FLAG-affinity adsorption were pooled, concentrated, and run on a 2-D electrophoresis gel to determine the purity of FLAG-purified samples (Figure 8). The 2-D gel reveals that Pfs25 sample was pure; the smear near bottom right-hand corner was probably lipids and/or chlorophyll pigment impurities. The band around the 30 kDa marker is the monomeric form of Pfs25. The band spread around pI of 5.0 (The program ProtParam was used to estimate the pI as 4.96) indicates that purified Pfs25 sample does not have a uniform isoelectric point and consists of several charge Pfs25 variants.

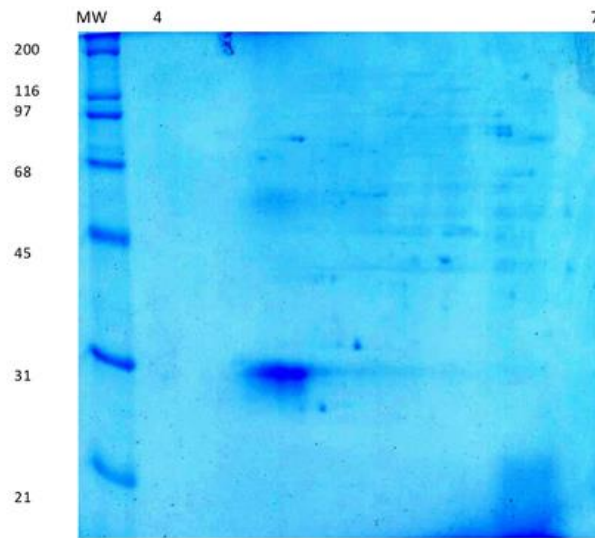


**Figure 8.** 2-D electrophoresis gel of FLAG-purified Pfs25 separated first by isoelectric point and then by molecular weight.

#### *2.4.3 Characterization of purified Pfs25 by SEC*

To determine the approximate amount and molecular weight (MW) distribution of the Pfs25 aggregates, FLAG-purified Pfs25 was analyzed by size exclusion chromatography (SEC) on a TSKGel G3000SWxl column. To confirm the SEC calibration curve developed by the column vendor (TOSOH), IgG (MW=156), BSA (MW=66.5kDa), and Lysozyme (MW=14kDa) were run on the same column and elution times recorded below (Table 1). The retention of thyroglobulin was taken from TOSOH.

**Table 1.** Elution of calibration proteins from TSKGel G3000SWxl column from TOSOH.

Sample	MW (kDa)	log (MW)	Elution (ml)
Thyroglobulin	660	2.8195439	6.7
IgG	156	2.1931246	8.7
BSA	67	1.8260748	9.5
Lysozyme	14	1.146128	12.5

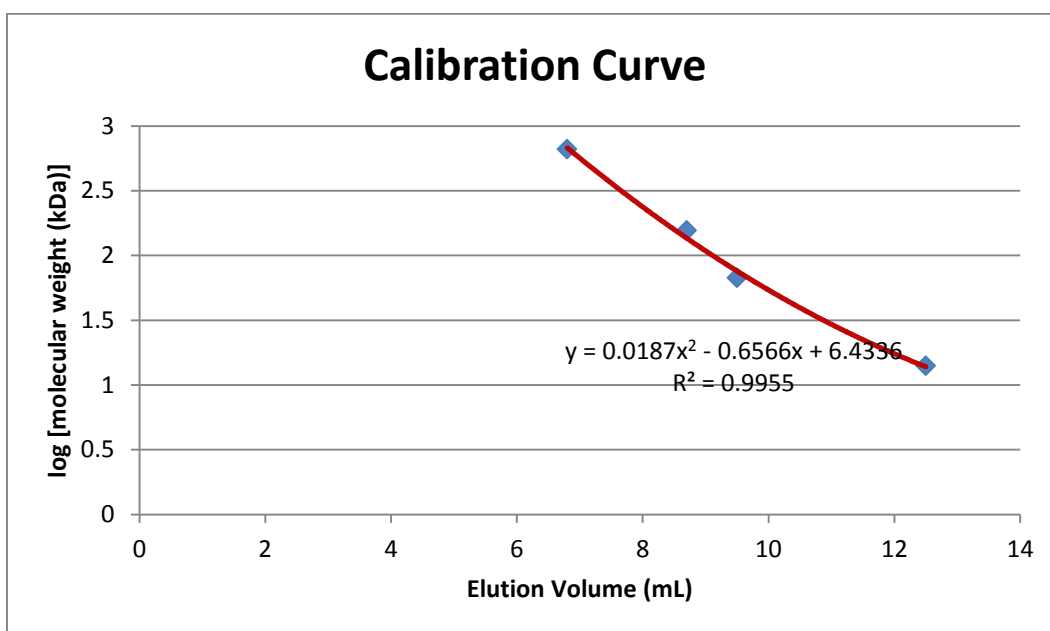


**Figure 9.** Calibration curve used for analysis of Pfs25 aggregates.

The resulting chromatogram of FLAG-purified Pfs25 is shown in Figure 10.

Using the calibration curve in Figure 10, the highest MW Pfs25 aggregate seen at 6.2

mL elution volume translates to a >600 kDa protein. The tallest peak at 10.5 mL elution volume correlates with 25 kDa, representative of the monomeric form of Pfs25.

Unfortunately, there was no baseline separation between the different aggregates that range from 25 to 600 kDa. Examination of the calibration curve confirms that proteins beyond 60 kDa in size would be difficult to separate unless they differ in size by a factor of 2. Therefore, the aggregates that were observed by SDS-PAGE of approximately 75, 100 and 125 kDa would not be easily discernable by SEC using TSKGel G3000SWx1.

What was surprising is the presence of species that eluted at volumes between 6 and 8 mL because Mayfield's laboratory and our SDS-PAGE gels only revealed Pfs25 complexes as high as 100 to 130 kDa. The last peak on the chromatogram does not contain any FLAG-tagged proteins, and based on the calibration curve is ~0.3 kDa, probably Tween 20.

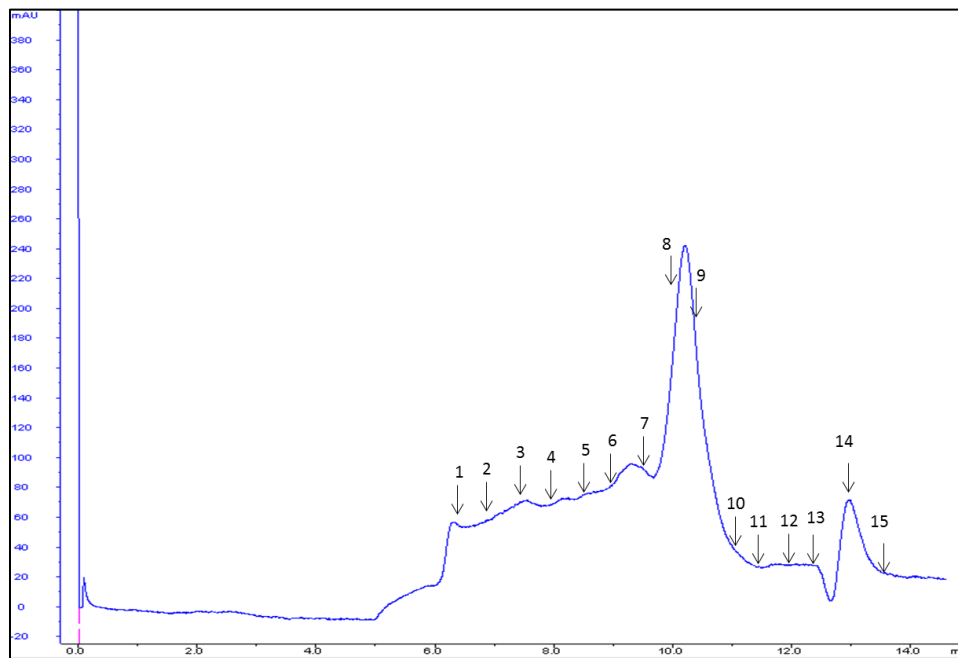


**Figure 10.** Chromatogram of Pfs25 without Tween 20 purified by anti-FLAG affinity chromatography separated by SEC TSKGEL G3000SWx1.

To determine that early eluting fractions contain Pfs25, selected fractions were run on a non-reduced Western blot (Figure 11a). The non-reduced Western blot reveals the protein in its native form, without breaking intramolecular disulfide bonds. Only high molecular weight bands are seen (Figure 11a) at the beginning of the chromatogram; then as the chromatogram progresses, lower molecular weight proteins come out of the column, finishing with dark, thick bands in fraction 8 and 9 corresponding to 28 kDa MW marker. The same samples were then run on a reduced Western blot (Figure 11b) to determine if aggregation pattern would change. The reduced Western blot, as expected, revealed that in the presence of 2-mercaptoethanol

and 70°C heating, Pfs25 monomer, dimer and higher MW species were released from the large aggregates under reducing conditions. The source or cause of the large agglomerates (200~600 kDa) is not clear, but one can speculate that a fraction of Pfs might be misfolded forming intermolecular disulfide bonds, due to disulfide bonds 2, 7, 8, 10, and 11 of Pfs25 not being completely formed in the chloroplast [2].

(a)

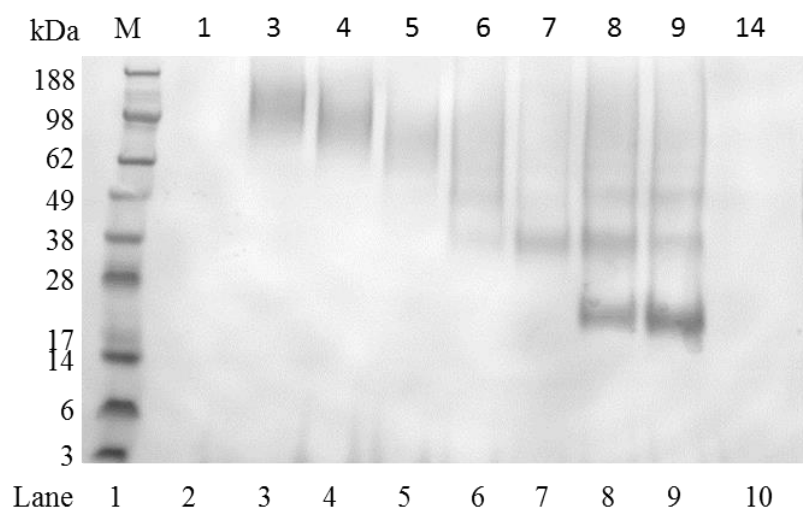
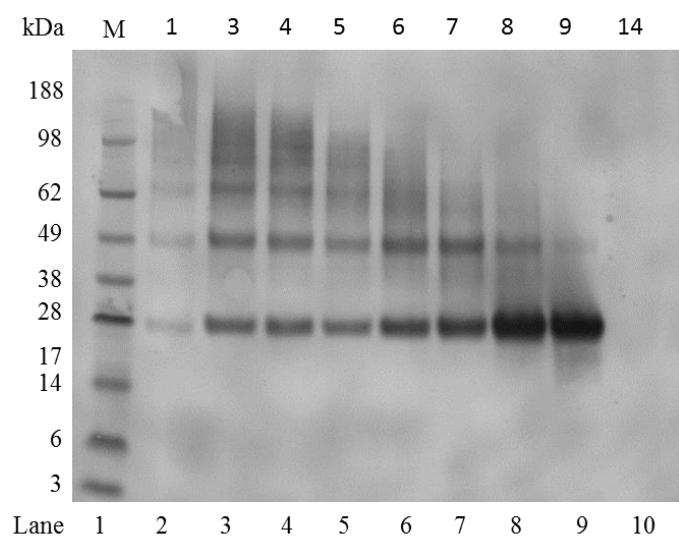


**Figure 11.** Western blotting of FLAG-purified Pfs25 separated by SEC using anti-FLAG-AP conjugated antibody (a) under non-reducing conditions, (b) under reducing conditions without Tween 20, and (c) under reducing conditions in the presence of Tween 20.

(b)



(c)

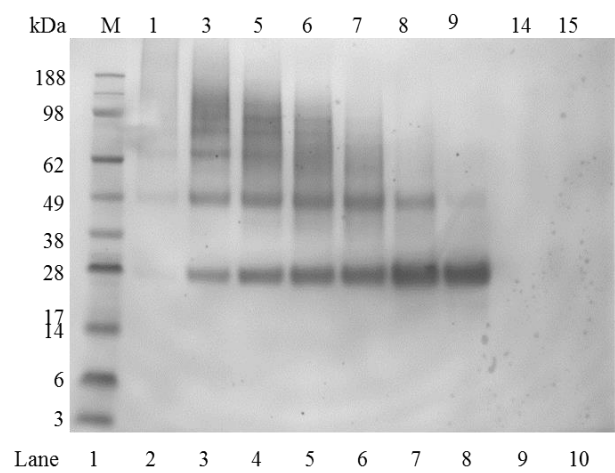


**Figure 11.** Continued.

Because the presence of 600 kDa in the SEC chromatogram was unexpected, we wanted to confirm that these large aggregates were not formed solely due to hydrophobic

protein-protein interactions. Therefore, 0.25% of Tween 20, was added to the FLAG-purified Pfs25 sample, and mixed for 30 min at room temperature using an end-over-end rotor. The sample with Tween 20 was run on the same SEC column and the resulting chromatogram is shown in a Figure 13. The protein elution profile in the presence of Tween 20 is the exactly the same as that in the absence of Tween 20 treatment (Figure 12). However, the peak heights of the aggregates were half on the peak height of the sample without Tween 20; this difference in peak height can be attributed to the dilution of sample with the addition of the detergent. The tall peak at 15mL elution volume is the detergent coming out of the column. Selected SEC fractions of the sample in the presence of Tween 20 were analyzed by a Western blot under reducing conditions (Figure 11c). Thus, the presence of high MW aggregates in the chromatogram was not an SEC product.

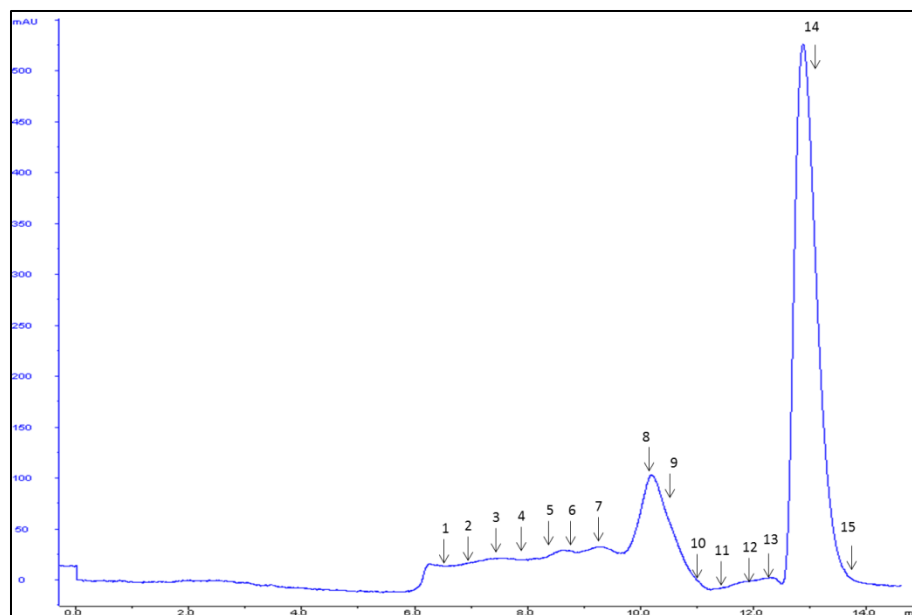


**Figure 12.** Chromatogram of Pfs25 with 0.25% Tween 20 purified by anti-FLAG affinity chromatography separated by SEC TSK GEL G3000SWx1.

Another concern we had is the possibility of Pfs25 partially unfolding and aggregation during pH 3.5 elution, which has been often observed with low pH elution of monoclonal antibodies and other affinity purified proteins. Therefore, instead of using five CVs of pH 3.5 elution buffer, six CVs of 100  $\mu\text{g}/\text{mL}$  FLAG-peptide in TBS of pH 8.0 was used to elute Pfs25 off the FLAG-affinity resin. Figure 13 is the SEC chromatogram of FLAG-peptide elution of Pfs25 at wavelength 220 nm. Even though FLAG-peptide elution has a different profile than regular elution method, the large complexes of Pfs25 are still present in the extract. It appears that Pfs25 complexes were not exclusively formed during the low pH elution step, although the low pH elution could have contributed to aggregation.

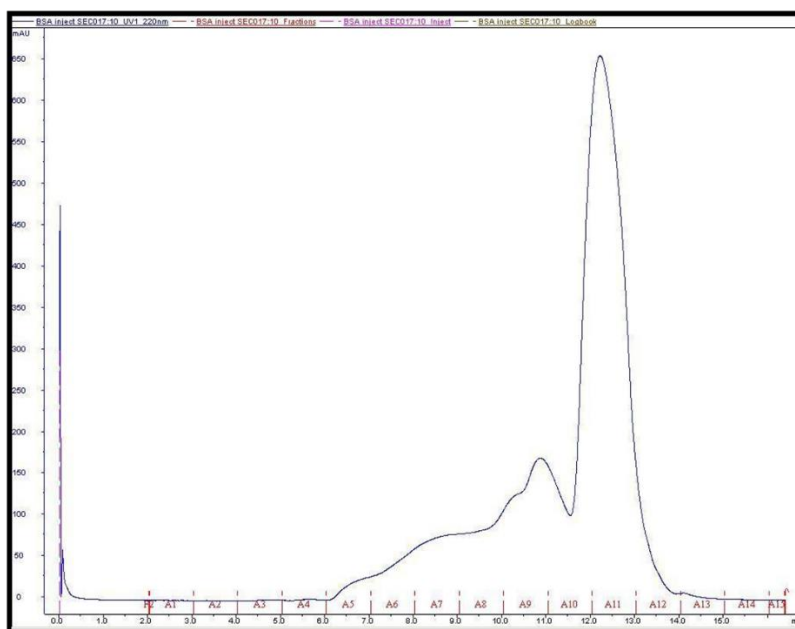


**Figure 13.** Chromatogram of FLAG-purified Pfs25 eluted using FLAG-peptide pH 8.0, separated using SEC.

Having established that all SEC fractions cross-react with anti-FLAG monoclonal antibodies, selected fractions of the SEC were probed with mAb 4B7 to determine which fractions were recognized by the conformationally-dependent mAb (Figure 14). Most of the fractions reacted with the mAb, except for Fractions 1, 12, 13, and 14. Fractions 1, 12, and 13 is where the chromatogram reached baseline indicating undetectable protein at wavelength 220nm and Fraction 14 is the detectible peak of Tween 20. It seems that fractions in the middle of the chromatogram (5, 7, 8, 9, 10, and 11) have the strongest reaction with 4B7 mAb. However, the higher molecular weight

fractions (4 and 5) have a sharp decrease in absorbance between sample dilutions 2 and 4.

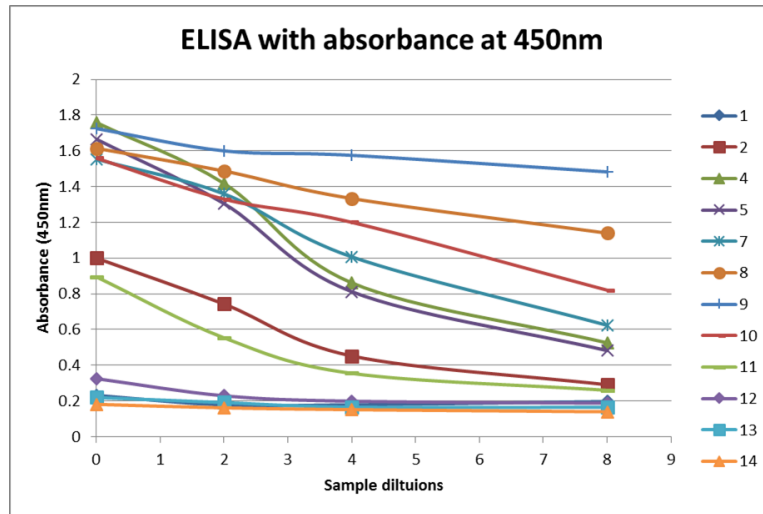


**Figure 14.** Reactivity of selected fractions from SEC probed with dilutions of 4B7 mAb on ELISA.

## 2.5 Summary

Our lab found that supplying fresh nutrients to cultures before light exposure drastically helps facilitate a more efficient downstream processing of recombinant proteins produced in the chloroplast of algae. Resuspending cell culture in fresh TAP media 24 hours before exposing the culture to light increased the cell concentration by 30% and almost doubled the amount of Pfs25 extracted from the cells.

SDS-PAGE analysis of FLAG-purified elutions revealed a predominant band at 28 kDa, the gel also revealed bands at the 50, 75, 100, and 125 kDa marks. Analysis of the Western blot confirmed the appearance of aggregates containing Pfs25 at those

markers as well (identical to Gregory and Vinetz's published results). To further characterize Pfs25 after extraction from the chloroplast of *C. reinhardtii*, FLAG-purified Pfs25 was run on a SEC. Using the standards for the SEC, it was determined that purified Pfs25 sample contained a molecular weight range from 25-600 kDa. The SEC fractions were run on non-reducing and reducing Western blots. The higher molecular weight FLAG-tagged proteins slightly break down into monomeric and dimeric forms of Pfs25 in the presence of reducing agents. Tween 20, a detergent, was mixed with the SEC fractions to ensure the aggregates were not formed due to hydrophobic protein-protein interactions; however, the aggregates seemed to remain intact with the same original distribution of multimeric forms of Pfs25. Another concern of ours was that the low pH elution used to desorb Pfs25 off the affinity column caused the protein to partially unfold and aggregate, as seen with monoclonal antibodies and other purified protein during low pH elutions. Therefore, instead of using low pH to elute bound proteins off the anti-FLAG affinity column, FLAG-peptide was used to displace the bound proteins off the column. The FLAG-peptide eluted proteins were analyzed by SEC. The resulting chromatogram showed a different Pfs25 profile, but still contained a large range of multimeric forms of Pfs25. The low pH elution may encourage multimeric forms of Pfs25 to form, but high molecular weight forms of Pfs25 are present before the low pH elution step. When the fractions were probed with conformationally-dependent mAb 4B7, the middle range aggregates showed a higher reactivity compared to the smaller forms.

The higher molecular weight FLAG-tagged proteins Gregory and Vinetz reported on their Western blots are in stable forms, even in the presence of detergents and reducing agents. The only other system that has reported self-formed Pfs25 aggregates was when Pfs25 secreted from *P. pastoris* and was chemically conjugated to EPA. PpPfs25-EPA was measured as a nanoparticle with a size of ~600kDa, about the same size as the largest aggregate found in our FLAG-purified sample. The conjugated protein, when administered with Alhydrogel®, was well tolerated by humans in Phase 1 clinical trials and it elicited a strong immunogenic response with high TBA. Pfs25 produced in the chloroplast of *C. reinhardtii* naturally forms large multimeric forms and interacts with the anti-Pfs25 mAb 4B7. Naturally formed Pfs25 aggregates are advantageous because additional steps to chemically conjugate the vaccine to a carrier protein are eliminated and there is no need to worry about the effects of the carrier protein during human clinical trials. The immunogenicity and TBA of the multimeric forms of Pfs25 need to be evaluated to further evaluate the chloroplast of *C. reinhardtii* as a possible production system for the malaria vaccine.

## CHAPTER III

### DEVELOPMENT OF A NON-AFFINITY PURIFICATION METHODS FOR RECOMBINANT PROTEINS PRODUCED IN *CHLAMYDOMONAS REINHARDTII*

#### 3.1 Overview

Protein therapeutics is advancing rapidly and in the past 25 years has become the fastest growing division in drug development. Researchers are exploring new therapeutic production systems depending on the size and complexity of the protein being produced. No matter the expression system, downstream processing accounts for a large majority of the total manufacturing costs of therapeutic proteins.

Pretreatment of clarified cell lysates is the first step in downstream processing designed to minimize impurities before loading the lysate onto a chromatographic column. When dealing with intracellular products, simple clarification steps like centrifugation and depth filtration do not sufficiently remove soluble impurities to achieve downstream process robustness. Additional pretreatment methods like ammonium sulfate precipitation [72], isoelectric precipitation [73, 74], and polymer precipitation have been applied to green tissue extracts to remove a significant fraction of host soluble protein such as ribulose bis-phosphate carboxylase/oxygenase (rubisco), chlorophyll pigments and DNA [73-75]. Polymer precipitation with cationic polymers, such as polyethylenimine and chitosan, has been shown to efficiently remove DNA.

Our lab previously studied the effects of the three precipitation methods mentioned above on the recovery of single-chain antibody fragment ( $\alpha$ CD22scFv) [3] produced in the chloroplast of *Chlamydomonas reinhardtii* [34]. The fragment was recovered and quantified from clarified lysates after each pretreatment using anti-FLAG-affinity resin. The 1M ammonium sulfate and isoelectric precipitation at pH 4.5 pretreatments significantly reduced the percent of residual chlorophyll and host cell protein without significantly reducing the target protein yield. On the other hand, chitosan precipitation at pH 5.0 significantly reduced the percentage of residual DNA, chlorophyll, and host cell protein; however, there was also a significant drop in scFv yield. The scFv from pretreated lysates was purified using anti-FLAG-affinity resin. Anti-FLAG-affinity resin is not a scalable capture step for large scale purification of therapeutics because the resin is extremely expensive, has a low binding capacity, and is easily compressible.

The objectives of this study were (i) to determine the stability of  $\alpha$ CD22scFv during adsorption to Capto Q resin of, (ii) compare the effects of pretreatment methods on  $\alpha$ CD22scFv adsorption to Capto Q and Phenyl Sepharose resins, (iii) scout Phenyl Sepharose and hydroxyapatite (HAP) resins as possible intermediate chromatography steps, and (iv) purify  $\alpha$ CD22scFv using isoelectric precipitation at pH 4.5, an anion exchange capture chromatography, and FLAG-affinity polishing step.

## 3.2 Introduction

### 3.2.1 *Single-chain antibody fragments ( $\alpha$ CD22scFv) applications*

The main line of defense against pathogenic organisms and toxins in humans are antibodies due to their highly specific targeting. IgG is the main serum antibody and is a highly complex molecule. A full-size IgG antibody is Y-shaped composed of two light chains and two heavy chains. Each light chain is made of a variable and constant domain and each heavy chain has one variable and three constant domains. There are three disulfide bonds total, one connecting each heavy chain to a light chain and one connecting the two heavy chains. The variable regions on the tips of the light chain define antigen specificity of the antibody [76]. Engineered monoclonal antibodies (mAbs) are already on the biotechnology market and more are on their way in clinical trials. To date, twenty-two mAbs have been approved in the US for therapeutic use and account for \$20 billion of healthcare spending [77]. Currently, the market is dominated by mAb products composed of the full-size form of IgG but smaller single-chained antibody fragments (scFvs) are now emerging as credible alternatives to whole mAbs [78]. A scFv is the smallest functional domain of an antibody (~30kDa) comprised of only a variable heavy chain and a variable light chain connected by a peptide linker. The linker is composed of hydrophilic residues using stretches of glycine and serine sequences (Gly<sub>4</sub>Ser)<sub>3</sub>, the most common linker sequence for scFv, to make the linker flexible [79-81]. Antibody fragments have several advantages over full-bodied mAbs including: (i) the fragments are able to penetrate tissues and tumors more rapidly and deeply than mAbs due to their size [82-84]; (ii) they are relatively small, unglycosylated

proteins allowing them to be produced in microbial expression systems (cheaper and quicker than mammalian cultures) [78, 85] while maintaining the targeting specificity of a mAb; (iii) they lack the Fc region of the full mAb resulting in a low immunogenicity; and (iv) the fragments can be bound to other fragments or fused with a range of molecules to produce new, unique molecules for therapeutic applications [78]. However there are several disadvantages to antibody fragments: (i) fragments have short half-lives in humans causing insufficient accumulation at the target site, making them undesirable for therapeutic applications [86-88]; (ii) they are cleared out of humans during kidney clearance because the fragments lack a neonatal Fc receptor-mediated recycling found on full-length mAbs [89, 90]; and (iii) fragments are less stable than full mAbs and are more likely to form undesirable aggregates [91].

The scFv used in this study was designed by our collaborator from University of California at San Diego to recognize the CD22 antigen from B-cells leukemia and lymphomas. The  $\alpha$ CD22scFv fragment was produced in the chloroplast of *C. reinhardtii* at relatively low titers in the order of 0.1 % of total soluble protein. To purify recombinant proteins expressed in microalgae FLAG-tagged recombinant proteins relied exclusively on immunoaffinity batch adsorption [71].

### 3.2.2 Purification of scFv

Downstream processing is a critical part for the development of commercially feasible protein products such as scFvs; a successful process should be able to efficiently (high purity and high yield) purify the target product while maintaining low operation

costs. A typical purification process is comprised of three stages: (1) primary recovery step, (2) capture step, and (3) polishing step. Because the constant Fc region is missing in scFvs, traditional purification methods (Protein A or G) monoclonal antibodies cannot be applied.

Natural binding ligands and tag ligands are two affinity-based chromatography methods that have been developed to specifically capture and purify scFvs. Peptostreptococcal Protein L (PpL) has been used to purify scFvs due to its high affinity to mammalian  $\kappa$ -light chains on the Fab portion of antibodies [92, 93]. About five years ago, a commercial chromatography resin with Protein L ligand has been made available to ease the purification of antibodies lacking Fc domains. However, not all mammalian immunoglobulins have a high affinity to Protein-L based resin [94]. The scFv investigated in this study has a mouse  $\kappa$ -light chain; which has a weak affinity to Protein-L resins. Short polypeptide sequences or whole proteins co-expressed as fusion partners with the target protein can be used to facilitate affinity tag chromatography [95]. Currently, immobilized metal affinity chromatography (IMAC) is one of the most utilized methodologies to purify scFvs [96, 97] by attaching a stretch of 6 histidines to N or C terminus of expressed recombinant fragment. Several labs have reported >90% purity by binding scFv-His<sub>6</sub> to IMAC [96, 98, 99] after being secreted into the culture media. IMAC has several distinct advantages over other affinity systems related to large-scale purification: low cost, high protein loading, ligand stability, mild elution conditions, and easy regeneration [100]. However, lower final purity has been achieved with IMAC compared to PpL-based chromatography [101]. Other disadvantages of

IMAC include: need to control the oxidative and reduction conditions inside the column, potential metal-induced cleavage of protein backbone, and toxicity of metal ions leaching from the solid support. Another tag developed to facilitate affinity purification was designed by the RPAS® Purification Module from Amersham Biosciences. They used an Anti-E-Tag monoclonal antibody to recognize a 13 amino acid peptide tag (E-Tag) fused to the C-terminal of a scFv produced from *E. coli* [102]. When designing downstream purification processes that utilize tag affinity chromatography, it is important to consider the additional steps needed to remove the tag from the protein, which could lead to a more complicated process. A FLAG tag, which consists of 9 amino acids, was fused to the N-terminus of the scFv analyzed in this study. Anti-FLAG® M2 Affinity Gel was developed by Sigma-Aldrich for the rapid purification of FLAG fusion proteins and was the resin used for rapid purification and detection of the target protein [34].

Even though affinity-based chromatography is the most frequently used methodology for first capture of scFvs, other chromatographic methods (ion exchange, size exclusion, and hydrophobic interaction) can also be used to purify antibody fragments. Several research groups have reported purifications of scFv using only non-affinity-based chromatographic methods. However, the fragment had either been secreted into the culture medium [103, 104] or previously purified using affinity-based chromatography [105]. To our knowledge, there is no reported data of using only non-affinity-based chromatographic methods to purify scFvs from cell lysates.

Mixed-mode chromatography has made a large impact on the purification of several recombinant proteins from various expression systems. Usually two or more of the following types of interactions have been combined to create a chromatography resin with unique selectivity: anion exchange, cation exchange, hydrophobic interaction, hydrophilic interaction, hydrogen bonding, pi-pi bonding, and metal affinity [106]. Current downstream processes often consist of two to three major separation steps by combining multiple purification steps into one, the overall cost of purification could drastically decrease. Even though mixed-mode chromatography can have high selectivity towards the desired product, method development is complicated and unpredictable. One mixed-mode chromatography is hydroxyapatite affinity chromatography (HAC), which is used for polishing purification of antibodies, from partially purified preparations. HAC combines two modes of interaction: metal affinity of protein carboxyl clusters for crystal atoms and cation exchange of positively charged protein amino residues with negatively charged crystal phosphates [106].

### 3.2.3 Purification of scFv from algae

To establish the feasibility of microalgae as a platform for recombinant protein production one has to demonstrate that target protein can be isolated and purified without relying on affinity resins. There are only few examples of purification of recombinant proteins produced in the chloroplast of *C. reinhardtii* and those rely on FLAG affinity tags [3-5] for ease of purification and detection. However, using anti-FLAG-affinity resin to purify recombinant proteins from clarified lysate is not a scalable

solution for several reasons: (i) the resin cannot handle high pressures necessitating the lysate to be loaded onto the column at unacceptably low flow rates (low productivity); (ii) the resin is extremely expensive; and (iii) the binding capacity of the resin is only 0.6mg/mL requiring a large bed volume. For these reasons, anti-FLAG-affinity resin seems more suitable as an analytical tool and batch purification method for FLAG-tagged proteins from cell lysates. Thus, one of the objectives of the study was to determine if FLAG-affinity could be employed as a polishing step after an anion exchange capture chromatography step.

### **3.3 Materials and methods**

#### *3.3.1 Gene construct for $\alpha$ CD22scFv*

In the construct, the endogenous *psbA* locus was replaced by  $\alpha$ CD22scFv via direct homologous recombination. Thus, transgene expression in these strains is regulated by the *psbA* promoter and the 5' and 3' untranslated regions (UTRs) and, therefore, is light inducible. A kanamycin resistance cassette was incorporated for selection. The variable domains of a human antibody against the B-cell surface antigen CD22 were separated by a linker sequence coding consisting of four glycines and a serine repeated four times, (Gly<sub>4</sub>Ser)<sub>4</sub>, to create an scFv [3]. The gene cassettes ( $\alpha$ CD22scFv) was ligated with a sequence coding for a 1× Flag peptide (DYKDDDDKS) and separated by a sequence that encodes a Tobacco etch virus (TEV) protease cleavage site (ENLYFQG) [3].

### 3.3.2 *Cultivation of $\alpha$ CD22scFv Chlamydomonas reinhardtii strains*

Algal biomass from a single agar plate (Tris-Acetate-Phosphate (TAP) agar with 150  $\mu\text{g}/\text{mL}$  kanamycin) was transferred to 100 mL of TAP media without kanamycin and grown for 3 days. A subsequent volumetric culture scale up was performed using 10% inoculum in the exponential phase (100 mL) in 1 L of fresh TAP media containing 25  $\mu\text{g}/\text{mL}$  kanamycin. One-liter cultures were grown heterotrophically for 5 days, reaching  $\sim 4$  to  $5 \times 10^6$  cells/mL. The cultures were then exposed to light for 24 hours consecutively at a photon irradiance of  $101 \mu\text{mol m}^{-2} \text{s}^{-1}$  to induce recombinant protein synthesis.

### 3.3.3 *Protein Extraction*

At the end of the light exposure period, cells were harvested by centrifugation at 3,000 rpm for 5 min at  $4^\circ\text{C}$ . Pelleted algal biomass was washed with fresh TAP media, weighted, and then resuspended at 1:5 biomass-to-lysis buffer ratio 50 mM Tris-HCl, 400 mM NaCl, and 0.5% Tween 20, pH 8.0. The buffer contained a complete protease inhibitor cocktail (Roche-Mannheim, Germany) dissolved in 200 mL of the buffer. Algal cells were lysed by sonication for 10 min with 30 seconds on/off intervals at  $4^\circ\text{C}$  using sonicator (Sonifier 250, Branson, USA) at 30% output control and 30% duty cycle with a micro probe (1/8" microtip A3-561 Branson, USA). Cell lysates were centrifuged (10,000 rpm for 20 min) to produce cell-free extracts.

#### 3.3.4 *Pretreatment of cell free lysates*

The three pretreatment methods (polymer precipitation, isoelectric precipitation, and ammonium sulfate precipitation) were performed on lysates free of cell debris. After cell disruption by sonication, the cell debris was removed by centrifugation at 10,000 rpm for 20 minutes and then by filtration using polyethersulfone (PES) 0.45 $\mu$ m syringe filters.

Polymer precipitation was performed using a stock solution of 10 mg/mL chitosan in 1% acetic acid solution (Sigma Aldrich Company, USA). For every gram of biomass purified, 30 mg of chitosan was added to the clarified lysate and quickly vortexed for 30 seconds to mix the polymer and lysate. The pH of the lysate was adjusted to pH 5.0 using 0.2M HCl, mixed end-over-end for 30 minutes at room temperature, and centrifuged for 20 minutes at 10,000 rpm. The formed pellet consisted of precipitated chitosan and chitosan bound proteins from the lysate. The supernatant from the pellet was readjusted to pH 8.0 using 1N sodium hydroxide (NaOH). The lysate was centrifuged again at 10,000 rpm for 20 minutes and filtered using a PES 0.45 $\mu$ m syringe filter.

Isoelectric precipitation was accomplished by adding 0.2M HCl drop wise to the cell free lysate until the pH of the mixture reached 4.5. The lysate was mixed end-over-end at room temperature for 15 minutes and then centrifuged for 20 minutes at 10,000 rpm. The pH of the supernatant was readjusted to 8.0 using 1N NaOH and filtered using a PES 0.45 $\mu$ m syringe filter.

Ammonium sulfate (Sigma Aldrich Company, USA) precipitation was performed by adding a stock solution of 3.6 M ammonium sulfate to the cell free lysate until the final concentration of ammonium sulfate in solution reached 1.0M and 1.5M (31% and 53% saturation, respectively). Agitation was provided by end-over-end mixing for 30 minutes at room temperature, centrifuged at 10,000 rpm for 20 minutes, and filtered through a PES 0.45 $\mu$ m syringe filter.

### 3.3.5 Anion exchange chromatography (AXC)

To ensure  $\alpha$ CD22scFv would bind to the anion exchange column (Capto<sup>TM</sup> Q (Sigma Aldrich, St. Louis, MO, USA)) before and after pretreatment, the clarified lysate was dialyzed against 50mM Tris-Base pH 8.0 to reduce the conductivity of the lysate to below 4 mS. The lysate was added to SnakeSkin<sup>®</sup> Dialysis Tubing 3,500 MWCO (Thermo Scientific, Meridian Rd., Rockford, IL, USA) and left in the exchange buffer for 24 hours in a 4°C cold room. A stir bar was added to the buffer to facilitate buffer exchange. Conductivity of dialyzed sample was measured by a conductivity meter (Model 2052, VWR, Pennsylvania, USA) to ensure low conductivity. After dialysis, Capto Q resin was incubated with the lysate for 30 minutes on an end-over-end rotor at room temperature. Similar to FLAG-affinity purification, the lysate was placed in a centrifuge for 5 minutes at 3,000 rpm to settle the resin. The resin was loaded onto a Bio Spin disposable chromatography column (Bio Rad, Hercules, CA, USA), washed with 10 CVs of washing buffer (50mM Tris-Base, pH 8.0), and eluted step-wise with washing buffer plus increasing amounts of salt (0.2, 0.4, 0.6, 0.8, 1.0M NaCl). Two CVs of

elution buffer was used before moving to the next elution buffer of additional NaCl. Supernatants at the end of the batch adsorption period, washes, and elutions were analyzed by western blotting to evaluate adsorption and specific binding to the resin.

### *3.3.6 Hydrophobic interaction chromatography (HIC)*

Stock solution of 3.6M ammonium sulfate (Sigma Aldrich Company, USA) was added to clarified lysate to a final concentration of 1 M ammonium sulfate. The lysate was incubated with Phenyl Sepharose<sup>™</sup> 6 Fast Flow (high sub) (Sigma Aldrich, St. Louis, MO, USA) resin on an end-over-end rotor at room temperature for 30 minutes. After incubation, the resin was centrifuged for 5 minutes at 3,000 rpm to settle the resin and then transferred to a Bio Spin disposable chromatography column (Bio Rad, Hercules, CA, USA). The resin was then washed with 10 CVs of washing buffer (50mM Tris-Base, 1 M ammonium sulfate, pH 8.0) and eluted using washing buffer plus decreasing amounts of ammonium sulfate (0.8, 0.6, 0.4, 0.2, 0M ammonium sulfate). Two CVs of elution buffer was used before moving to the next elution buffer of less ammonium sulfate. Supernatants at the end of the batch adsorption period, washes, and elutions were analyzed by western blotting to assess adsorption and specific binding to the resin.

A final concentration of 1.5M ammonium sulfate in the clarified lysate was also tested to increase the adsorption and specific binding to Phenyl Sepharose resin. Methodology was similar to 1 M ammonium sulfate except after incubation with resin; the washing buffer was 50mM Tris-base, pH 8.0 in 1.5M ammonium sulfate. The

recombinant protein was eluted from the resin using the washing buffer with decreasing amounts of ammonium sulfate (1.2, 1.0, 0.8, 0.6, 0.4, 0.2, 0M ammonium sulfate). Two CVs of elution buffer was used before moving to the next elution buffer of less ammonium sulfate. Supernatants at the end of the batch adsorption period, washes, and elutions were analyzed by western blotting to gauge increased adsorption and specific binding to the resin.

When HIC was tested as a possible orthogonal purification step after isoelectric precipitation and AXC, the elutions from AXC were pooled together and 3.6M ammonium sulfate was added to the pool elution to a final concentration of 1.5M ammonium sulfate. The pool elution were then mixed end-over-end for 30 minutes at room temperature and centrifuged for 20 minutes at 10,000 rpm. Phenyl Sepharose<sup>TM</sup> 6 Fast Flow (high sub) (Sigma Aldrich, St. Louis, MO, USA) resin was incubated with the clarified partially purified sample for 30 minutes at room temperature. After incubation, the resin was settled by centrifugation at 3,000 rpm for 5 minutes then transferred into a Bio Spin disposable chromatography column (Bio Rad, Hercules, CA, USA). The resin was washed with 10 CVs of 50mM Tris-Base, 1.5M ammonium sulfate, pH 5.0. Protein was eluted off the HIC washing buffer plus decreasing amounts of ammonium sulfate (1.2, 1.0, 0.8, 0.6, 0.4, 0.2, 0M ammonium sulfate). Two CVs of elution buffer was used before moving to the next elution buffer of less ammonium sulfate. Supernatants at the end of the batch adsorption period, washes, and elutions were analyzed by western blotting to assess adsorption and specific binding to the resin.

### 3.3.7 *Mixed-mode chromatography*

Macro-Prep Ceramic Hydroxyapatite (HAP) TYPE I 80  $\mu\text{m}$  is a mixed-mode chromatography resin. HAP chromatography was tested as a possible orthogonal purification step after isoelectric precipitation and AXC. Pooled elutions after AXC were added to SnakeSkin<sup>®</sup> Dialysis Tubing 3,500 MWCO (Thermo Scientific, Meridian Rd., Rockford, IL, USA) and left in the exchange buffer (5mM sodium phosphate, pH 6.8) for 24 hours in a 4°C cold room. The partially purified sample was incubated with HAC resin for 1 hour at room temperature on an end-over-end rotor. After incubation, the resin was settled by centrifugation at 3,000 rpm for 5 minutes then transferred into a Bio Spin disposable chromatography column (Bio Rad, Hercules, CA, USA). The resin was washed with 10 CVs of 5mM sodium phosphate, pH 6.8 buffer and eluted with 2 CVs of 200mM sodium phosphate, pH 6.8 followed by 2 CVs of 500mM sodium phosphate, pH 6.8. Supernatants at the end of the batch adsorption period, washes, and elutions were analyzed by western blotting to assess adsorption and specific binding to the resin.

### 3.3.8 *Anti-FLAG-affinity purification*

Partially purified  $\alpha\text{CD22scFv}$  samples were mixed with anti-FLAG affinity resin (Sigma Aldrich, St. Louis, MO, USA); approximately 1 mL of resin was used for every 20mL of sample. Binding of the recombinant protein to the affinity resin was performed for 2 hours at 4 °C by continuous end-over-end mixing in a Glas-Col rotor (Glas-Col LLC, Terre Haute, IN, USA) at ~33 rpm (40% speed control). The resin was settled by centrifugation at 3,000 rpm for 5 minutes. Affinity resin was transferred into Bio Spin

disposable chromatography columns (Bio Rad, Hercules, CA, USA) and washed with 10 column volumes (CV) of buffer respective to buffer sample is in. Recombinant protein was eluted at pH 3.5 using 5 CV of 100 mM glycine buffer, pH 3.5, containing 400 mM NaCl. Eluted protein fractions were collected in 5 tubes containing a predetermined amount of 1M Tris-HCl, pH 8.0, to immediately neutralize the pH of the eluted protein and avoid protein degradation. Typically, three elution fractions (E2 to E4) were used for the estimation of purity and yield, although some losses occurred by not taking into account E1 (Elution Fraction 1). By pooling these three fractions, more than 80% of extracted FLAG-tagged proteins were recovered. Extraction buffer and all of the materials used, including the sonication probe (1/8" microtip A3-561 Branson, Danbury, CT, USA), were cooled before use.

The FLAG affinity purification method was used as a convenient analytical tool to determine the recombinant yield after pretreatment/capture chromatography methods and orthogonal purification steps. The resin was added in sufficient amounts to bind all available FLAG fusion protein present in clarified extracts. Supernatants at the end of the batch adsorption period were regularly analyzed by western blotting to assure complete adsorption and specific binding to the resin. Although minor recombinant protein losses have occurred during resin washing and pH 3.5 elution from the anti-FLAG resin, this determination of recombinant protein concentration was considered appropriate for estimating recombinant protein in crude extracts.

Column purification of AEX pool by FLAG-affinity resin was performed with a 12 mL column (1.6×6 cm). Twelve milliliters of AEX pool were loaded at 0.1 mL/min

(3 cm/h). The column was then washed with 5 CVs of 50mM Tris, pH 8.0 followed by 6 CVs of 100 mM glycine buffer, pH 3.5, containing 400 mM NaCl. Resulting peaks separated by the affinity column were analyzed by SDS-PAGE and western blotting.

### *3.3.9 Protein Analysis*

Total soluble protein in clarified lysate and purified fractions were analyzed using the Bradford assay with a working range from 25 to 1500 µg/mL. The samples were quantified using Coomassie Plus assay kit (Thermo Scientific, Waltham, MA, USA) measured using VERSA max plate reader (Molecular Devices, Sunnyvale, CA, USA) at wavelength 595 nm.

Supernatants and purified fractions were also analyzed using SDS-PAGE and Western Blots; all gels, stains, membranes, and chemicals were acquired from Invitrogen™ (Carlsbad, CA, USA). Samples were prepared with a reducing buffer (composed of NuPAGE LDS Sample Buffer 4x and 10% 2-mercaptoethanol), thoroughly mixed, and placed on a heating block, set at 70°C, for 10 minutes. After cooling, the samples were loaded onto a NuPAGE® Novex® Bis-Tris pre-packed gradient gel (1.5mm x 10 wells). A running buffer (1X MES SDS Running Buffer) was used to carry the current and create a uniform electric field on the gel. Antioxidant was also present in the running buffer to ensure proteins would remain in their linear form during electrophoresis. The system ran for 35 minutes at a constant voltage of 200V. The gels were then blocked with a 10% acetic acid, 40% ethanol, 50% reverse osmosis (RO) water fixing solution for 45 minutes to prevent diffusion of proteins, ensuring sharp and

resolved bands during the staining process. The fixing solution was rinsed off the gel and stained using Coomassie™ G-250 stain for 3 hours. Pictures of the stained gels were taken using a Gel Logic 100 Imaging System.

For Western blot analysis, the samples were run on a NuPAGE® Novex® Bis-Tris pre-packed gradient gel (1.5mm x 10 wells) in the same manner as SDS-PAGE. However, after running the gel, it was transferred to a nitrocellulose membrane using iBlot® 7-Minute Blotting System. After protein transfer, the membrane was blocked with 2.5% non-fat milk in a solution of Tris-Buffered Saline and Tween 20 (TBS-T) for 1 hour to prevent non-specific binding of the antibody. The membrane was washed three times with TBS-T then incubated with anti-FLAG M2 AP for one hour. The antibody was at a concentration of 1:2000 for detection of anti-FLAG-tagged  $\alpha$ CD22scFv. The membrane was washed again three times with TBS-T to remove any remaining antibody that did not bind to FLAG-tagged proteins. Nitro-blue tetrazolium (NBT) and 5-bromo-4-chloro-3'-indolylphosphate p-toluidine salt (BCIP) dissolved in 10 mL of ROW was used to develop the membrane. Gel Logic 100 Imaging System was used to take pictures of the developed membrane.

### **3.4 Results and discussion**

#### *3.4.1 Stability of $\alpha$ CD22scFv during adsorption to Capto Q resin*

During large scale purification of protein therapeutics, depending on how quickly the clarified extract can be processed, the target protein could be exposed to potential proteolytic activities present in clarified extracts for several hours. Before proceeding

with the investigation of alternative non-affinity chromatography steps, we wanted to demonstrate  $\alpha$ CD22scFv remains intact in clarified lysates for a lengthy amount of time at room temperature. The typical lysate volume in our experiments to be purified using packed column purification was 60mL. The time required for 60 mL of non-pretreated lysate to be manually loaded onto a column with a bed volume of 4.7 mL (0.7x10cm) at a linear velocity of 50 cm/h was 5 hours. To subsequently wash the column of any non-specifically bound proteins (mimicking batch purification process, 8 CVs of washing is sufficient) would require an additional 2.5 hours. Assuming the proteases were also bound to the column and remained on the column with the target protein, we had to demonstrate that  $\alpha$ CD22scFv would remain intact for 7 hours at room temperature. Using batch in determine  $\alpha$ CD22scFv stability, clarified lysate was mixed for 7 hours with Capto Q at room temperature. The stability of the  $\alpha$ CD22scFv fragment during the Capto Q adsorption process can be found on the Western blot in Figure 15. Lanes 2-4 show the initial presence of  $\alpha$ CD22scFv at time zero and lanes 5-10 are samples taken after 7 hours. There were minor losses of the fragment during adsorption and washing of the resin (Lanes 5 and 6), but a majority of  $\alpha$ CD22scFv were concentrated in the elution fractions (Lanes 7-10). The strong single bands in the elution fractions indicate no measurable degradation of  $\alpha$ CD22scFv after being bound to Capto Q resin for 7 hours at room temperature.

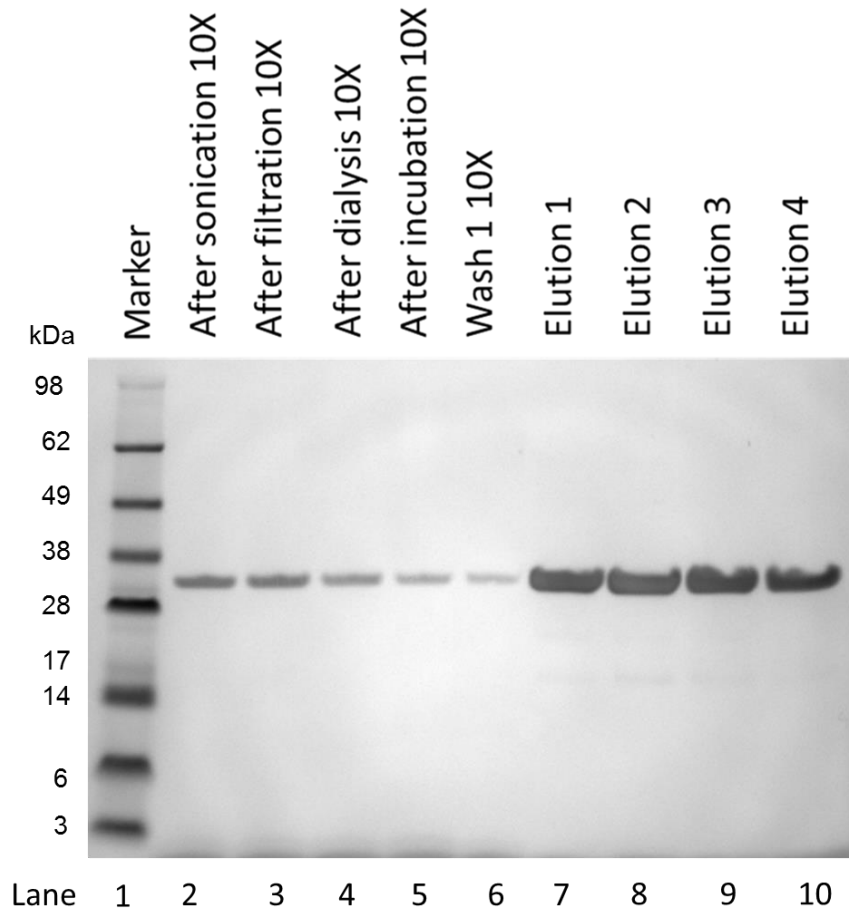


**Figure 15.** Stability of  $\alpha$ CD22scFv bound to Capto Q resin in clarified lysate for 7 hours at room temperature. Western Blot analysis of  $\alpha$ CD22scFv using anti-FLAG-AP conjugated antibody. Lane 1: molecular weight marker (kDa); Lane 2: 10X diluted supernatant after sonication of cells; Lane 3: 10X diluted supernatant after filtration through PES 0.22 $\mu$ m syringe filter; Lane 4: 10X diluted supernatant after dialysis; Lane 5: 10X diluted supernatant after 7 hours binding with anti-FLAG resin; Lane 6: 10X diluted washes before elution; Lane 7-10: 50mM Tris-base, 1M NaCl pH 8.0 eluted fractions.

### *3.4.2 Comparing effect of pretreatment methods with $\alpha$ CD22scFv adsorption to Capto Q and Phenyl Sepharose resin*

Our lab [34] previously analyzed the effects of three pretreatment methods (ammonium sulfate precipitation at pH 8.0, isoelectric precipitation at pH 4.5, and chitosan precipitation at pH 5.0) on residual chlorophyll, DNA, host cell protein, and  $\alpha$ CD22scFv yield (Table 2). Isoelectric precipitation was determined to be the ideal pretreatment method, with ammonium sulfate a close second choice, for significantly reducing the amount of chlorophyll and host cell protein, while maintaining a high  $\alpha$ CD22scFv yield. Even though there was a significant loss (35%) in recombinant protein after chitosan precipitation, the significant reduction in DNA, host cell protein, and chlorophyll prompted us to also evaluate chitosan pretreatment. Batch affinity adsorption was used to determine the amount of  $\alpha$ CD22scFv left in the supernatant after each pretreatment. Because we established that anti-FLAG-affinity resin is not an acceptable option for large scale purification. Each of these pretreatments evaluated was paired with most compatible non-affinity adsorption. After polymer precipitation and isoelectric precipitation, the conductivity of the pretreated sample is relatively low; therefore, the next logical step for capture chromatography would be AXC because of the acidic pI of  $\alpha$ CD22scFv (pI=4.5). Because 1M ammonium sulfate produces a high-conductivity lysate, the most logical step would be to bind the protein to HIC.

**Table 2.** Effect of pretreatment method stage of implementation on residual DNA, chlorophyll, host cell protein, and  $\alpha$ CD22scFv yield in algae extract. Values given are averages from 3 replicates  $\pm$  standard deviations. <sup>a,b,c,d,e</sup> For each observation that do not share a common superscript letter are significantly different from the control no pretreatment ( $P < 0.05$ ).

	Residual DNA (%)	Residual Chlorophyll (%)	Residual host cell protein (%)	$\alpha$ CD22 scFv Yield (%)
Control (No pre-treatment)	100 <sup>a</sup> $\pm$ 9.12	100 <sup>a</sup> $\pm$ 4.8	100 <sup>a</sup> $\pm$ 14.5	100 <sup>a</sup> $\pm$ 16.3
Ammonium sulfate precipitation (1M) at pH 8.0	100 <sup>a</sup> $\pm$ 1.3	60.1 <sup>b</sup> $\pm$ 6.3	56.7 <sup>b</sup> $\pm$ 6.7	87.5 <sup>a</sup> $\pm$ 5.06
Isoelectric precipitation at pH=4.5	91.7 <sup>a</sup> $\pm$ 7.6	28.4 <sup>c</sup> $\pm$ 14.7	31.1 <sup>c</sup> $\pm$ 9.3	118.8 <sup>a</sup> $\pm$ 21.8
Chitosan precipitation at pH=5.0	8.9 $\pm$ 7.9 <sup>b</sup>	1.4 <sup>d</sup> $\pm$ 1.1	18 <sup>d</sup> $\pm$ 7.1	66 <sup>c</sup> $\pm$ 7.4

Each pretreatment method was performed on the lysate and then incubated with its respective resin for 30 minutes at room temperature (uptake experiments in Appendix II). After adsorption to the respective resin, the bound protein was then eluted off the resin. The supernatants after batch adsorption and washing step for 1M ammonium sulfate (Figure 16a), chitosan precipitation (Figure 16b), and isoelectric precipitation (Figure 16c) were analyzed by western blotting. Finding  $\alpha$ CD22scFv in the supernatant after binding and in the wash is undesirable indicating a weak interaction between the FLAG-tagged protein and resin under those conditions (i.e. loss of  $\alpha$ CD22scFv during the purification process). Comparing the three Western blots, it is clear that the 1M ammonium sulfate pretreatment resulted in significant  $\alpha$ CD22scFv loss in both

supernatant and wash fractions (Figure 16a). Chitosan pretreatment affected primarily the adsorption of  $\alpha$ CD22scFv (Figure 16b). The Western blot in Figure 16c shows that isoelectric precipitation at pH 4.5 has the faintest band in the supernatant and washing fractions. This indicates that isoelectric precipitation-anion exchange chromatography is potentially the best pretreatment-capture step combination because almost all of  $\alpha$ CD22scFv binds to the resin and the binding is strong enough for the protein to remain on the resin after washing.

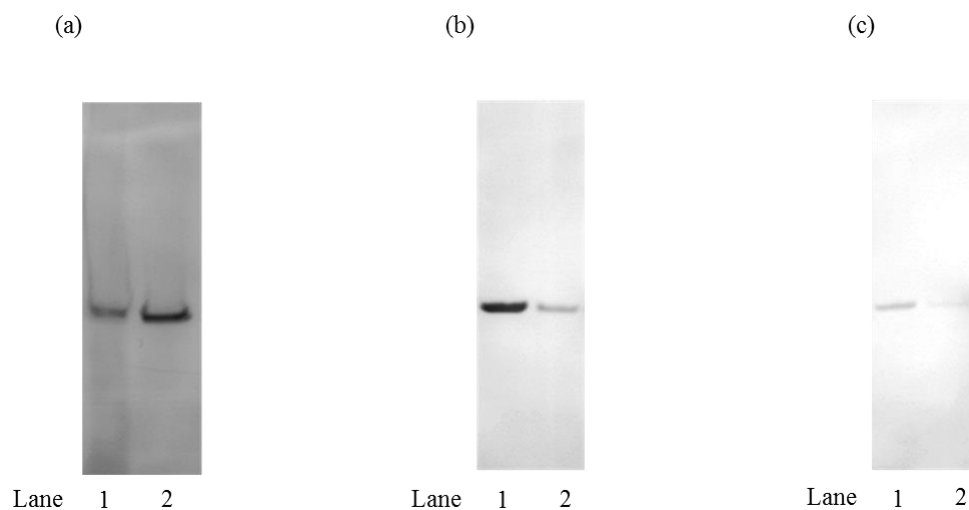


**Figure 16.** (a) 1M ammonium sulfate precipitation Western blot analysis of  $\alpha$ CD22scFv using anti-FLAG-AP conjugated antibody. Lane 1: supernatant after 30 minutes of binding with Phenyl Sepharose resin; Lane 2: wash of Phenyl Sepharose resin after 30 minutes of incubation with supernatant. (b) Chitosan precipitation Western blot analysis of  $\alpha$ CD22scFv using anti-FLAG-AP conjugated antibody. Lane 1: supernatant after 30 minutes of binding with Capto Q resin; Lane 2: wash of Capto Q resin after 30 minutes of incubation with supernatant. (c) Isoelectric precipitation at pH 4.5 Western blot analysis of  $\alpha$ CD22scFv using anti-FLAG-AP conjugated antibody. Lane 1: supernatant after 30 minutes of binding with Capto Q resin; Lane 2: wash of Capto Q resin after 30 minutes of incubation with supernatant.

Since isoelectric precipitation-Capto Q was identified as the best pretreatment-capture step combination, a SDS-PAGE (Figure 17a) and Western blot (Figure 17b) of the pretreatment and AXC process was performed to determine  $\alpha$ CD22scFv purity after the first capture step. The eluted fractions from AXC (Lanes 6-10) strongly reacted on the Western blot when probed with anti-FLAG-AP conjugated antibody. Furthermore, the elution fractions also have a reduced amount of total soluble protein, compared to the clarified lysate (Lane 2), indicating an increased purity of  $\alpha$ CD22scFv after the capture chromatography step. It is interesting to note that  $\alpha$ CD22scFv is detected by Western blot in all of the elution fractions (Lanes 6-10), suggesting a rather broad range of pIs for CD22scFv. Using anti-FLAG affinity resin to quantify the FLAG-tagged protein remaining in solution, it was determined that the AEX step yielded a CD22scFv purity of 1.7%. With a starting purity of 0.14% TSP, isoelectric precipitation followed by AXC provided a 12-fold increase in purity.

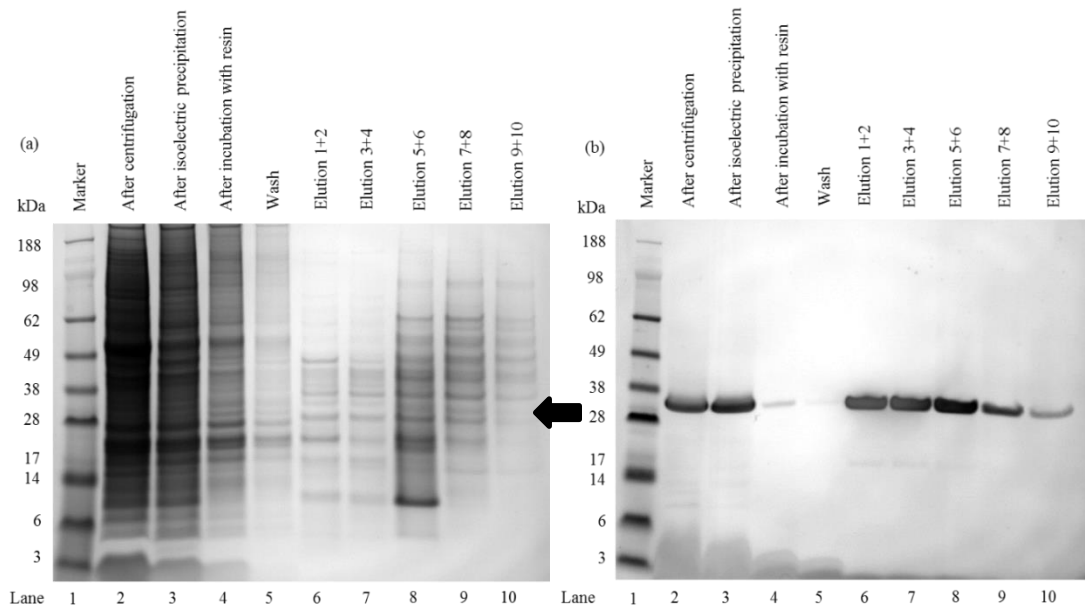


**Figure 17.** Purification of  $\alpha$ CD22scFv after isoelectric precipitation and AXC. (a) Coomassie-stained SDS-PAGE of  $\alpha$ CD22scFv. Lane 1: molecular weight marker (kDa); Lane 2: clarified algae extract; Lane 3: supernatant after isoelectric precipitation from pH 4.5 to pH 8.0; Lane 4: supernatant after 30 minutes of binding with Capto Q resin at room temperature; Lane 5: washing of Capto Q resin before elution; Lane 6-10: elution fractions by step-wise elutions with increasing concentrations of salt. (b) Western blot analysis of  $\alpha$ CD22scFv samples run on SDS-PAGE using anti-FLAG-AP conjugated antibody. Black arrow indicates  $\alpha$ CD22scFv.

### 3.4.3 Screening of Phenyl Sepharose and HAP as possible intermediate purification steps

To increase the purity of  $\alpha$ CD22scFv, an orthogonal chromatography step needs to be implemented. Elution fractions after AXC were pooled together. A final concentration of 1.5M ammonium sulfate was added to the pooled elution fractions and batch purified with Phenyl Sepharose resin for 30 minutes at room temperature. The

elution fractions were run on SDS-PAGE gels to analyze purity of the fractions (Figure 18). The first two elution fractions (Lanes 1 and 2) show very little protein in solution. Total soluble protein increases in the elution fractions as the conductivity of eluent decreases, with Lanes 8-10 containing the largest amounts of total protein. Even though the total protein detected on the SDS-PAGE increased as the conductivity of the elution buffer decreased, the elution of  $\alpha$ CD22scFv did not correlate in the same manner according to analysis of elutions run on the Western blot (Figure 19). The target protein comes off the resin as soon as the elution starts (Lanes 2 and 3). The intensity of the bands on the Western blot increases until Lane 5. However,  $\alpha$ CD22scFv is still detected in Lanes 6-10. Comparing the impurities in the SDS-PAGE to the  $\alpha$ CD22scFv response in the Western blot, it was determined that the first four elution fractions (Lanes 2-5) would provide the highest recombinant protein purity.

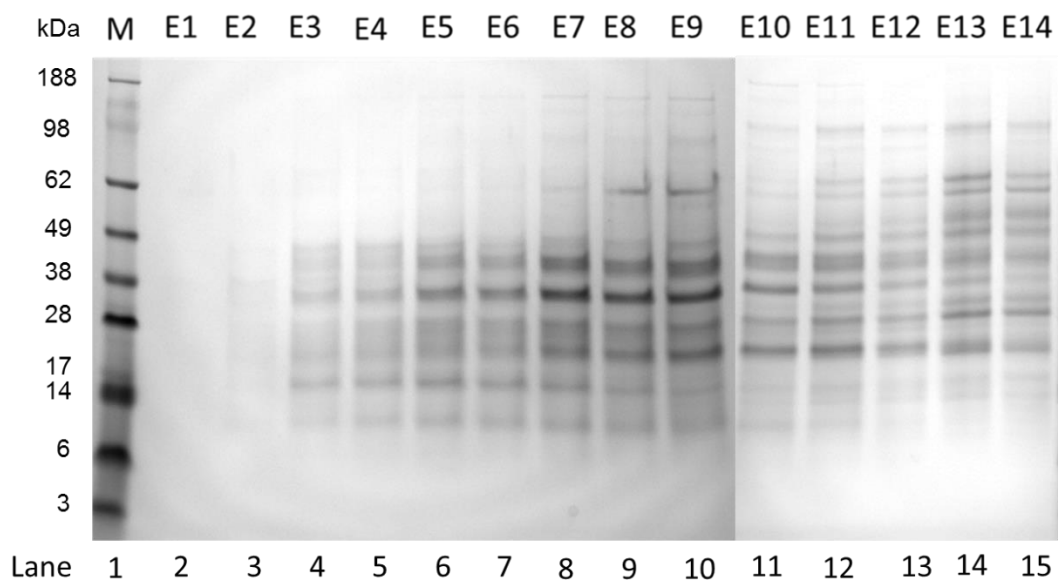


**Figure 18.** Purification of  $\alpha$ CD22scFv using Phenyl Sepharose resin as intermediate purification step after isoelectric precipitation and AXC. Coomassie-stained SDS-PAGE of  $\alpha$ CD22scFv. Lane 1: molecular weight marker (kDa); Lanes 2-3: 1.2M ammonium sulfate elution fractions; Lanes 4-5: 1.0M ammonium sulfate elution fractions; Lanes 6-7: 0.8M ammonium sulfate elution fractions; Lanes 8-9: 0.6M ammonium sulfate elution fractions; Lanes 10-11: 0.4M ammonium sulfate elution fractions; Lanes 12-13: 0.2M ammonium sulfate elution fractions; Lanes 14-15: 0M ammonium sulfate elution fractions. Black arrow indicates  $\alpha$ CD22scFv.

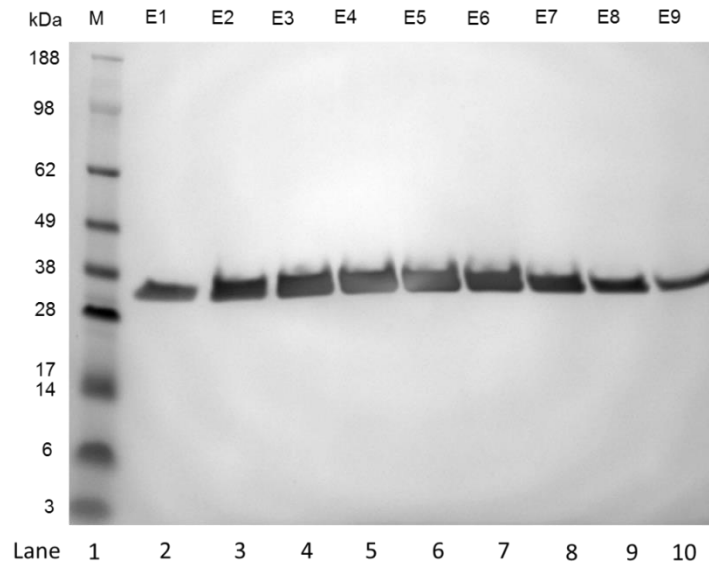


**Figure 19.** Western blot analysis of reduced  $\alpha$ CD22scFv using anti-FLAG-AP conjugated antibody after elution from Phenyl Sepharose resin as an orthogonal step to isoelectric precipitation at pH 4.5 and elution from Capto Q resin. Lane 1: molecular weight marker (kDa); Lanes 2-3: 1.2M ammonium sulfate elution fractions; Lanes 4-5: 1.0M ammonium sulfate elution fractions; Lanes 6-7: 0.8M ammonium sulfate elution fractions; Lanes 8-9: 0.6M ammonium sulfate elution fractions; Lane 10: 0.4M ammonium sulfate elution fractions.

The selected elution fractions (Lane 2-5) were pooled together and lyophilized to remove the water and concentrate all soluble proteins. The lyophilized proteins were resuspended in 0.5 mL RO water and run on an SDS-PAGE (Figure 20) to more accurately determine the purity of  $\alpha$ CD22scFv. The arrow identifies  $\alpha$ CD22scFv on the gel in comparison to the other proteins also in solution.

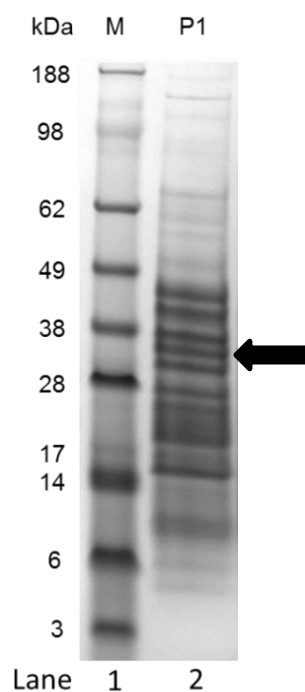


**Figure 20.** Coomassie-stained SDS-PAGE of highly concentrated  $\alpha$ CD22scFv after HIC as orthogonal chromatography step. Lane 1: molecular weight marker (kDa); Lane 2: concentrated pooled elution fractions (Lanes 2-5 from Figures 19 and 20). Black arrow indicates  $\alpha$ CD22scFv.

Based on the concentrated pool,  $\alpha$ CD22scFv is about 5% pure; only a 3-fold increase in purity from the isoelectric precipitation and anion exchange purification. After a pretreatment step and two chromatography steps, a final purity of only 5% is unacceptable (a minimum of 10-fold increase in purity is considered acceptable in manufacturing). Therefore, a different resin was screened as a possible orthogonal chromatography step to increase  $\alpha$ CD22scFv purity.

HAP is a mixed-mode chromatography resin commonly used for polishing purification of monoclonal antibodies and was tested as a possible orthogonal step after

isoelectric precipitation and AXC. Elution fractions 1-8 (Figure 17, Lanes 6-9) after isoelectric precipitation/AXC were pooled together and batch purified using HAP resin for 30 minutes at room temperature. Supernatants after batch adsorption, washing fractions, and elution fractions were qualitatively analyzed using SDS-PAGE gels (Figure 21a) and Western blots (Figure 21b).

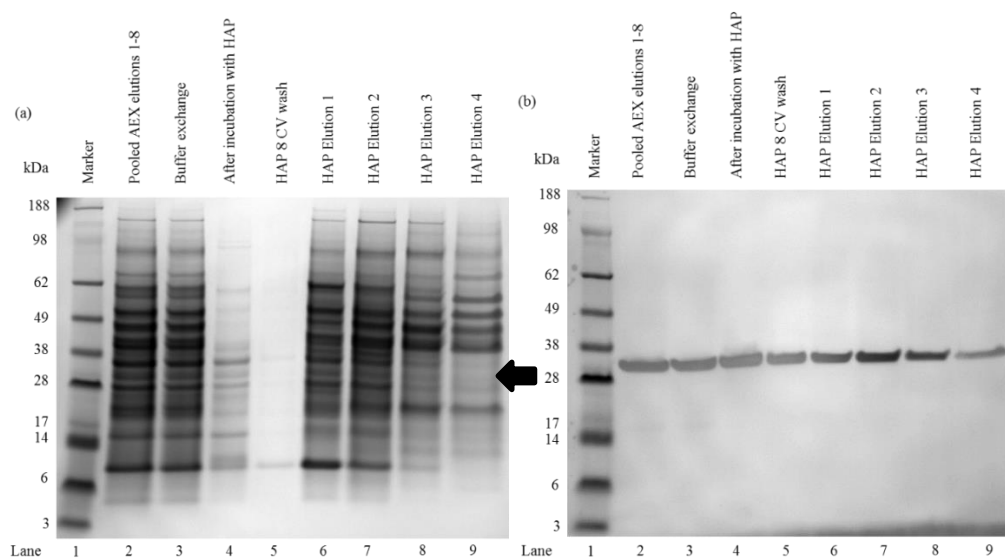


**Figure 21.** Purification of  $\alpha$ CD22scFv using HAP as intermediate purification step after isoelectric precipitation and AXC. (a) Coomassie-stained SDS-PAGE of reduced  $\alpha$ CD22scFv. Lane 1: molecular weight marker (kDa); Lane 2: Pooled elutions from Capto Q resin; Lane 3: partially purified sample after buffer exchange into 5mM sodium phosphate pH 6.8; Lane 4: supernatant after 30 minutes binding with HAP resin; Lane 5: washing HAP resin before elution; Lanes 6-7: 200mM sodium phosphate pH 6.8 elutions; Lane 8-9: 500mM sodium phosphate pH 6.8 elutions. (b) Western blot analysis of  $\alpha$ CD22scFv using anti-FLAG-AP conjugated antibody on same samples as SDS-PAGE.

Very little protein is detected by SDS-PAGE in the supernatant after purification with HAP and during the washing step. This means that a majority of the soluble proteins in the partially purified sample was bound to the resin. Elution fractions with 200mM sodium phosphate eluent (Lanes 6 and 7) contained a majority of the soluble proteins bound to the resin while the elution fractions with 500mM sodium phosphate (Lanes 8 and 9) contained the proteins that have the strongest affinity toward HAP resin (Figure 21a). Based on previous data,  $\alpha$ CD22scFv has shown to elute off the resin needing only 200mM sodium phosphate (data not shown). Unfortunately qualitative analysis of the Western blot (Figure 21b) shows Lanes 4 and 5 to contain thick, dark bands, indicating a substantial amount of  $\alpha$ CD22scFv not bound to the resin and washed off the resin. The main fractions capturing  $\alpha$ CD22scFv (Lanes 6 and 7) also had a large concentration of impurities, resulting in a low  $\alpha$ CD22scFv yield and purity after the orthogonal chromatography step. Therefore, HAP is not a suitable orthogonal chromatography step for intermediate purification of  $\alpha$ CD22scFv.

#### 3.4.4 Purification of $\alpha$ CD22scFv by Capto Q and FLAG-affinity chromatography

The bench scale purification process consisting of isoelectric precipitation and AXC was scaled up using AktaPurifier. The chromatogram of Capto Q purification of pretreated lysate is shown in Figure 22.

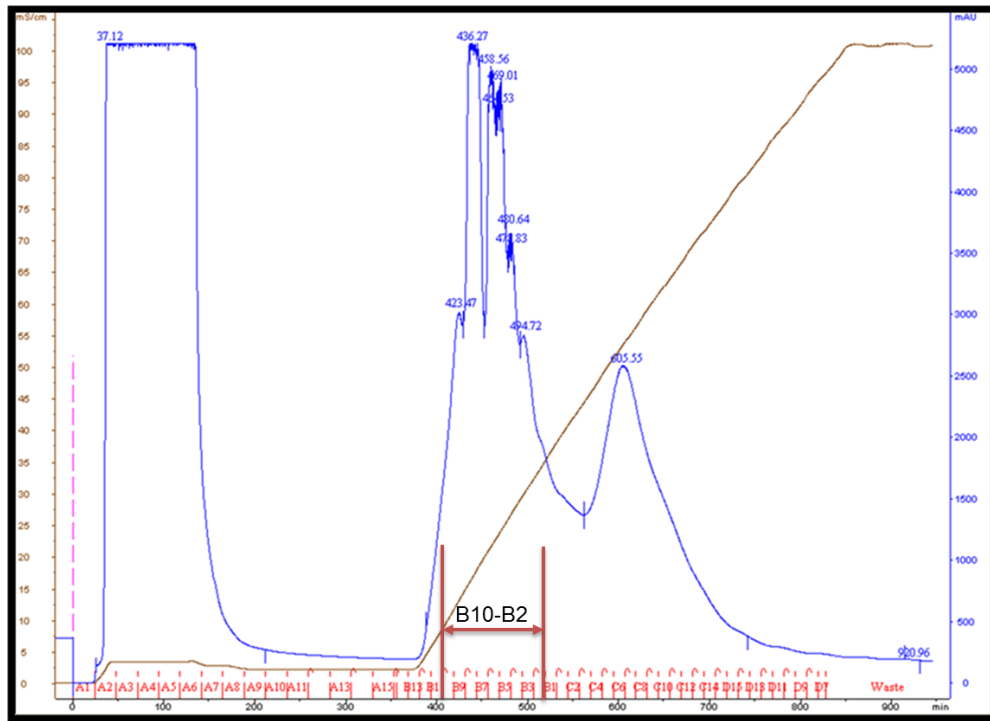


**Figure 22.** Chromatogram of *Chlamydomonas reinhardtii* and pretreated lysate purified using AXC Cpto Q resin. The chromatogram is plotted with absorbance at 280nm (mAU) and conductivity (mS/cm) against time (min). Sample Injection is marked by pink dashed line and each sample collected are labeled at the bottom of the chromatogram.

The flow through fractions (soluble protein that did not bind to the column) encompassed Fractions A2-A9, column wash fractions A10-A15. The elution gradient started at A15. Gradient elution resulted in several distinct peaks. In order to determine which peak contains  $\alpha$ CD22scFv, samples from selected fractions were run on a Western blot (Figure 23a). The same samples were also run on a SDS-PAGE to determine the purity (Figure 23b).

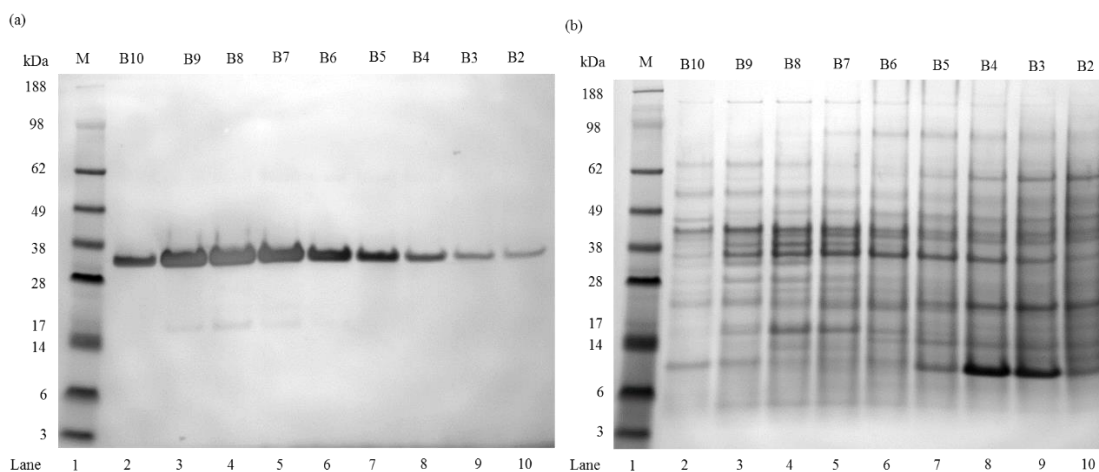


**Figure 23.** Analysis of fractions collected by AktaPurifier after binding and elution to Capto Q column. (a) Western blot analysis of  $\alpha$ CD22scFv using anti-FLAG-AP conjugated antibody. Lane 1: molecular weight marker (kDa); Lane 2-10: Fractions collected from AktaPurifier. (b) Coomassie-stained SDS-PAGE of same samples on Western blot.

The Western blot shows that  $\alpha$ CD22scFv eluted in fractions B10-B2 (between conductivities 10 and 35 mS/cm). The wide distribution of  $\alpha$ CD22scFv can be explained by the range of isoelectric points pI 4.5-5 found in  $\alpha$ CD22scFv determined by 2-D electrophoresis (See Appendix III). The SDS-PAGE showed an initial low concentration of soluble proteins but as the conductivity of the eluent increased, so did the concentration of impurities. To minimize the loading volume onto anti-FLAG-affinity resin, only fractions B10-B5 (Lanes 2-7) were pooled and run on the affinity column. The 12mL pooled sample was loaded on a 12mL FLAG affinity column at a linear velocity of 3 cm/h and 4°C. The low linear velocity was used to ensure a 2 hour contact time of  $\alpha$ CD22scFv with the resin. A chromatogram of the FLAG purified sample is shown in Figure 24.

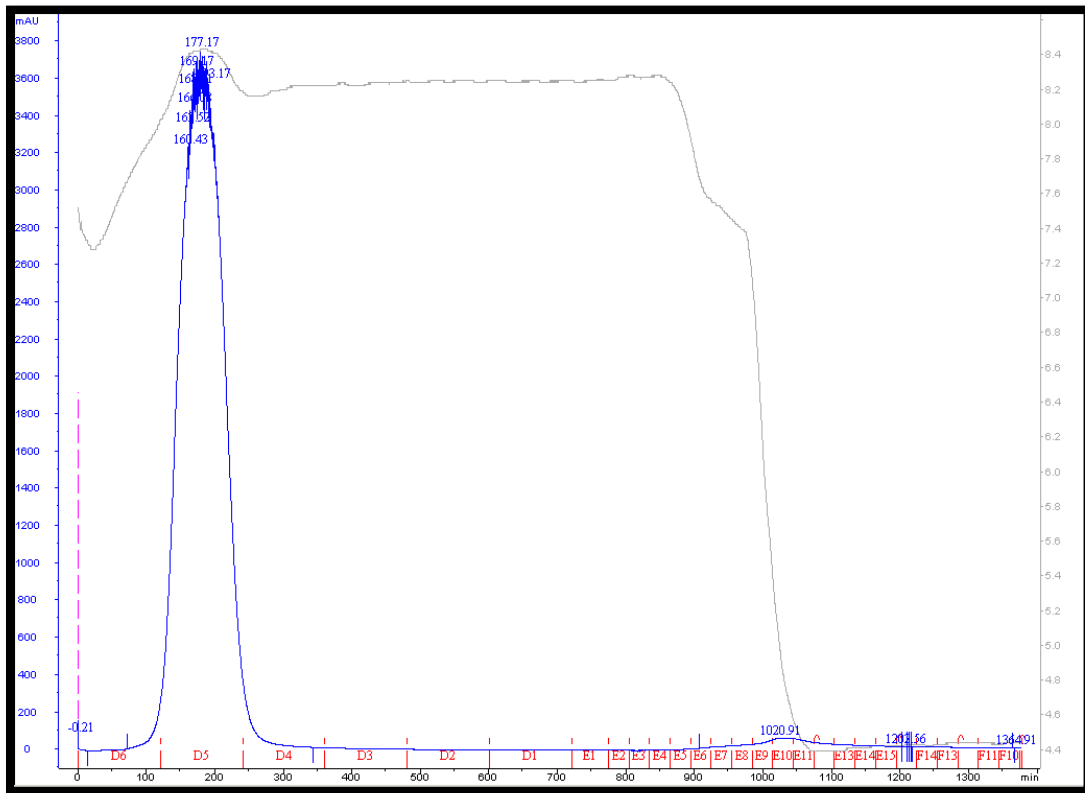


**Figure 24.** Chromatogram of partially purified *Chlamydomonas reinhardtii*  $\alpha$ CD22scFv, by Capto Q resin, further purified using anti-FLAG affinity resin. The chromatogram is plotted with absorbance at 280nm (mAU) against time (min). Injection of sample is marked by pink dashed line and fractions collected are noted at the bottom of the chromatogram.

Two peaks are shown on the chromatogram, the first coming out mainly in fraction D5 and the other is distributed over fractions E6-E14. The first peak contains algal proteins that did not bind to the anti-FLAG resin. The second peak was eluted during the pH-step change from pH 7.5 to pH 4.4. The fractions under each peak were concentrated and run on a Western blot (Figure 25a) and a SDS-PAGE (Figure 25b).

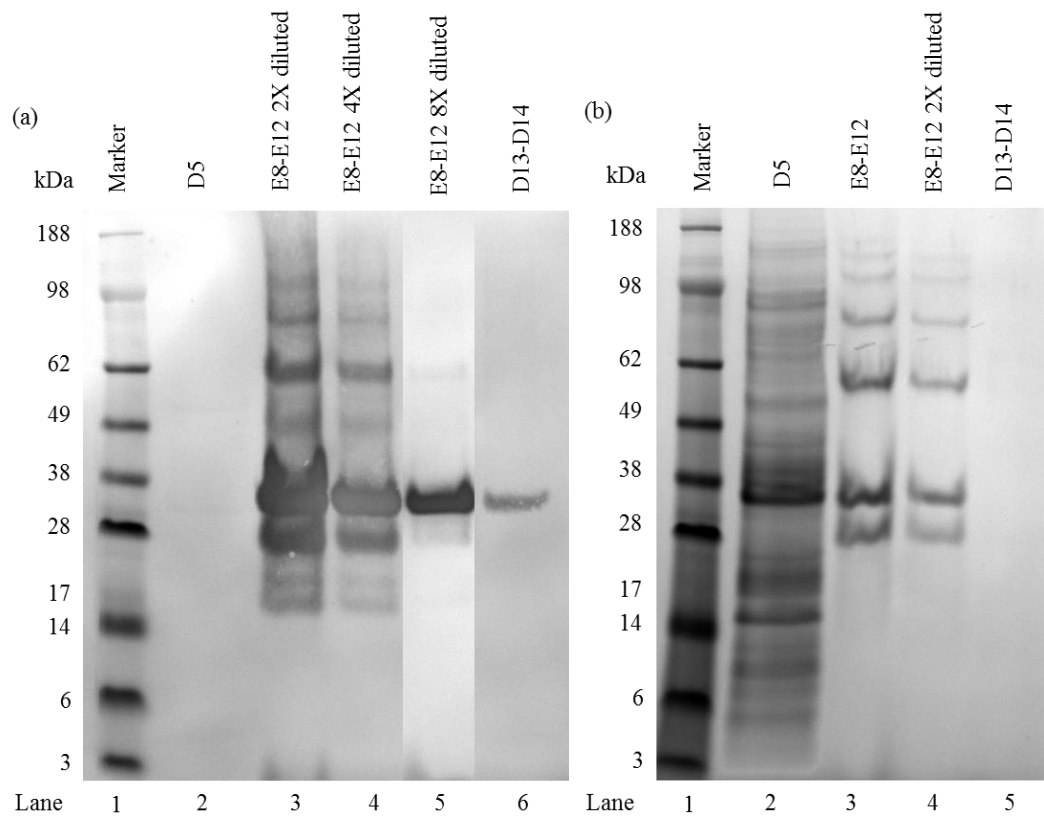


**Figure 25.** (a) Western blot analysis of concentrated  $\alpha$ CD22scFv using anti-FLAG-AP conjugated antibody. Lane 1: molecular weight marker (kDa); Lane 2: concentrated Fraction D5; Lane 3: 2X diluted pooled Fractions E8-E12; Lane 4: 4X diluted pooled Fractions E8-E12; Lane 5: 8X diluted pooled Fractions E8-E12; Lane 6: concentrated pooled Fractions D13-D14. (b) Coomassie-stained SDS-PAGE of concentrated  $\alpha$ CD22scFv purified with FLAG affinity chromatography. Lane 1: molecular weight marker (kDa); Lane 2: concentrated Fraction D5; Lane 3: concentrated pooled Fractions E8-E12; Lane 4: 2X diluted pooled Fractions E8-E12; Lane 5: concentrated pooled Fractions D13-D14.

Analysis of the Western blot showed that  $\alpha$ CD22scFv was completely bound to the FLAG-affinity resin since there was no cross-reaction band in Lane 2 when probed with the anti-FLAG-AP conjugated antibody. The pooled elution fractions (Lanes 3-5) of the same sample were analyzed at different dilutions to qualitatively compare  $\alpha$ CD22scFv band thickness to the other bands in the lane. The eluted peak (Lanes 3-5) shows multiple bands on the SDS-PAGE, indicating multiple sized proteins are found in the sample. However, the same sample run on the Western blot also shows multiple bands similar to the bands on the SDS-PAGE. Therefore, the bands on the SDS-PAGE are all FLAG-tagged proteins. The eluted peak purified by FLAG-affinity resin contains highly purified  $\alpha$ CD22scFv (Table 3).

**Table 3.** Purity and yield of  $\alpha$ CD22scFv after each clarification/chromatography step.

Sample	Process step	Purity	Purification fold	Yield
Clarified lysate	Initial	0.14%	1	100%
Isoelectric precipitation at pH 4.5	Pretreatment	0.4%	2.9	100%
Anion exchange chromatography	Capture	1.7%	12	78%
FLAG-affinity chromatography	Polishing	>98% FLAG-tagged proteins (~50% monomeric form)	700	~77% (~40% monomeric form)

Pretreatment resulted in a 3-fold enrichment of  $\alpha$ CD22scFv and AEX in an additional 4-fold enrichment. As expected, significant increase in purification was achieved during affinity step, which resulted in 700-fold enhancement. A final  $\alpha$ CD22scFv yield of 77% and >98% purity are incredibly good results, especially since the initial product titer was so low, larger losses in yield could have easily occurred.

### 3.5 Summary

Single-chain antibody fragments are becoming a more promising possibility for pharmaceutical industries because they can be produced quicker and cheaper than full-size antibodies while still maintaining the target specificity of whole mAbs. Being only a fraction of mAbs (~30kDa), provides the fragments with several advantages such as, rapid and deep penetration into tissues and tumors, and numerous therapeutic applications when bound or fused to other fragments or molecules. Since scFvs are small in size, simple in structure, and non-glycosylated, the chloroplast of eukaryotic microalgae *C. reinhardtii* could be a potential production system for scFvs.

Our lab previously analyzed the effects of three pretreatment methods (ammonium sulfate precipitation at pH 8.0, isoelectric precipitation at pH 4.5, and chitosan precipitation at pH 5.0) on residual chlorophyll, DNA, host cell protein, and  $\alpha$ CD22scFv yield. Isoelectric precipitation was determined to be the ideal pretreatment method, with ammonium sulfate a close second choice. Both methods significantly reduced the amount of chlorophyll and host cell protein, while maintaining a high  $\alpha$ CD22scFv yield. Even though the pretreatment methods have been shown to benefit protein recovery, no

previous research has been done with algal extracts to show their effects on downstream processing. Therefore, this study tested the effect of the pretreatment methods on purification of  $\alpha$ CD22scFv using the two commercial resins, Phenyl Sepharose and Capto Q.

At 1M ammonium sulfate, a large percentage of the target protein came off the resin during the wash; indicating that the hydrophobicity of  $\alpha$ CD22scFv at 1M ammonium sulfate was not strong enough to bind to the resin. Using 1M ammonium sulfate as a pretreatment method before capture chromatography provides little to no effect on downstream processing, it only increases the final production cost. However, chitosan and isoelectric precipitation yielded the same final purity. Unfortunately, anion exchange chromatography could not capture all of the target protein after chitosan precipitation and some of the target protein was non-specifically bound to the resin and came out in the wash. Therefore, it was concluded that the isoelectric precipitation-anion exchange chromatography combination was the best for initial recovery and concentration of  $\alpha$ CD22scFv.

After the AEX capture step  $\alpha$ CD22scFv was 1.7%, a 4-fold increase from precipitation step in purity which is a reasonable increase for a capture step. To increase the final purity an orthogonal chromatography step was implemented using Phenyl Sepharose resin using a final concentration of 1.5M ammonium sulfate. Even with the increased concentration of ammonium sulfate, not all of  $\alpha$ CD22scFv bound to the HIC resin and still some of the target protein was non-specifically bound to the column and came off during the wash. The final purity of the cleanest elution fractions was only 5%,

an unacceptable purity after a pretreatment method and 2 chromatography steps. A second attempt of scouting an orthogonal chromatography step to further purify  $\alpha$ CD22scFv was made by using HAP resin. Not only did HAP fail to completely take up  $\alpha$ CD22scFv from the partially purified solution, a bit larger proportion of the protein came off the column during the washing step before elution. Also,  $\alpha$ CD22scFv eluted off the column with other impurities, resulting in a poor yield. Therefore, no viable orthogonal non-affinity chromatographic step was identified.

The batch purification process of isoelectric precipitation, AXC, and FLAG-affinity chromatography was scaled up using AktaPurifier. By pooling and running the partially purified elution fractions through a FLAG-affinity column, yielded highly purified  $\alpha$ CD22scFv (>98% purity).

## CHAPTER IV

### CONCLUSIONS AND RECOMMENTATIONS

#### 4.1 Conclusions

The chloroplast of eukaryotic green algae has shown its ability to produce correctly folded complex recombinant proteins. This study attempted to better understand downstream processing of acidic proteins in algal lysate. The research increased the current scientific knowledge on the viability of microalgae as possible commercial platforms for recombinant proteins. The major challenges identified in this study were: (i) extremely low transgene expression levels, (ii) broad range of charge variances of target proteins, and (iii) trouble separating the acidic recombinant protein from impurities, mainly rubisco, which is almost identical to the recombinant protein in size and charge.

Our collaborators, Mayfield's laboratory in San Diego, California, proved that a malaria transmission blocking vaccine (TBV), Pfs25, and a single-chained antibody,  $\alpha$ CD22scFv, were correctly produced in the chloroplast of *Chlamydomonas reinhardtii*. Gregory reported that affinity-purified Pfs25 was cross-reacting with anti-Pfs25-mAb 4B7 at a 4×higher molecular weight than expected. Pfs25 has shown success of high immunogenicity in humans and transmission blocking activity when produced in other expression systems (like yeast and tobacco). However, to further drive down the cost of production, algae is an excellent potential candidate for cheaply made Pfs25. Therefore, Chapter II of this research is dedicated to increasing the accumulation of Pfs25 in the

chloroplast of *C. reinhardtii* and to characterize the size and stability of higher molecular weight Pfs25 proteins reported by Gregory and Vinetz. By suspending algal cells in fresh media after 5 days of growth, 24 hours before exposure to light, the accumulation of Pfs25 increased 1.7-fold. The affinity-purified Pfs25 was separated on a size exclusion column (SEC) and, based off the calibration curve of the column, the size of the aggregates ranged in size from 25 kDa to >600 kDa. The aggregates were found to remain intact even in the presence of reducing agents and detergent. Another concern of ours was that the aggregates were being formed during the low pH elution step during affinity-purification. Therefore, FLAG-peptide was used to desorb Pfs25 from the column at neutral pH. The eluted protein was separated on the SEC and even though the profile of the chromatogram was different, high molecular weight proteins >600 kDa were still found in the FLAG-peptide eluted Pfs25 sample. The Pfs25 complexes were not exclusively formed during the low pH elution step. Previous research on Pfs25 (no matter the expression system) has shown that Pfs25 in its monomeric form does not induce an immunogenic response. Therefore, researchers must either chemically conjugate Pfs25 to itself or other proteins or combine it with an adjuvant. Algae, since Pfs25 has shown it naturally forms complexes of itself, could have the potential of inducing an immunogenic. Therefore, the immunogenicity of Pfs25 complexes should be studied to further understand the viability of using microalgae as a possible production platform for recombinant proteins.

Previously our lab studied different process variables affecting extraction and recovery of recombinant protein in algal lysate. It was determined that out of three

pretreatment options studied (chitosan precipitation, ammonium sulfate precipitation, and isoelectric precipitation), ammonium sulfate and isoelectric precipitation significantly reduced residual chlorophyll and host cell proteins while recovering a large portion of  $\alpha$ CD22scFv. The pretreatment options were compared using anti-FLAG-affinity resin as a quantitative method. Unfortunately, FLAG-affinity resin is not a practical resin for commercial use due to it being extremely expensive, has a low binding capacity, and is easily compressible. Therefore, in Chapter III of this research, compares the three pretreatment methods on its effects on  $\alpha$ CD22scFv adsorption to non-affinity commercial resins, Capto Q and Phenyl Sepharose. It was determined that isoelectric precipitation at pH 4.5 and anion exchange chromatography combination was the best for initial recovery and concentration of  $\alpha$ CD22scFv, resulting in a 12-fold increase in purity of  $\alpha$ CD22scFv. Hydroxyapatite resin and Phenyl Sepharose resin were then scouted to further increase the purity of  $\alpha$ CD22scFv; unfortunately no viable orthogonal non-affinity chromatographic step was identified. Using FLAG-affinity resin after isoelectric precipitation and AXC resulted in a purity of  $\alpha$ CD22scFv >98% and a 77% yield.

## **4.2 Recommendations**

The suggestions for future work include:

1. Increase the expression level of both Pfs25 and  $\alpha$ CD22scFv.
2. Study the immunogenic response of Pfs25 complexes in mice.

3. To screen more resins as possible intermediate purification chromatography steps, to hopefully remove affinity chromatography entirely from the purification process.

## REFERENCES

1. Dove, A., *Uncorking the biomanufacturing bottleneck*. Nature biotechnology, 2002. **20**(8): p. 777-779.
2. Gregory, J.A., et al., *Algae-produced Pfs25 elicits antibodies that inhibit malaria transmission*. PLoS One, 2012. **7**(5): p. e37179.
3. Tran, M., et al., *Production of unique immunotoxin cancer therapeutics in algal chloroplasts*. Proceedings of the National Academy of Sciences, 2013. **110**(1): p. E15-E22.
4. Mayfield, S.P., S.E. Franklin, and R.A. Lerner, *Expression and assembly of a fully active antibody in algae*. Proceedings of the National Academy of Sciences, 2003. **100**(2): p. 438-442.
5. Tran, M., et al., *Synthesis and assembly of a full-length human monoclonal antibody in algal chloroplasts*. Biotechnology and bioengineering, 2009. **104**(4): p. 663-673.
6. Rasala, B.A. and S.P. Mayfield, *The microalga Chlamydomonas reinhardtii as a platform for the production of human protein therapeutics*. Bioengineered bugs, 2011. **2**(1): p. 50-54.
7. Dauvillée, D., et al., *Engineering the chloroplast targeted malarial vaccine antigens in Chlamydomonas starch granules*. PLoS One, 2010. **5**(12): p. e15424.
8. Wurm, F.M., *Production of recombinant protein therapeutics in cultivated mammalian cells*. Nature biotechnology, 2004. **22**(11): p. 1393-1398.
9. Zhang, H., et al., *Engineering considerations for process development in mammalian cell cultivation*. Current pharmaceutical biotechnology, 2010. **11**(1): p. 103-112.
10. Adamson, S., *Experiences of virus, retrovirus and retrovirus-like particles in Chinese hamster ovary (CHO) and hybridoma cells used for production of protein therapeutics*. Developments in biological standardization, 1997. **93**: p. 89-96.
11. Swartz, J.R., *Advances in Escherichia coli production of therapeutic proteins*. Current Opinion in Biotechnology, 2001. **12**(2): p. 195-201.

12. Baneyx, F. and M. Mujacic, *Recombinant protein folding and misfolding in Escherichia coli*. Nature biotechnology, 2004. **22**(11): p. 1399-1408.
13. Decker, E.L. and R. Reski, *The moss bioreactor*. Current opinion in plant biology, 2004. **7**(2): p. 166-170.
14. Twyman, R.M., *Host plants, systems and expression strategies for molecular farming*. Molecular Farming: Plant-Made Pharmaceuticals and Technical Proteins, 2006: p. 338.
15. Twyman, R.M., et al., *Molecular farming in plants: host systems and expression technology*. TRENDS in Biotechnology, 2003. **21**(12): p. 570-578.
16. Rasala, B.A., et al., *Production of therapeutic proteins in algae, analysis of expression of seven human proteins in the chloroplast of Chlamydomonas reinhardtii*. Plant biotechnology journal, 2010. **8**(6): p. 719-733.
17. Rosenberg, J.N., et al., *A green light for engineered algae: redirecting metabolism to fuel a biotechnology revolution*. Current opinion in Biotechnology, 2008. **19**(5): p. 430-436.
18. Potvin, G. and Z. Zhang, *Strategies for high-level recombinant protein expression in transgenic microalgae: a review*. Biotechnology advances, 2010. **28**(6): p. 910-918.
19. Griesbeck, C., I. Kobl, and M. Heitzer, *Chlamydomonas reinhardtii*. Molecular biotechnology, 2006. **34**(2): p. 213-223.
20. Kukuruzinska, M. and K. Lennon, *Protein N-glycosylation: molecular genetics and functional significance*. Critical Reviews in Oral Biology & Medicine, 1998. **9**(4): p. 415-448.
21. Porro, D., et al., *Recombinant protein production in yeasts*. Molecular biotechnology, 2005. **31**(3): p. 245-259.
22. Eichler-Stahlberg, A., et al., *Strategies to facilitate transgene expression in Chlamydomonas reinhardtii*. Planta, 2009. **229**(4): p. 873-883.
23. Lauersen, K.J., et al., *Efficient recombinant protein production and secretion from nuclear transgenes in Chlamydomonas reinhardtii*. Journal of biotechnology, 2013. **167**(2): p. 101-110.
24. Faye, L. and H. Daniell, *Novel pathways for glycoprotein import into chloroplasts*. Plant biotechnology journal, 2006. **4**(3): p. 275-279.

25. Liu, H.F., et al. *Recovery and purification process development for monoclonal antibody production*. in *MAbs*. 2010. Taylor & Francis.
26. Hughes, J., D. Ramsden, and K. Symes, *The flocculation of bacteria using cationic synthetic flocculants and chitosan*. *Biotechnology techniques*, 1990. **4**(1): p. 55-60.
27. Persson, I. and B. Lindman, *Flocculation of cell debris for improved separation by centrifugation*. *Flocculation in Biotechnology and Separation Systems*, Elsevier, Amsterdam, 1987: p. 457-466.
28. Kumar, A., I.Y. Galaev, and B. Mattiasson, *Precipitation of proteins: non specific and specific*. *Isolation and purification of proteins*. CRC Press, Boca Raton, 2003: p. 225-276.
29. Bermejo, R., E. Ruiz, and F. Acien, *Recovery of B-phycoerythrin using expanded bed adsorption chromatography: Scale-up of the process*. *Enzyme and microbial technology*, 2007. **40**(4): p. 927-933.
30. Bermejo, R., E.M. Talavera, and J.C. Orte, *Chromatographic purification of biliproteins from Spirulina platensis high-performance liquid chromatographic separation of their  $\alpha$  and  $\beta$  subunits*. *Journal of Chromatography A*, 1997. **778**(1): p. 441-450.
31. Rossano, R., et al., *Extracting and purifying R-phycoerythrin from Mediterranean red algae Corallina elongata Ellis & Solander*. *Journal of biotechnology*, 2003. **101**(3): p. 289-293.
32. Jian-Feng, N., et al., *Large-scale recovery of C-phycoerythrin from Spirulina platensis using expanded bed adsorption chromatography*. *Journal of Chromatography B*, 2007. **850**(1): p. 267-276.
33. Patra, K.P., et al., *Algae-produced malaria transmission-blocking vaccine candidate Pfs25 formulated with a human use-compatible potent adjuvant induces high affinity antibodies that block Plasmodium falciparum infection of mosquitoes*. *Infection and immunity*, 2015: p. IAI. 02980-14.
34. Munjal, N., *Evaluation of extraction conditions and pretreatment methods for production of an antibody fragment from Chlamydomonas reinhardtii*. 2014.
35. Achan, J., et al., *Quinine, an old anti-malarial drug in a modern world: role in the treatment of malaria*. *Malaria Journal*, 2011. **10**(1): p. 144.

36. Sharma, B., *Structure and mechanism of a transmission blocking vaccine candidate protein Pfs25 from P. falciparum: a molecular modeling and docking study*. In silico biology, 2008. **8**(3-4): p. 193-206.
37. Miller, L.H., et al., *Research toward malaria vaccines*. Science, 1986. **234**(4782): p. 1349-56.
38. Zavala, F., et al., *Synthetic peptide vaccine confers protection against murine malaria*. The Journal of Experimental Medicine, 1987. **166**(5): p. 1591-1596.
39. *First Results of Phase 3 Trial of RTS,S/AS01 Malaria Vaccine in African Children*. New England Journal of Medicine, 2011. **365**(20): p. 1863-1875.
40. *A Phase 3 Trial of RTS,S/AS01 Malaria Vaccine in African Infants*. New England Journal of Medicine, 2012. **367**(24): p. 2284-2295.
41. Jones, R.M., et al., *A plant-produced Pfs25 VLP malaria vaccine candidate induces persistent transmission blocking antibodies against Plasmodium falciparum in immunized mice*. PLoS one, 2013. **8**(11): p. e79538.
42. Miyata, T., et al., *Plasmodium vivax ookinete surface protein Pvs25 linked to cholera toxin B subunit induces potent transmission-blocking immunity by intranasal as well as subcutaneous immunization*. Infection and immunity, 2010. **78**(9): p. 3773-3782.
43. The mal, E.R.A.C.G.o.V., *A Research Agenda for Malaria Eradication: Vaccines*. PLoS Med, 2011. **8**(1): p. e1000398.
44. Outchkourov, N.S., et al., *Correctly folded Pfs48/45 protein of Plasmodium falciparum elicits malaria transmission-blocking immunity in mice*. Proceedings of the National Academy of Sciences, 2008. **105**(11): p. 4301-4305.
45. Chowdhury, D.R., et al., *A Potent Malaria Transmission Blocking Vaccine Based on Codon Harmonized Full Length Pfs48/45 Expressed in Escherichia coli*. PLoS ONE, 2009. **4**(7): p. e6352.
46. Tachibana, M., et al., *N-Terminal Prodomain of Pfs230 Synthesized Using a Cell-Free System Is Sufficient To Induce Complement-Dependent Malaria Transmission-Blocking Activity*. Clinical and Vaccine Immunology : CVI, 2011. **18**(8): p. 1343-1350.
47. Kaslow, D.C., et al., *A vaccine candidate from the sexual stage of human malaria that contains EGF-like domains*. Nature, 1988. **333**(6168): p. 74-6.

48. Barr, P.J., et al., *Recombinant Pfs25 protein of Plasmodium falciparum elicits malaria transmission-blocking immunity in experimental animals*. The Journal of experimental medicine, 1991. **174**(5): p. 1203-8.
49. Gozar, M.M.G., V.L. Price, and D.C. Kaslow, *Saccharomyces cerevisiae-Secreted Fusion Proteins Pfs25 and Pfs28 Elicit Potent Plasmodium falciparum Transmission-Blocking Antibodies in Mice*. Infection and Immunity, 1998. **66**(1): p. 59-64.
50. Paton, M.G., et al., *Structure and expression of a post-transcriptionally regulated malaria gene encoding a surface protein from the sexual stages of Plasmodium berghei*. Molecular and biochemical parasitology, 1993. **59**(2): p. 263-75.
51. Fries, H.C., et al., *Biosynthesis of the 25-kDa protein in the macrogametes/zygotes of Plasmodium falciparum*. Experimental Parasitology, 1990. **71**(2): p. 229-35.
52. Kaslow, D.C., et al., *Induction of Plasmodium falciparum transmission-blocking antibodies by recombinant Pfs25*. Memorias do Instituto Oswaldo Cruz, 1992. **87**: p. 175-177.
53. Kumar, R., E. Angov, and N. Kumar, *Potent Malaria Transmission-Blocking Antibody Responses Elicited by Plasmodium falciparum Pfs25 Expressed in Escherichia coli after Successful Protein Refolding*. Infection and Immunity, 2014. **82**(4): p. 1453-1459.
54. Kaslow, D.C., et al., *Saccharomyces cerevisiae recombinant Pfs25 adsorbed to alum elicits antibodies that block transmission of Plasmodium falciparum*. Infection and immunity, 1994. **62**(12): p. 5576-80.
55. Kaslow, D.C. and J. Shiloach, *Production, purification and immunogenicity of a malaria transmission-blocking vaccine candidate: TBV25H expressed in yeast and purified using nickel-NTA agarose*. Nature Biotechnology, 1994. **12**(5): p. 494-499.
56. Gozar, M.M.G., et al., *Plasmodium falciparum: immunogenicity of alum-adsorbed clinical-grade TBV25–28, a yeast-secreted malaria transmission-blocking vaccine candidate*. Experimental parasitology, 2001. **97**(2): p. 61-69.
57. Carter, R. and A. Stowers, *Current developments in malaria transmission-blocking vaccines*. Expert opinion on biological therapy, 2001. **1**(4): p. 619-628.

58. Zou, L., et al., *Expression of malaria transmission-blocking vaccine antigen Pfs25 in Pichia pastoris for use in human clinical trials*. *Vaccine*, 2003. **21**(15): p. 1650-1657.
59. Wu, Y., et al., *Phase I trial of malaria transmission blocking vaccine candidates Pfs25 and Pvs25 formulated with montanide ISA 51*. *PLoS ONE*, 2008. **3**(7): p. e2636.
60. Wu, Y., et al., *Sustained high-titer antibody responses induced by conjugating a malarial vaccine candidate to outer-membrane protein complex*. *Proceedings of the National Academy of Sciences of the United States of America*, 2006. **103**(48): p. 18243-8.
61. Kubler-Kielb, J., et al., *Long-lasting and transmission-blocking activity of antibodies to Plasmodium falciparum elicited in mice by protein conjugates of Pfs25*. *Proceedings of the National Academy of Sciences*, 2007. **104**(1): p. 293-298.
62. Qian, F., et al., *Conjugating recombinant proteins to Pseudomonas aeruginosa ExoProtein A: a strategy for enhancing immunogenicity of malaria vaccine candidates*. *Vaccine*, 2007. **25**(20): p. 3923-33.
63. Shimp, R.L., et al., *Development of a Pfs25-EPA malaria transmission blocking vaccine as a chemically conjugated nanoparticle*. *Vaccine*, 2013. **31**(28): p. 2954-2962.
64. Qian, F., et al., *Addition of CpG ODN to recombinant Pseudomonas aeruginosa ExoProtein A conjugates of AMA1 and Pfs25 greatly increases the number of responders*. *Vaccine*, 2008. **26**(20): p. 2521-7.
65. ClinicalTrials.gov. *Initial Study of Malaria VAccine Pfs25-EPA/Alhydrogel*. 2013 [cited 2015 April 6]; Available from: <https://clinicaltrials.gov/ct2/show/NCT01434381?term=Pfs25-EPA&rank=2>.
66. Davidson, E.A. and D.C. Gowda, *Glycobiology of Plasmodium falciparum*. *Biochimie*, 2001. **83**(7): p. 601-604.
67. Gowda, D. and E. Davidson, *Protein glycosylation in the malaria parasite*. *Parasitology today*, 1999. **15**(4): p. 147-152.
68. Tsai, C.W., et al., *Overproduction of Pichia pastoris or Plasmodium falciparum protein disulfide isomerase affects expression, folding and O-linked glycosylation of a malaria vaccine candidate expressed in P. pastoris*. *Journal of biotechnology*, 2006. **121**(4): p. 458-470.

69. Farrance, C.E., et al., *Antibodies to plant-produced Plasmodium falciparum sexual stage protein Pfs25 exhibit transmission blocking activity*. Human vaccines, 2011. **7**(sup1): p. 191-198.
70. Jones, R.M., et al., *A novel plant-produced Pfs25 fusion subunit vaccine induces long-lasting transmission blocking antibody responses*. Human vaccines & immunotherapeutics, 2014(ahead-of-print).
71. Mayfield, S.P., et al., *Chlamydomonas reinhardtii chloroplasts as protein factories*. Current Opinion in Biotechnology, 2007. **18**(2): p. 126-133.
72. Lai, H., et al., *Monoclonal antibody produced in plants efficiently treats West Nile virus infection in mice*. Proceedings of the National Academy of Sciences, 2010. **107**(6): p. 2419-2424.
73. Barros, G.O., S.L. Woodard, and Z.L. Nikolov, *Phenolics removal from transgenic Lemna minor extracts expressing mAb and impact on mAb production cost*. Biotechnology progress, 2011. **27**(2): p. 410-418.
74. Woodard, S.L., et al., *Evaluation of monoclonal antibody and phenolic extraction from transgenic Lemna for purification process development*. Biotechnology and bioengineering, 2009. **104**(3): p. 562-571.
75. Garger, S.J., et al., *Process for isolating and purifying viruses, soluble proteins and peptides from plant sources*. 2000, Google Patents.
76. Nelson, A.L. and J.M. Reichert, *Development trends for therapeutic antibody fragments*. Nature biotechnology, 2009. **27**(4): p. 331-337.
77. Maggon, K., *Monoclonal antibody "gold rush"*. Current medicinal chemistry, 2007. **14**(18): p. 1978-1987.
78. Holliger, P. and P.J. Hudson, *Engineered antibody fragments and the rise of single domains*. Nature biotechnology, 2005. **23**(9): p. 1126-1136.
79. Whitlow, M., et al., *An improved linker for single-chain Fv with reduced aggregation and enhanced proteolytic stability*. Protein engineering, 1993. **6**(8): p. 989-995.
80. Alfthan, K., et al., *Properties of a single-chain antibody containing different linker peptides*. Protein engineering, 1995. **8**(7): p. 725-731.

81. Weisser, N.E. and J.C. Hall, *Applications of single-chain variable fragment antibodies in therapeutics and diagnostics*. Biotechnology advances, 2009. **27**(4): p. 502-520.
82. Jain, R.K., *Physiological barriers to delivery of monoclonal antibodies and other macromolecules in tumors*. Cancer research, 1990. **50**(3 Supplement): p. 814s-819s.
83. Ward, E.S., et al., *Binding activities of a repertoire of single immunoglobulin variable domains secreted from Escherichia coli*. 1989.
84. Yokota, T., et al., *Rapid tumor penetration of a single-chain Fv and comparison with other immunoglobulin forms*. Cancer research, 1992. **52**(12): p. 3402-3408.
85. Hudson, P.J. and C. Souriau, *Engineered antibodies*. Nature medicine, 2003. **9**(1): p. 129-134.
86. Larson, S., et al., *Localization of <sup>131</sup>I-labeled p97-specific Fab fragments in human melanoma as a basis for radiotherapy*. Journal of Clinical Investigation, 1983. **72**(6): p. 2101.
87. Cumber, A.J., et al., *Comparative stabilities in vitro and in vivo of a recombinant mouse antibody FvCys fragment and a bisFvCys conjugate*. The Journal of Immunology, 1992. **149**(1): p. 120-126.
88. King, D.J., et al., *Improved tumor targeting with chemically cross-linked recombinant antibody fragments*. Cancer research, 1994. **54**(23): p. 6176-6185.
89. Schott, M.E., et al., *Differential metabolic patterns of iodinated versus radiometal chelated anticarcinoma single-chain Fv molecules*. Cancer research, 1992. **52**(22): p. 6413-6417.
90. Arend, W. and F. Silverblatt, *Serum disappearance and catabolism of homologous immunoglobulin fragments in rats*. Clinical and experimental immunology, 1975. **22**(3): p. 502.
91. Bird, R.E., et al., *Single-chain antigen-binding proteins*. Science, 1988. **242**(4877): p. 423-426.
92. Åkerström, B., et al., *On the interaction between single chain Fv antibodies and bacterial immunoglobulin-binding proteins*. Journal of immunological methods, 1994. **177**(1): p. 151-163.

93. Zahid, M., et al., *Design and reshaping of an scFv directed against human platelet glycoprotein VI with diagnostic potential*. Analytical biochemistry, 2011. **417**(2): p. 274-282.
94. Chateau, M.d., et al., *On the interaction between protein L and immunoglobulins of various mammalian species*. Scandinavian journal of immunology, 1993. **37**(4): p. 399-405.
95. Ayyar, B.V., et al., *Affinity chromatography as a tool for antibody purification*. Methods, 2012. **56**(2): p. 116-129.
96. Kurasawa, J.H., et al., *Insect cell-based expression and characterization of a single-chain variable antibody fragment directed against blood coagulation factor VIII*. Protein expression and purification, 2013. **88**(2): p. 201-206.
97. Miethe, S., et al., *Production of single chain fragment variable (scFv) antibodies in Escherichia coli using the LEX™ bioreactor*. Journal of biotechnology, 2013. **163**(2): p. 105-111.
98. Freyre, F.M., et al., *Very high expression of an anti-carcinoembryonic antigen single chain Fv antibody fragment in the yeast Pichia pastoris*. Journal of biotechnology, 2000. **76**(2): p. 157-163.
99. Sushma, K., et al., *Cloning, expression, purification and characterization of a single chain variable fragment specific to tumor necrosis factor alpha in Escherichia coli*. Journal of biotechnology, 2011. **156**(4): p. 238-244.
100. Porath, J., *Immobilized metal ion affinity chromatography*. Protein expression and purification, 1992. **3**(4): p. 263-281.
101. Das, D., T.M. Allen, and M.R. Suresh, *Comparative evaluation of two purification methods of anti-CD19-c-myc-His 6-Cys scFv*. Protein expression and purification, 2005. **39**(2): p. 199-208.
102. Mechaly, A., E. Zahavy, and M. Fisher, *Development and implementation of a single-chain Fv antibody for specific detection of Bacillus anthracis spores*. Applied and environmental microbiology, 2008. **74**(3): p. 818-822.
103. Damasceno, L.M., et al., *An optimized fermentation process for high-level production of a single-chain Fv antibody fragment in Pichia pastoris*. Protein expression and purification, 2004. **37**(1): p. 18-26.

104. Willems, A., et al., *Optimizing expression and purification from cell culture medium of trispecific recombinant antibody derivatives*. Journal of Chromatography B, 2003. **786**(1): p. 161-176.
105. Moosmann, A., et al., *Purification of a PEGylated single chain Fv*. Journal of Chromatography A, 2012. **1236**: p. 90-96.
106. Gagnon, P.S., *Enhanced capacity and purification of antibodies by mixed mode chromatography in the presence of aqueous-soluble nonionic organic polymers*. 2010, Google Patents.

## APPENDIX

### **Appendix I Chromatogram of FLAG-purified Pfs25 separated by QA monolithic disk.**

The 2-D electrophoresis gel (Figure 8) revealed that purified Pfs25 has several charge variants, the same characteristic was assumed to hold true with aggregates comprised of Pfs25 as well. Therefore, purified Pfs25 was run on a QA monolithic disk to try to separate the monomeric forms of Pfs25 from its multimeric forms. Figure 26 is the chromatogram of purified Pfs25 bound and desorbed from the QA monolithic disk. Unfortunately, baseline separation was not achieved between the eluted peaks; therefore, the QA monolithic disk was not an effective method to separate the different aggregates of Pfs25.

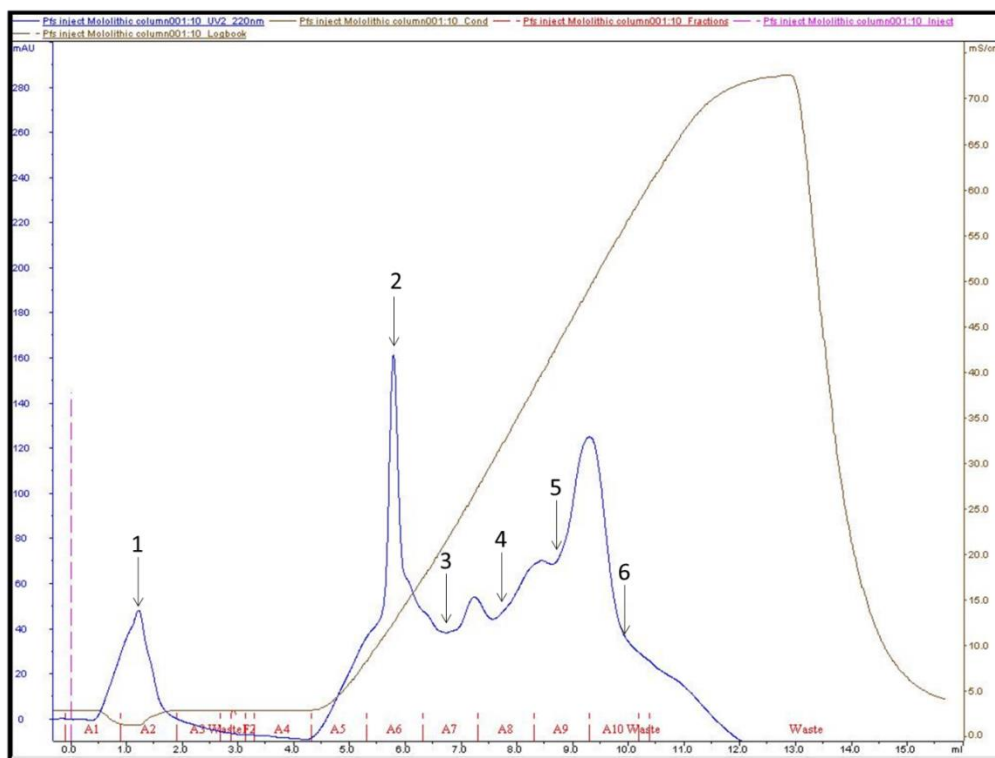


**Figure 26.** Chromatogram of FLAG-purified Pfs25 separated by QA monolithic disk.

## **Appendix II Uptake experiments to determine possibility for binding to Capto Q and Phenyl Sepharose resin**

During a continuous purification process, for a column with a bed volume of 4.7 mL (0.7x10cm) at a linear velocity of 50 cm/h,  $\alpha$ CD22scFv has a retention time of 20 minutes to bind to the column before the solution has traveled out of the column. Non-pretreated lysate was batch purified with Capto Q resin for 5, 15, 30, and 60 minutes to determine the minimum amount of time needed for maximum amount  $\alpha$ CD22scFv to bind to the resin. The supernatant of the lysate after incubation with Capto Q resin at each time point was run on a Western Blot to determine how much  $\alpha$ CD22scFv

remained in the solution. The supernatant after binding to the resin after 5 minutes (Figure 27, Lane 5) had a relatively darker band on the Western blot than the supernatants at the other incubation time points (Lanes 6-8) indicating a greater amount of FLAG-tagged protein did not adsorb to the resin after 5 minutes of uptake. The supernatants after time points 15, 30, and 60 minutes seem to have the same band thickness of FLAG-tagged recombinant protein; approximately the same amount of  $\alpha$ CD22scFv is left in the supernatants. This qualitative analysis suggests that 15 minutes of incubation with the Capto Q resin is the minimum amount of time for maximum protein binding to the resin; increased incubation time will not increase the amount of  $\alpha$ CD22scFv bound to the resin. To ensure consistency in subsequent batch experiments, 30 minutes was used as the incubation time of pretreated lysate and Capto Q resin. This experiment also serves as a baseline to test the efficiency of pretreatment methods and its ability to reduce the amount of impurities in solution and increase the interaction between  $\alpha$ CD22scFv and the resin.

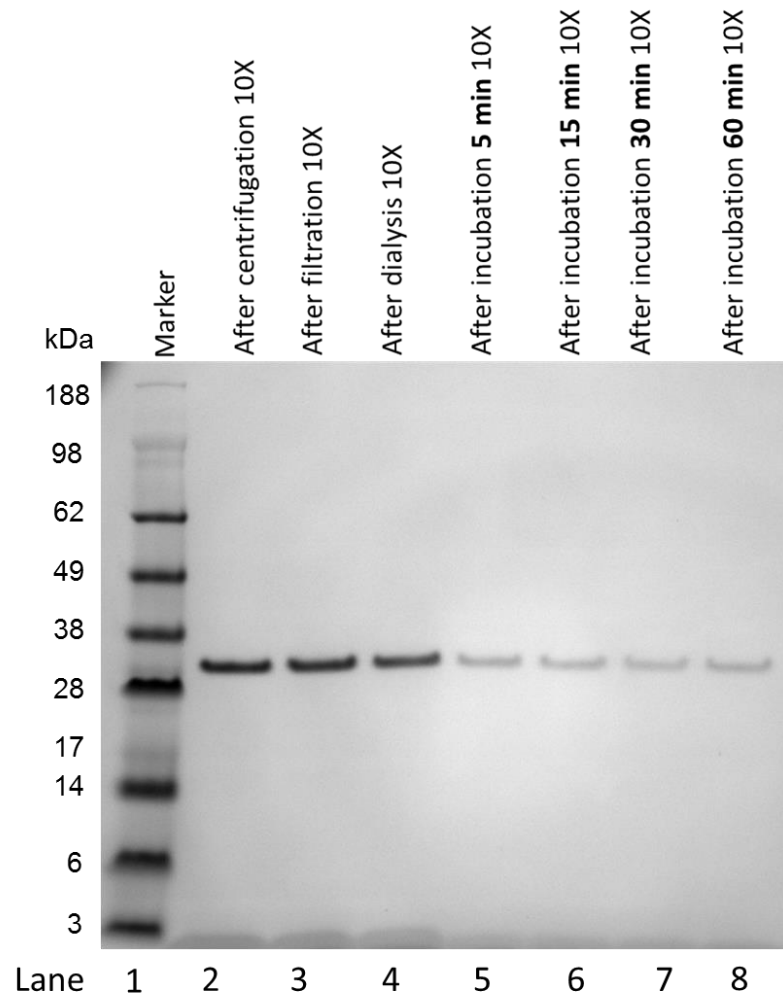


**Figure 27.** Uptake experiment with Capto Q resin. Western Blot of  $\alpha$ CD22scFv using anti-FLAG-AP conjugated antibody. Lane 1: molecular weight marker (kDa); Lane 2: 10X diluted supernatant after centrifugation; Lane 3: 10X diluted supernatant after filtration through PES 0.22 $\mu$ m syringe filter; Lane 4: 10X diluted supernatant after dialysis; Lane 5: 10X diluted supernatant after 5 minutes of binding with Capto Q resin; Lane 6: 10X diluted supernatant after 15 minutes of binding with Capto Q resin; Lane 7: 10X diluted supernatant after 30 minutes of binding with Capto Q resin; Lane 8: 10X diluted supernatant after 60 minutes of binding with Capto Q resin.

Another non-affinity commercial resin being tested as a capture chromatography step is hydrophobic interaction resin, Phenyl Sepharose. A similar experiment to the anion exchange purification was performed on the hydrophobic interaction resin. However, instead of removing the conductivity in the lysate by dialysis, the conductivity of the lysate increased by adding ammonium sulfate to a final concentration of 1M ammonium sulfate. Batch binding purification was performed on the clarified lysate with 1M ammonium sulfate and Phenyl Sepharose resin for 5, 15, 30, and 60 minutes to determine how much time is needed for  $\alpha$ CD22scFv to completely bind to the resin. Samples of the supernatant after the time points and the first column volumes of wash were analyzed by western blotting to determine affinity and specificity of  $\alpha$ CD22scFv to Phenyl Sepharose resin. Elution fractions after 60 minutes of binding time were also analyzed by western blotting (Figure 28).

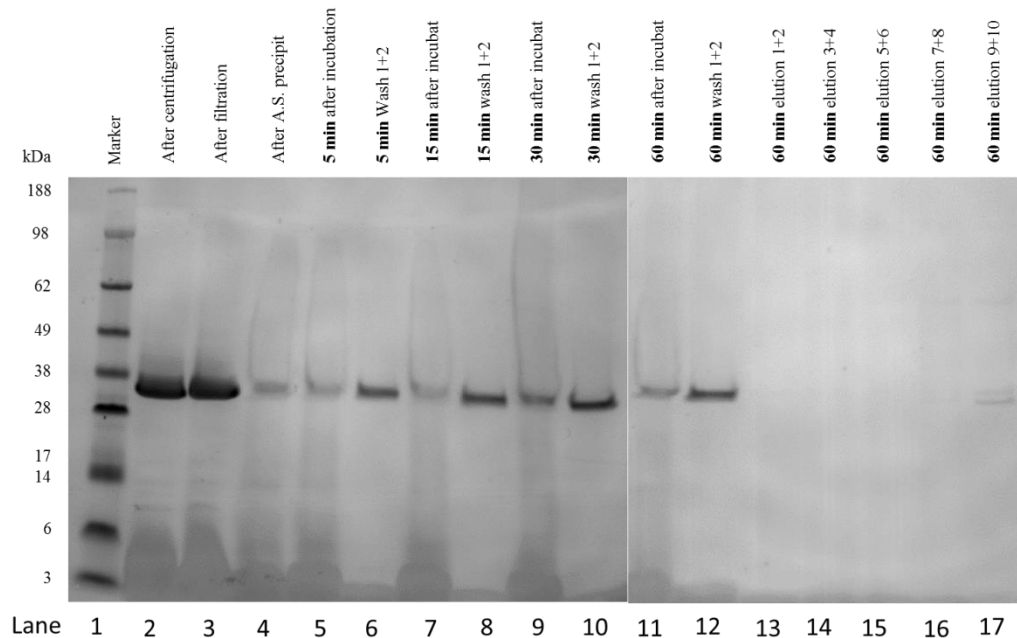


**Figure 28.** Uptake experiment with 1M ammonium sulfate and Phenyl Sepharose resin. Western Blot using anti-FLAG-AP conjugated antibody to detect  $\alpha$ CD22scFv. Lane 1: molecular weight marker (kDa); Lane 2: supernatant after centrifugation; Lane 3: supernatant of clarified lysate; Lane 4: supernatant after 1M ammonium sulfate precipitation; Lanes 5, 7, 9, and 11: supernatant after mixing with Phenyl Sepharose resin for 5, 15, 30, and 60 minutes; Lanes 6, 8, 10, and 12: 1<sup>st</sup> and 2<sup>nd</sup> CVs of washing column before elution; Lanes 13-17: elution fractions of resin mixed with clarified lysate for 60 minutes at room temperature.

Strong bands are seen on the Western blot in the lanes containing supernatant after protein uptake to Phenyl Sepharose resin and washing fractions. However, no reaction took place on the membrane in Lanes 13-17 when probed with anti-FLAG-AP conjugated antibody (no FLAG-tagged proteins came off the column during the low

conductivity elution). This indicates that  $\alpha$ CD22scFv was unable to adsorb to the resin under current binding conditions. Enough resin was available during the residence period; hence there was plenty of binding sites for  $\alpha$ CD22scFv to bind to the resin. Therefore the only way to increase the binding to Phenyl Sepharose is to increase the concentration of ammonium sulfate in the lysate to further expose the hydrophobic sites on  $\alpha$ CD22scFv giving the protein a higher specificity to the resin.

To increase the adsorption of  $\alpha$ CD22scFv to Phenyl Sepharose resin, ammonium sulfate was added to clarified lysate to a final concentration of 1.5M ammonium sulfate. The lysate was batch purified with Phenyl Sepharose resin for 5, 15, 30, and 60 minutes at room temperature. Supernatants of the lysate after incubation with the resin was run on a Western Blot to determine how much protein was left in the supernatant; the first column volume of wash was also run on the Western Blot to determine non-specific binding to the column. After binding with the Phenyl Sepharose resin after the time points, the supernatants (Figure 29, Lanes 3, 5, 7, and 9) reveal a thick band on the Western blot. The washing fractions (Figure 29, Lanes 4, 6, 8, and 10) also contained significant amount of  $\alpha$ CD22scFv. The Western Blot reveals that even at 1.5M ammonium sulfate, the hydrophobicity of  $\alpha$ CD22scFv is not enough to bind to the HIC and even if the recombinant protein gets taken up during the load, it interacts weakly with the resin and easily comes off in the wash. Clarified lysates have many proteins that competitively interact with Phenyl Sepharose resin. For  $\alpha$ CD22scFv to have a strong affinity to the HIC resin, the protein needs: (a) more binding sites on the resin to accommodate all the proteins that have an affinity to the resin (increasing bed volume)

and/or (b) reduce the amount of competing proteins in solution (different pretreatment methods). By increasing the concentration of ammonium sulfate in the clarified lysate from 1M to 1.5M, about half of  $\alpha$ CD22scFv is lost due to precipitation. Even though increasing the concentration of ammonium sulfate could further increase the specificity of  $\alpha$ CD22scFv to the resin, a majority of the protein will be lost before the capture chromatography step and is, therefore, not a viable option as a capture chromatography step. However, Phenyl Sepharose resin could be used as an intermediate purification step.

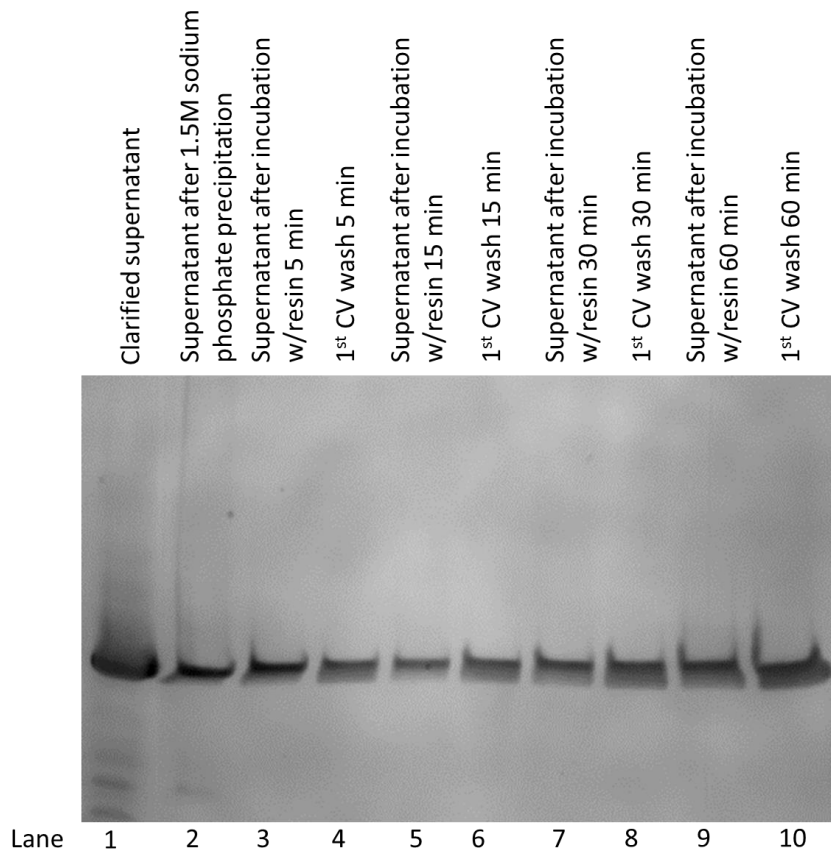


**Figure 29.** Uptake experiment with 1.5M ammonium sulfate and Phenyl Sepharose resin. Western blot analysis of  $\alpha$ CD22scFv, using anti-FLAG-AP conjugated antibody. Lane 1: supernatant of clarified lysate; Lane 2: Supernatant after 1.5M sodium phosphate precipitation; Lane 3: supernatant after 5 minutes of binding with Phenyl Sepharose resin; Lane 4: wash of Phenyl Sepharose resin after 5 minutes of incubation with supernatant; Lane 5: supernatant after 15 minutes of binding with Phenyl Sepharose resin; Lane 6: wash of Phenyl Sepharose resin after 15 minutes of incubation with supernatant; Lane 7: supernatant after 30 minutes of binding with Phenyl Sepharose resin; Lane 8: wash of Phenyl Sepharose resin after 30 minutes of incubation with supernatant; Lane 9: supernatant after 60 minutes of binding with Phenyl Sepharose resin; Lane 10: wash of Phenyl Sepharose resin after 30 minutes of incubation with supernatant.

### Appendix III 2-D electrophoresis of FLAG-purified $\alpha$ CD22scFv

The Texas A&M Protein Chemistry lab ran FLAG-purified  $\alpha$ CD22scFv on a 2D electrophoresis gel (Figure 30). The gel reveals a very pure sample with a protein train consisting of highly purified  $\alpha$ CD22scFv. The protein train shows that  $\alpha$ CD22scFv has several differently charged variants.

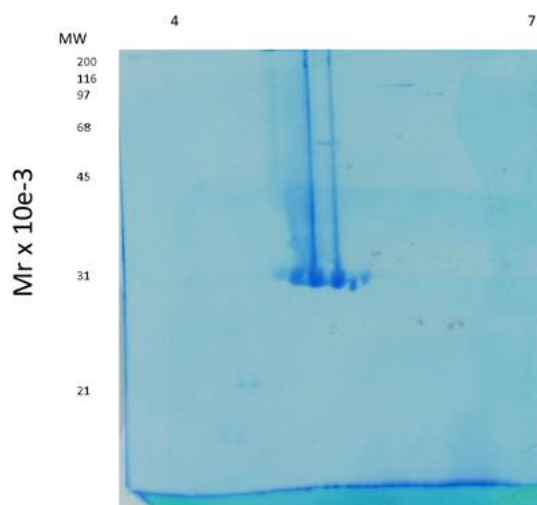


**Figure 30.** 2D electrophoresis gel on FLAG-purified  $\alpha$ CD22scFv.